Scholar Commons
USF University of South Florida

University of South Florida
Scholar Commons

Graduate Theses and Dissertations | Graduate School

1-1-2014

Quantification of Protein Adhesion Strength to Surface Attached Poly (N- isopropylacrylamide) Networks by Hydrodynamic Detachment Shear Stresses

Gulnur Sanden
University of South Florida, gefe@mail.usf.edu

Follow this and additional works at: http://scholarcommons.usf.edu/etd

 Part of the Biomedical Engineering and Bioengineering Commons

Scholar Commons Citation

Sanden, Gulnur, "Quantification of Protein Adhesion Strength to Surface Attached Poly (N- isopropylacrylamide) Networks by Hydrodynamic Detachment Shear Stresses" (2014). *Graduate Theses and Dissertations.*
http://scholarcommons.usf.edu/etd/5615

This Dissertation is brought to you for free and open access by the Graduate School at Scholar Commons. It has been accepted for inclusion in Graduate Theses and Dissertations by an authorized administrator of Scholar Commons. For more information, please contact scholarcommons@usf.edu.

Quantification of Protein Adhesion Strength to Surface Attached Poly (N-isopropylacrylamide) Networks by Hydrodynamic Detachment Shear Stresses

by

Gulnur Sanden

A dissertation submitted in partial fulfillment
of the requirements for the degree of
Doctor of Philosophy
Department of Chemical and Biomedical Engineering
College of Engineering
University of South Florida

Major Professor: Ryan Toomey, Ph.D.
Aydin Sunol, Ph.D.
Nathan Gallant, Ph.D.
William Lee, Ph.D.
Sameer Varma, Ph.D.

Date of Approval:
November 4, 2014

Keywords: Thermoresponsive Hydrogel, IgG Adsorption, Spinning Disk, Polystyrene Microsphere, Peptide-Polymer Conjugate

Copyright © 2014, Gulnur Sanden

DEDICATION

This dissertation is dedicated to my wonderful mother, Mukaddes Efe, my father Orhan Efe, my sisters, Gulcan Alothman, Gulgun Efe, Gulin Meckeli, and my beloved husband Steven Sanden for their unrelenting and unconditional support, encouragement, care and love.

ACKNOWLEDGMENT

It is still hard to believe that it is time to leave and move on to different adventures. Years of research needs to be passed on to new explorers. Throughout my journey I have experienced situations that made me sad, happy, doubtful, excited, overwhelmed, vigorous, fearful, and confident. There have been many times that I did not believe that I was capable of completing this journey.

I would like to express my deepest gratitude to my advisor Dr. Ryan Toomey. He has never doubted of my capabilities and he has always given me his confidence. He gave me his constant support, encouragement, guidance, understanding and patience. He has not only been my teacher but also my mentor, my scholar. I will always be grateful for all of his help to make me a better scientist, researcher, engineer and most of all a better person.

I also would like to convey my sincere appreciation to my dissertation committee members, Dr. Aydin Sunol, Dr. Nathan Gallant, Dr. William Lee and Dr. Sameer Varma for their invaluable help and support on this study. My special thanks to Dr. Sunol for his mentorship and countless help throughout my study at USF. I also would like to give my special thanks to Dr. Nathan Gallant for making me a part of his research group and for all of his guidance and help.

Lastly, I express my appreciation to my family and friends from the bottom of my heart. I could not make this happen without their constant support, care and love.

TABLE OF CONTENTS

LIST OF TABLES

LIST OF FIGURES

ABSTRACT

Stimuli responsive coatings offer a versatile method by which to manipulate interfacial interactions of proteins in a desired way. However, there exists little guidance as to how the structure of a responsive polymer coating influences adsorption of proteins. In this dissertation, the adsorption behavior of immuglobulin-G (IgG) on poly (N-isopropylacryamide) (PNIPAAm) hydrogel coatings was investigated as a function of film thickness. PNIPAAm exhibits a hydrophilic to hydrophobic transition above a critical temperature of ~32°C in aqueous solutions. In this research, through the use of quartz crystal microbalance with dissipation (QCM-D) it was observed that the adsorption was thickness dependent and became non-reversible as the temperature was decreased. Interestingly, QCM-D results also suggested a similar amount of protein adsorption on both hydrated and dehydrated PNIPAAm surfaces. A rigid film analysis using Sauerbrey equation revealed a multi-layer formation on the collapsed PNIPAAm coatings. Although it is allegedly reported that PNIPAAm favors adsorption above the critical temperature due to hydrophobic interactions, there have been several studies that reported adsorption of proteins below the critical temperature. To better understand the QCM-D results, hydrodynamic shear force assays in a spinning disk configuration were performed in order to quickly measure and quantify adhesion of polystyrene (PS) probe spheres (10μm) to the PNIPAAm coatings in both the solvated (hydrophilic) and collapsed (hydrophobic) state. The influence of polymer coating thickness, polymer chain cross-link density, microsphere concentration and adsorption time on the

adhesion characteristics of the coatings was investigated in relation with volume phase transition of the polymer coatings.

A series of experiments on quantification of the temperature dependent adhesion of proteins adsorbed on surface attached PNIPAAm coatings of thicknesses was performed as the surface chemistry was switched from hydrophilic to hydrophobic. First, adhesion of polystyrene (PS) microspheres on PNIPAAm coatings was quantified in order to have a guideline for temperature dependent adhesion performance of these coatings. PS particles were subjected to a range of detachment shear stresses through hydrodynamic flow in a spinning disk configuration. These experiments provide an indirect method to determine the force of adhesion since it is proportional to the hydrodynamic force. Model protein, IgG, was then linked to PS microspheres and the mean adhesion strength of the IgG coated PS microspheres were determined through the detachment shear stresses. The influence of PS deposition time, PS bead concentration, PNIPAAm coating thickness and PNIPAAm cross-link density on the adhesion strength were addressed. The results indicated that in the collapsed state, the adhesion of bare hydrophobic PS microspheres depends strongly on coating thickness. For hydrophilic charged PS microspheres the adhesion was always higher on the hydrated PNIPAAm surfaces and appeared not to be strongly affected by the increase in PNIPAAm coating thickness. The adhesion of IgG was higher on the collapsed PNIPAAm surfaces and the adhesion trend did not significantly change as the PNIPAAm film thickness was increased. For PNIPAAm coatings with the cross-link density reduced by factor of 10, the adhesion was again higher on the collapsed PNIPAAm surface and scaled linearly with thickness. Moreover, the influence of

thickness became prominent at the higher thickness values (165 nm-185 nm). In addition, the adhesion of carboxylated microspheres on PNIPAAm did not reach equilibrium and increased linearly with microsphere deposition time.

A study on the sensing characteristics of PNIPAAm coatings in response to heavy metal ions was also conducted in this dissertation. The temperature-dependent swelling behavior of poly(N-isopropylacrylamide) and tripeptide Gly-Gly-His/poly(NIPAAm) conjugate hydrogel coatings were investigated using a quartz crystal microbalance with dissipation (QCM-D) while in contact with NaCl, $ZnCl_2$, $NiCl_2$, and $CuCl_2$ solutions. To fabricate the tripeptide conjugated gels, precursor gels of poly(NIPAAm-co-3-aminopropylmethacrylamide[3.5 mole%]) were synthesized via free radical polymerization. The metal binding tripeptide, Gly-Gly-His, was subsequently synthesized in the gel via a Merrifield solid phase peptide synthesis (SPPS) technique, in which the amino group of the copolymer gel provided a functional site to support peptide synthesis. It was found that the logarithm of the transition temperature of the tripeptide Gly-Gly-His/poly(NIPAAm) conjugate hydrogel was proportional to the ionic strength, showing two distinct regions at low and high ionic strengths for the divalent ions. In the low ionic strength regime, the salting out constants were 0.08 M^{-1}, 0.07 M^{-1}, and 0.06 M^{-1} for Cu^{2+}, Ni^{2+}, and Zn^{2+}, respectively, which follows the known trend for binding of the ions to Gly-Gly-His. In the high ionic strength region, when the metal-ion binding sites in the tripeptide conjugate hydrogel were saturated, the salting out constants were similar to the salting out constants associated with pure poly(NIPAAm).

CHAPTER 1 : SURFACE MOIFICATION THROUGH STIMULI RESPONSIVE POLYMERS

1.1 Introduction

Modification of a surface with stimuli responsive polymers offers great potential to control surface interactions of proteins and thereby, to attain desired protein functioning in biological activities. Stimuli responsive polymers are often called smart polymers due to their ability to sense very slight environmental changes such as change in temperature, pH, ionic strength, external additives (ions, bioactive molecules, etc.), light irradiation, specific analytes, electric/magnetic fields, and mechanical forces.[1, 2] Such polymers respond to these triggers by undergoing a dramatic reversible and/or irreversible change in their physical property and/or chemical structure. Polymers that undergo these types of changes in response to temperature variations are called thermoresponsive polymers and they exhibit a conformational change at a critical temperature called lower critical solution temperature (LCST). Induced conformational changes in polymer structures can be controlled and tuned in a predictable manner, which makes them very practical in a wide range of applications related to biotechnology and biomedicine. These applications involve control over the adsorption of proteins at interfaces. The adsorption of proteins is the first event observed between a material and a biological fluid, therefore, controlling the adsorption of proteins at interfaces is imperative in biomedical field such as designing biomaterials for surgical

implants, creating drug delivery systems and developing scaffolds for tissue colonization. In spite of the advances made for understanding the adsorption phenomena of proteins, the exact mechanism has not yet been established.[3] The details of the protein adsorption are discussed in the next chapter of this dissertation. The use of stimuli responsive polymers as a biomaterial surface has introduced promising developments in modulating the protein-surface interactions. The adsorption behavior of protein on the polymer surface is shown in figure 1.1. Upon contact with the polymer surface, water molecules are repositioned from contact sites between amino acid residues and polymer surface. This induces conformational change in the protein that leads to a strong binding of the protein to the surface.[4]

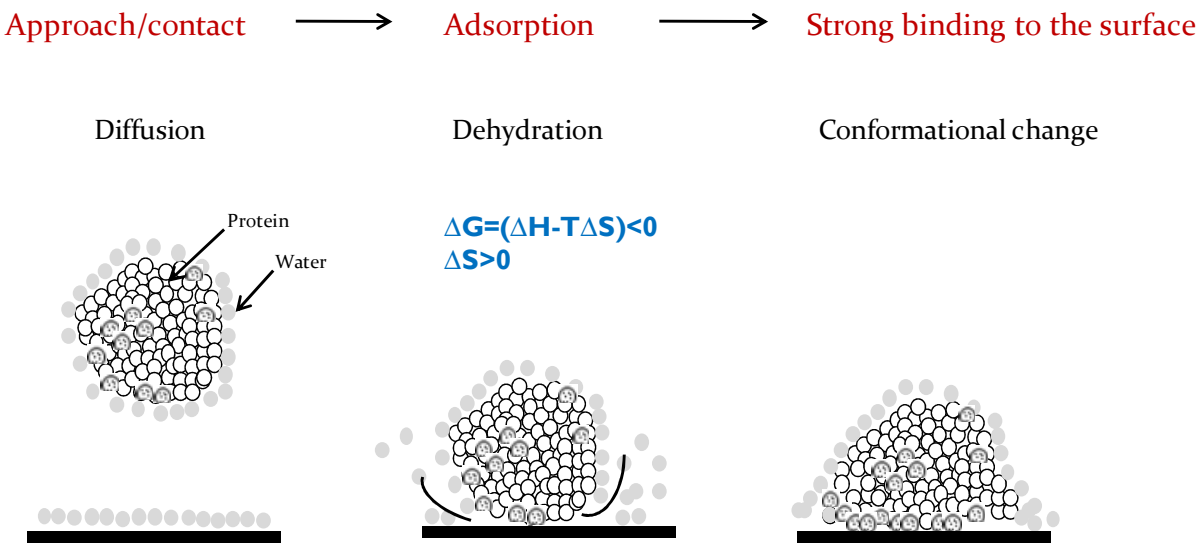

Figure 1.1 Protein adsorption on polymer surfaces (Image from Y. Iwasaki Et al., Proteins at Solid-Liquid Interfaces, Ed. P. Dejardin, Springer, 2006)

Stimuli responsive polymers can have different architectures such as linear chains, cross-linked networks of the bulk form or surface anchored. In cross-linked thermoresponsive polymers, polymer chains are chemically linked to one another forming a three dimensional network that can undergo extensive swelling and

contraction behavior in all three directions. Regardless the tremendous swelling capacity, macroscopic gels in bulk form exhibit a slow response time as the swelling rate is inversely proportional to the square of the characteristic dimension of the gel[5] and their collective diffusion is a rate limiting step. It is, therefore, necessary to reduce their size in order to get to a usable level of response time. Chemical linkage of the polymer network to an underlying surface results in lateral confinement that restricts the swelling of the network in parallel direction and allows it only in perpendicular direction or normal to the surface (figure 1.2). This reduces the degree of freedom of the gel and leads to significant changes in the structure, mechanical properties, dynamics and permeability of the network. The response time of the confined gel to a stimulus would be faster since the rate of response is related to the amount of water contained within the gel network. The chemical attachment of the network to a solid substrate also gives more stability to the network. As a result, surface confinement should considerably improve performance of the gel. Although the swelling is observed to be less in surface-attached networks as compared to the nonattached bulk networks at the same cross-link density it is larger than that suggested by simple geometric considerations for swelling in one dimension.[6] It was reported by Harmon and coworkers that surface attached Poly(N-isopropylacrylamide) PNIPAAm networks experienced a volume change of around 15 fold while this change was as large as 100 fold in unconstrained networks.[7] Other studies reported that surface attachment of the PNIPAAm network resulted in a lower LCST at the thick film regime as the film thickness increased and surface attached PNIPAAm did not completely collapse above the LCST.[8, 9] Surface attachment allows for remarkable design flexibility and surface anchored

thermoresponsive polymer networks offer great opportunities for microfluidic systems that are used in sensing, fluid regulating, mechanical actuating and the controlled uptake of the proteins from the solution.[10]

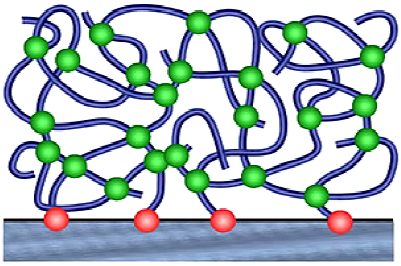

Figure 1.2 Surface attached polymer networks

Poly(N-isopropylacrylamide) or PNIPAAm is one of the most studied responsive polymers, which shows a sensitivity to temperature change at a critical point called cloud point or lower critical solution temperature (LCST). [11-14] The polymer goes through a reversible conformational change called volume phase transition at around 32°C due to the presence of a hydrogen-binding group (amide) and a hydrophobic group (isopropyl) in its structure. At temperatures below LCST, the polymer chains exist as coils due to favorable mixing of amide groups and water. Above the LCST, the hydrogen bonding of water with the amide groups is disrupted. Attractive inter-segment interactions between the isopropyl groups dominate and the chains collapse to globules (Figure 1.3). The sharpness of the volume phase transition, the transition temperature close to physiological temperature and the robustness of the polymer itself make PNIPAAm often be exploited as a model system in bio-based applications.

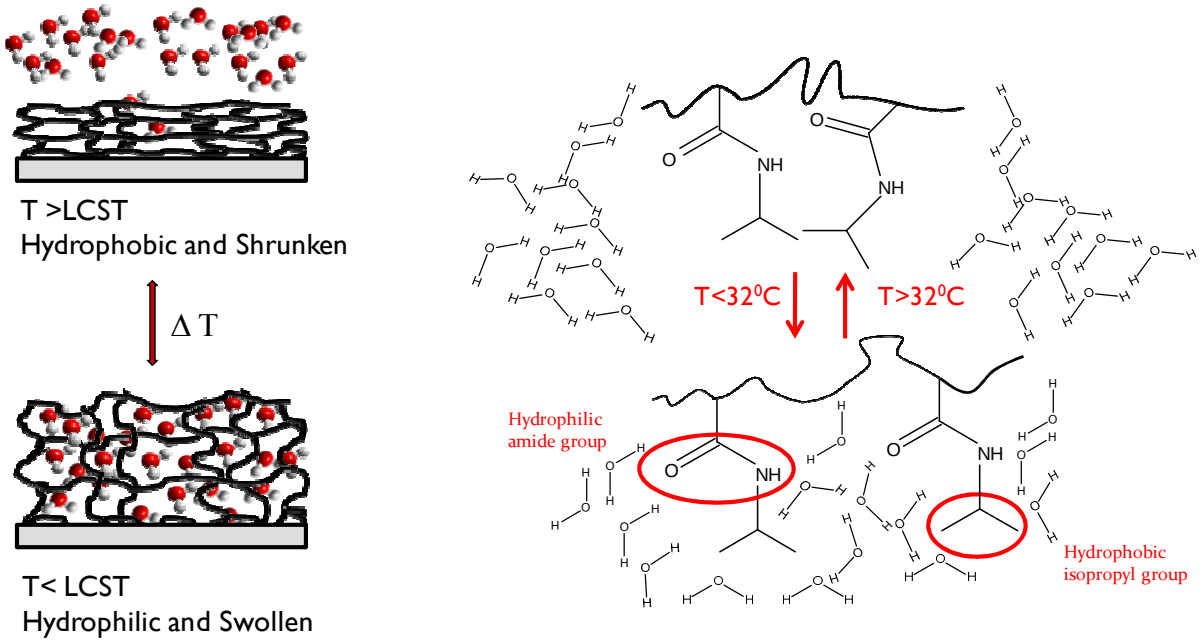

Figure 1.3 Volume phase transition of surface attached PNIPAAm. Increase in temperature brings hydrophobic groups closer to each other and swollen PNIPAAm chains collapse to globules.

Protein interactions with PNIPAAm immobilized surfaces have been studied by monitoring the amount of adsorbed proteins as a function of temperature. [15, 16] Figure 1.4 presents a schematic of the adsorption behavior of proteins on PNIPAAm above and below the LCST. PNIPAAm surfaces are, in general, observed to adsorb more protein above its LCST than below and the activity of proteins was better preserved below the LCST than above it. This was attributed to the difference in protein confirmation/orientation above and below the LCST.[17] Bovine serum albumin (BSA) and lysozyme (Lys) adsorption on PNIPAAm coatings were investigated at below (20°) and above (37°) the LCST of the polymer.[3] The results demonstrated no measurable fouling on the PNIPAAm coating at the hydrated state while proteins are retained on dehydrated PNIPAAm coatings. In another study, the protein adsorption on thermo-

responsive PNIPAAm-grafted silicon surfaces was found to be thickness dependent.[18] In the thickness range below 15nm, changes in adsorption in response to temperature was not notable, however, the temperature sensitivity of protein adsorption was significant for thicker PNIPAAm grafted surfaces. In addition, they found a certain extent size-sensitive protein adsorption property for the grafted surface of 38.1 nm.

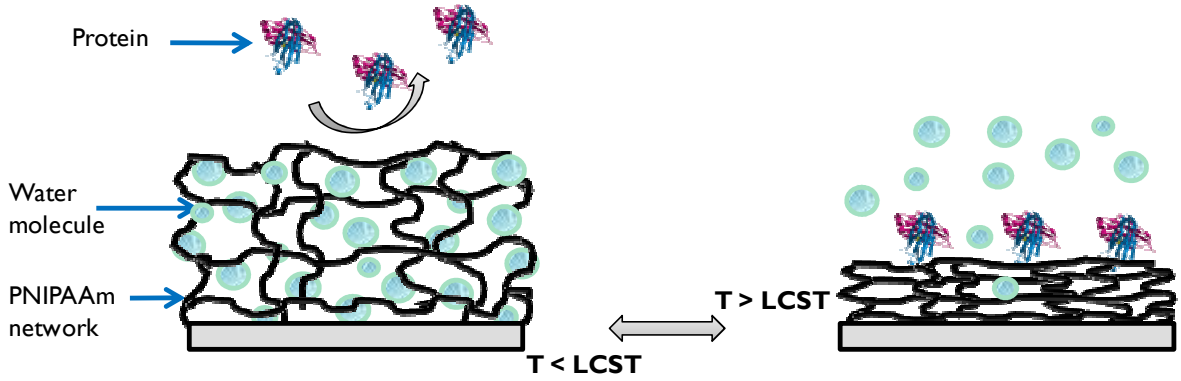

Figure 1.4 Modification through surface attached PNIPAAm networks to control protein adsorption

1.1.2 The Relevant Application: Cell Attachment-Detachment/Tissue Engineering

The development, organization and maintenance of the tissues are vital processes for life and interaction of cells with immobilized components of extracellular matrix (ECM) is necessary in order to carry out these processes. Once cells anchor to solid substrates they can perform their normal functions and then they can proliferate and produce an extracellular matrix, which leads to formation of confluent cell monolayers. This process can be done under controlled conditions normally outside of their natural environment by in vitro cell culturing. Conventional cell culturing methods harvest cells by dissolving ECM through proteolyatic activities; however, this can be detrimental to critical cell surface proteins and thereby, causes the disruption of the newly produced tissue like structure. Creation of thermoresponsive substrates for cell

harvesting constitutes a promising method to prevent this drawback encountered in the conventional cell culturing method. Such switchable substrate coatings can establish a good platform for cells to attach on and growth and release of the adhered cells can be adjusted through temperature.

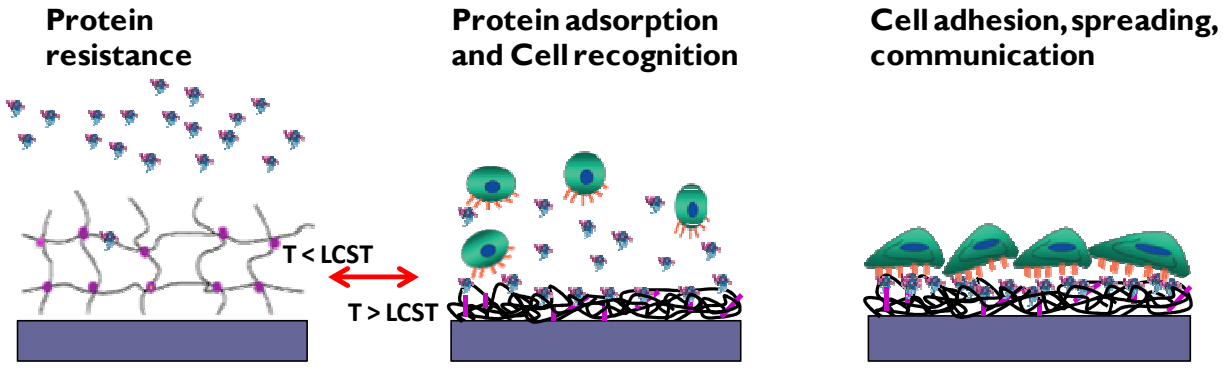

Figure 1.5 Schematic for control over protein adsorption through surface attached PNIPAAm coatings to promote cell adhesion

Tekazawa and his colleagues were, for the first time, able to detach a confluent cell sheet in culture without using conventional treatments but through the adjustment of temperature.[19] They cultured fibroblast monolayer in a physical blend of collagen and PNIPAAm coated dishes and found that lowering the temperature below LCST of PNIPAAm resulted in dissolution of the coating and thereby release (recovery) of the fibroblast sheet. Highly enzymatic harvesting sensitive bovine hepatocytes were successfully subcultured on PNIPAAm grafted tissue culture polystyrene (TCPS) surfaces by Yamada Et al.[2] Cell adhesion was promoted when grafted chains exposed their hydrophobic groups and became insoluble at the culture temperature (37.8°C), however, at temperatures below the LCST of PNIPAAm, the surface did not support cell adhesion due to hydration of the polymer chains. PNIPAAm surfaces are also quite

suitable to construct thicker tissue-like cell sheets that appear to be ideal for applications that involve with stratified tissue structures. Harimoto Et al. reported that they expelled confluent human aortic endothelial cells (HAECs) cultured on thermo-responsive culture dish grafted with PNIPAAm as an intact contiguous cell sheet by decreasing the temperature below the LCST of PNIPAAm.[20] They were able to produce double-layered cell sheets by placing a recovered confluent endothelial cell sheet directly onto rat hepatocytes monolayer. This offers a great improvement in liver tissue engineering because the layered co-culture of hepatocytes and HAEC sheets allows for the expression of differentiated functions of hepatocytes such as liver lobule. With the use of thermoresponsive coatings that can promote cell adhesion and proliferation, cell sheets that have more complex geometries resembling tissue shapes can potentially be engineered.

1.2 Motivation and Research Directions

1.2.1 Motivation

The surface modification of a material by using stimuli responsive polymers constitutes a powerful method to control the interactions of the material with its environment. Tailoring these interactions in a desired way has been indispensable in many biological and industrial applications. Numerous studies based on optimization of the surfaces with stimuli responsive polymers have reported very promising solutions to demanding challenges in many fields such as protein purification, biomaterials, tissue engineering, biosensors, drug delivery systems, and microfluidics. Most of the applications mentioned involve a very fundamental biological response: protein

adsorption/desorption. The intricacy of this phenomenon is great because majority of proteins change their structure and thereby their function upon adsorption and the biological functioning of a given protein is directly related to its specific three-dimensional structure. The accomplishments achieved in the past few decades with the aim of understanding the mechanism and thus, controlling the interactions of proteins with the environment via polymeric switchable surfaces have given us the necessary incentive and guidance to pursue this study. Our aspirations are to provide quantitative contributions to the existing practices and further elucidations to the challenges of the protein adsorption/desorption on thermoresponsive polymeric surfaces. Our findings will help in design of intelligent biomaterial surfaces in respective areas such as tissue engineering.

1.2.2 Objective

This research strives for attainment of substantial and reliable information regarding the adhesion properties of cross-linked and surface tethered PNIPAAm films as the water content of the films varies. With the use of a robust and quantitative measurement system, we, for the first time, intended to quantitatively ascertain the adhesion of the model protein, IgG (M_w~150kDa) attached on the surface tethered PNIPAAm networks as the surface activity of the polymer is altered from hydrophilic (also referred as protein repelling) to hydrophobic (protein binding) through temperature change. The observations obtained from this technique would help establish correlation between the adsorption characteristics of proteins and the phase transition behavior of the surface anchored thermoresponsive PNIPAAm surfaces. The knowledge gained will

present a useful guidance for biomedical applications based on controlling surface interactions of proteins.

1.2.3 Problem Statement and Dissertation Summary

Although there have been great prospects to control surface interactions of biomolecules using stimuli responsive thin films[21-23], the relationship between the structure of switchable surfaces and adhesion properties is still ambiguous. There have been conflicts among the reports regarding the adhesive properties of the stimuli responsive polymers with respect to volume phase transition behavior. Several studies have reported negligible adhesion below the LCST in grafted or adsorbed PNIPAAm chains[24-26] while other studies stated significant adhesion in cross-linked coatings below the LCST[27, 28] which might be due to thickness or structure dependence. As opposed to the well-established reversible volume phase transition behavior of PNIPAAm, the reversibility of its bio-fouling characteristics has not yet been defined. A number of investigations suggested temperature reversible adhesion and removal of proteins, mammalian and bacterial cells.[29-33] This is, however, not always observed as some studies showed partial cycling of protein adsorption/desorption.[34, 35] It is, consequently, crucial to better understand the factors that govern whether or not a PNIPAAm surface is completely non-fouling below its critical temperature. It is also important to have an improved comprehension of the factors that could inhibit the reversible adsorption of proteins since irreversibility would affect the effective lifetime of many applications.

As PNIPAAm goes through its phase transition over a small temperature variations, corresponding change in its volume due to the underlying fundamental interactions (Van der Waals interactions, hydrogen bonding) influences the properties of

the polymer layer such as elasticity, topography, osmotic compressibility, and water content at the surface. Each of these parameters is closely dependent on the degree of confinement of the PNIPAAm chains and affects the adhesive performance of a PNIPAAm surface. Therefore it is necessary to investigate how adhesion is correlated to the volume phase transition and surface confinement. This dissertation presents a comprehensive study to provide experimental data on the adhesive characteristics of PNIPAAm cross-linked networks.

Another aspect of the use of responsive polymers is that they can provide selective recognition mechanisms towards heavy metal ions. Responsive polymer-based sensing possesses unique advantages due to temperature induced “fingerprints” that can be measured with respect to phase-transition behavior when in contact with ionic solutions. Though phase transition behavior of responsive polymers has been of considerable interest for many bio related applications the studies on applying their feature of environment sensitivity towards selective separation and detection systems still remain in their initial stage. In this dissertation, the metal ion binding ability of the PNIPAAm hydrogel networks which a metal affinity tripeptide was directly grown within the network was also investigated.

Chapter 1 and 2 of this dissertation provide the background information regarding the adsorption phenomenon of proteins and use of thermoresponsive polymer surfaces to control protein adsorption.

In Chapter 3, experimental methods of polymer synthesis, thin film fabrication and characterization were discussed. Three major measurement techniques of this dissertation were introduced in detail. Ellipsometry was mainly used to characterize the

thickness of the PNIPAAm films as a function of temperature induced volume phase transition behavior. Quartz crystal microbalance with dissipation (QCM-D) was used to determine the adsorbed protein amount on the polymer surface as well as the qualitatively determine the rigidity of the adsorbed protein layer. It is also used to determine the change in the phase transition temperature of the peptide conjugated PNIPAAm networks as a result of metal ion binding. Fluorescence technique was used to visualize the adsorption of the model protein, IgG, on the PNIPAAm surface. Spinning disk technique was utilized to quantify the adhesion of the polystyrene (PS) microspheres and IgG on the PNIPAAm films.

Chapter 4 presents the results of our QCM-D investigations on temperature dependent adsorption of IgG on both gold and PNIPAAm surfaces. Our results indicated the similar amount of IgG adsorption on PNIPAAm surfaces at both 15°C and 40°C. The adherent protein layer on swollen PNIPAAm surface was observed to be soft as opposed to a rigid layer formation on the collapsed PNIPAAm surface. The IgG adsorption on gold surface displayed a behavior independent of temperature. Our analysis revealed a multilayer formation on the gold surface and collapsed PNIPAAm surface.

Chapter 5 considers how we can quickly quantify the adhesion of IgG on PNIPAAm films as a function of film thickness, cross-link density in correlation with volume phase transition of PNIPAAm. In order to achieve this, a mechanical technique, hydrodynamic shear flow essay in spinning disk configuration, was applied for the first time. IgG molecules were immobilized on carboxyl group functionalized PS microspheres and their adhesion on PNIPAAm surfaces was determined through

hydrodynamic detachment shear stresses. Our results indicated a significant difference between the IgG adsorption and PS microsphere adsorption on PNIPAAm surfaces. The adsorption of hydrophilic carboxylated PS microspheres was observed to be higher on the hydrophilic PNIPAAm surfaces by factor of two whereas this trend was reversed but not significantly different for IgG adsorption. This finding shows an agreement with our results from QCM-D. In addition, adhesion was observed to change linearly with microsphere adsorption time on PNIPAAm surfaces.

In Chapter 6, the binding affinity of peptide conjugated PNIPAAm networks was investigated towards heavy metal ions including Cu^{2+}, Ni^{2+}, Zn^{2+}, and Na^{+}. QCM-D results provided the ion induced change in the critical temperature of PNIPAAm networks. Through determination of salting out constants for each ion, two distinct regions were found at low and high ionic strengths. In the low ionic strength regime, the salting out constants followed the known trend for binding of the ions to Gly-Gly-His, which is $Cu^{2+} > Ni^{2+} > Zn^{2+} \sim Na^{+}$. In the high ionic strength region, the salting out constants were similar to the salting out constants associated with pure poly(NIPAAm).

Finally Chapter 7 presents an overall conclusion and suggestions for relevant future studies.

:

CHAPTER 2 : PROTEIN ADSORPTION

2.1 General Overview

Proteins are crucial components of living organisms because they play a major role in nearly every activity of cells. Interactions of molecules such as proteins with surfaces have tremendous importance throughout nature. Even the formation of the earliest living organisms might have originated from the structured congregation of molecules at mineral surfaces.

When proteins in a solution transport to a surface through diffusion, thermal convection, bulk flow or combination of all, they accumulate on the surface without penetrating. The formation of an adsorbed layer follows the attachment of proteins to the surface via hydrophobic and electrostatic interactions and spreading in a surface area through conformational changes.[4, 36] The process is known as protein adsorption. The simplicity of the definition is deceptive in regards to the complexity of the mechanism, which is yet not well understood. There have been number of comprehensive review articles and proceedings that document the fundamentals of the phenomenon, biocompatibility hypothesis and correlations, methods to study protein adsorption, and influence of the surface chemistry and protein properties.[37-44] However, the questions still remain regarding why and how proteins adsorb and which general rules protein adsorption mechanism follows.

When proteins come to a contact with a surface, they can interact with the surface in three possible ways depending on the water content at the interface as shown in figure 2.1. They might not adsorb to the surface or they might adsorb without undergoing any conformational change or they might change their conformation in order to minimize their energy and attain most stable state. Hydration of the surface determines how protein will interact with that surface.

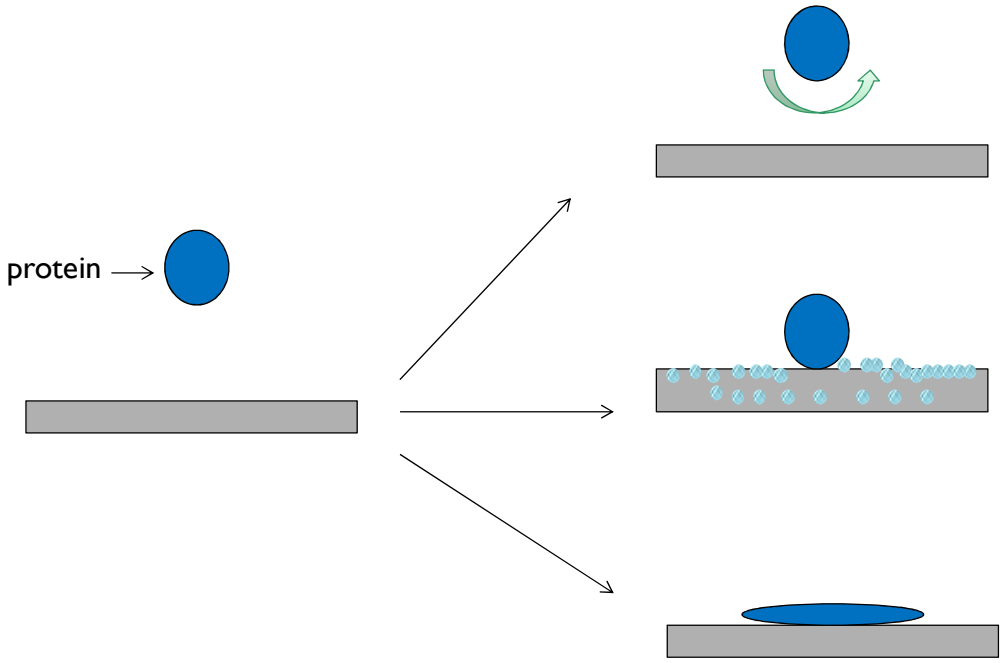

Figure 2.1 Interactions of proteins at solid-liquid interface depending on hydration of the surface

2.2 Significance and Challenges in Studying Protein Adsorption

Protein interactions with surfaces play a fundamental role in many vital biological and industrial processes. Cell adhesion, which is a primary process of embryogenesis and regulation of metabolism such as immune system response[45] and repair of damaged tissue[46], is essentially conducted by the attachment/detachment of proteins at the interfaces. Integrin containing junctions of the cells bind to the pre-adsorbed protein

interlayer on the extracellular matrix.[47] Hence, the attachment and detachment of cells are mediated by the behavior of the adsorbed proteins at the interface through varying the number and the activity of integrins. Garcia and his group have reported that the adsorption of a recombinant fragment of fibronectin ($FNIII_{7-10}$) on self-assembled monolayers of alkanethiols with different chemistries modified the structure of protein and modulated the $\alpha_5\beta_1$ integrin binding, cell adhesion, spreading and migration.[48]

Understanding the mechanism of protein adsorption is a key point to address numerous issues of biomedical and industrial applications such as bioseperation[30, 49], tissue engineering[46, 50], implant technology[51, 52], biosensors[53], microfluidic devices[30, 54-56] and drug delivery systems.[57, 58] Though, specific adsorption of cell matrix proteins are required for cell adhesion and proliferation, aberrant adsorption of proteins induces biofouling which causes various clinical disorders as well as problems in marine science. The main objective of the research in this area has been to gain the ability of quantitative prediction of how a given protein in a solution with specified properties behaves upon adsorption to a particular surface. Theoretical models on quantitative prediction of the adsorbed amount suffer from number of specific difficulties, such as the sheer complexity of the process which has not been captured by any current analytical model. Most models approach the protein as a rigid sphere with uniform charge whereas these simplifications are, in reality, not validated. Additionally, none of the models consider the influence of fluid flow and numerous interactions on the adsorption process. Another difficulty arises from the fact that the adsorption process is highly sensitive to the initial conditions such as pH, temperature and ionic strength. Minute

variations can change the amount of adsorbed protein on a large scale; it is therefore rather challenging to obtain reliable data with regards to reproducibility.

2.3 Factors that Dictate Protein Adsorption

Adsorption of proteins on a surface is driven by intermolecular and intramolecular forces including van der Waals interactions, electrostatic interactions, hydrogen bonding and hydrophobic interactions. Electrostatic interactions depend on the surface charge and protein charge which are the functions of pH and ionic content of the solution. Hydrophobic hydration results from bonding of the protein's hydrophobic residues to the hydrophobic regions on the adsorbent. Dehydration of the adsorbent surface and the structural rearrangements inside the protein molecule give rise to increase in entropy of the total system.

2.3.1 Protein Structure and Size

Proteins spontaneously fold into three-dimensional structure of native form from their primary structure in order to perform their specific functions. Fibrillar proteins have a regular structure (e.g., helices and pleated sheets, or secondary structure) and are usually insoluble in water and found in connective tissue. On the other hand, globular proteins having different structural elements such as helices, pleated sheets and parts that are unordered are folded up to a compact, densely packed structure (tertiary structure).[59] Although the adsorption of the globular proteins is most relevant with respect to practical applications and implications such as biomedical engineering, their intricate and highly specific structures have not yet endowed a development of a general theory of their adsorption behavior.

Another influence on the adsorption process is protein size. According to thermodynamics larger protein molecules are capable of contacting more sites of the surface resulting in greater interactions and stronger adsorption. Huber and his group have reported the competitive adsorption of myoglobin-Bovine Serum Albumin (BSA), Hemoglobin-BSA, and cytochrome C-BSA mixtures on PNIPAAm brush films at 50°C.[30] For solutions containing myoglobin (M_w=16 kDa) - BSA ((M_w=65 kDa), they initially observed immediate adsorption of smaller myoglobin to the surface. However, larger BSA removed myoglobin and formed a relatively pure monolayer. The same effect was monitored for cytochrome C-BSA mixture and hemoglobin-BSA mixture. This showed in consistence with literature that the adsorption is initially dictated by kinetics which indicates the inverse proportion between diffusion of a protein and the hydrodynamic radius. However, the final adsorption is concluded by the thermodynamics (larger the molecule larger the contact area to interact).

2.3.2 Protein Charge

Proteins contain charged, polar, nonpolar, hydrophobic, hydrophilic region. Generally, hydrophilic polar and charged amino acids are positioned on the exterior of protein and hydrophobic residues are on the interior. However, hydrophobic amino acids might exist on the protein exterior and interact with the surface of a substrate. Proteins are observed to exhibit higher surface activity close to their isoelectric point (IP) which is the pH level where they do not possess a net electrical charge.[60] At this point electrostatic repulsion between uncharged adsorbing molecules is reduced allowing more protein to bind to the surface. In addition, protein adsorption is affected by properties related to unfolding rate of a protein. Less stable proteins such as those

with low intramolecular cross-linking will have high unfolding rate that can allow protein to make contact with the surface more rapidly.

2.4 Monolayer Adsorption: Langmuir Isotherms

Proteins are biological polymers that are formed by covalent binding of amino acids into a linear chain which is known as their primary structure. Their adsorption behavior shares some features with those highly solvated and flexible synthetic polymers with a disordered coiled structure. Some proteins with nutritional functioning such as caseins and glutelins fall under this category. These polymers possess high conformational entropy due to various states that each of many segments in the chain can adopt. This conformational entropy decreases upon adsorption. Consequently, the adsorption takes place only if the loss in conformational entropy is compensated by sufficient attraction between the polymer segments and the surface. The resulting high affinity between the polymer and the surface leads to adsorption isotherm where the adsorbed amount, $\boldsymbol{\Gamma}$, is plotted against the polymer concentration in solution after adsorption. If the solution is sufficiently dilute, the adsorption isotherm can be determined according to the classical Langmuir theory[61, 62] at which surface coverage of a monolayer is determined by the following equation:

$$\Gamma = \Gamma_{max} \frac{K\,C}{1 + K\,C} \tag{2.1}$$

where K is the Langmuir equilibrium constant, C is the aqueous concentration and $\boldsymbol{\Gamma}_{\max}$ is the maximum amount adsorbed as the concentration is increased. The application of

Langmuir adsorption isotherm theory to adsorption of proteins is restricted by the following assumptions:

- Monolayer assumption that stipulates only one single molecule adsorption per site
- Homogenous surface that stipulates only one type of site
- No sideway interactions or cooperativity between the adsorbed molecules
- No other adsorbing species (no competitive adsorption)
- Dilute solution and reversible adsorption

CHAPTER 3 : EXPERIMENTAL METHODS

3.1 Synthesis of Poly(NIPAAm-co-MaBP) Hydrogel

NIPAAm is copolymerized with 3% photo cross-linking monomer, methacroyloxybenzaphenone (MaBP), through free radical reaction using 0.1 % azobisisobutyronitrile (AIBN) as the initiator (scheme 3.1). The solvent used for the polymerization was dioxane and was purified through distillation prior to the reaction. The certain amount of reactants was mixed in a Schlenk tube and the mixture was degassed under nitrogen by repetitive freezing and thawing. After several freeze-thaw cycles, the mixture was placed in water bath at 72°C for 18 hours and subsequently was precipitated in diethyl ether. The resultant product was then dried under vacuum to obtain the final product in the white powder form. The final product was characterized through proton (^{1}H) NMR.

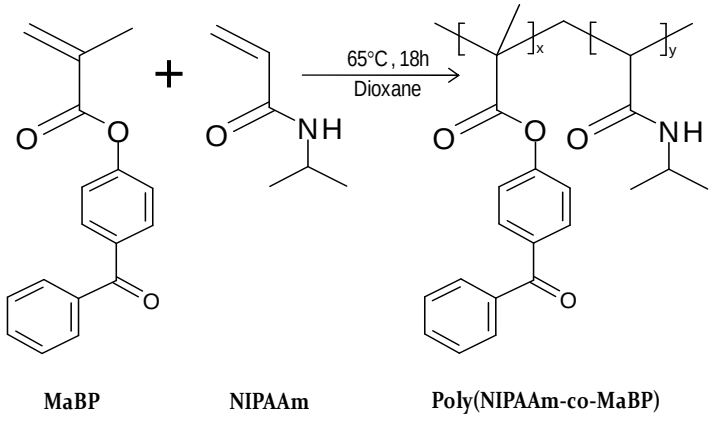

Figure 3.1 Chemical reaction scheme of poly(NIPAAm-co-MaBP) synthesis with x mol % MaBP.

The synthesis of photo cross-linking monomer MaBP can be found in a study by Vidyasagar and Toomey.[63] It involves the reaction of 4-hydroxybenzophenone and methacroyl chloride and an acid scavenger, triethylamine (TEA), in the ratio of 1:1:2 in dry acetone at 0°C.

The use of benzophenone (BP) moieties grants several advantages such as chemical stability and reactivity with C-H bonds even in the presence of water and bulk nucleophiles. They can be manipulated in the ambient light and can also be triggered at the wavelength range (350-360nm) which is the range that does not damage protein and polymer structure. Even first photo-cross linking polymers studied include copolymers with benzophenone (BP) moieties.[64, 65]

3.1.1 Characterization of Poly(NIPAAm-co-MaBP)

The confirmation of the poly(NIPAAm-co-MaBP [3%]) was done through proton NMR using Agilent direct drive 500MHz (dd500) spectrometer. The adequate amount of copolymer was dissolved in deuterated chloroform ($CdCl_3$) and the spectrum was obtained using tetramethylsilane as internal standard. The multiplet peaks between 7.2-8.0 ppm correspond to the 9H from the aromatic groups of MaBP. The singlet peaks at 4.0 ppm and 1.0 ppm correspond to the NH and CH_3 groups of the NIPAAm, respectively.

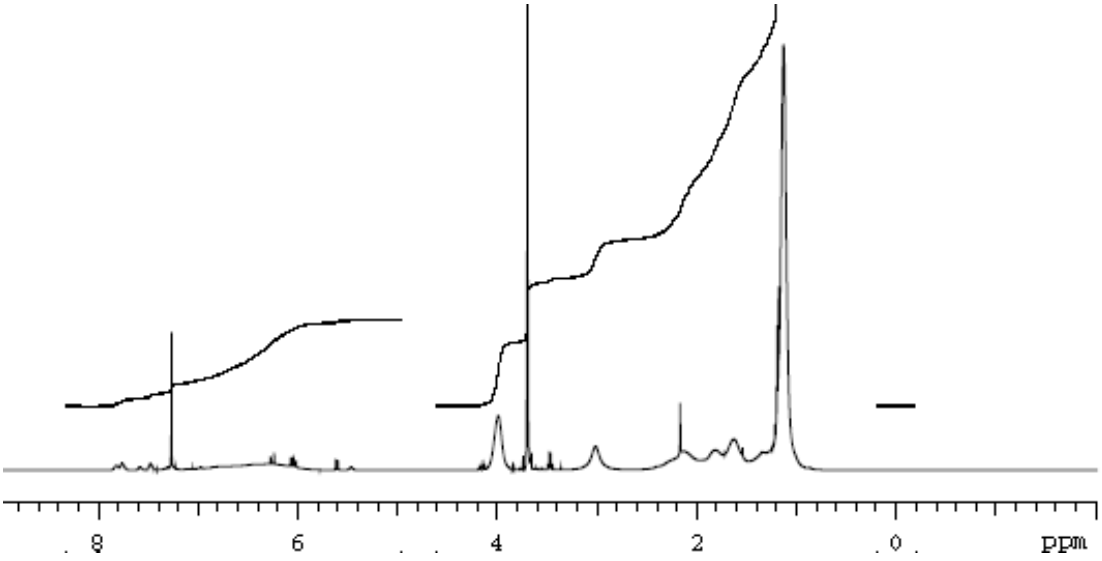

Figure 3.2 ^{1}H NMR spectrum of poly(NIPAAm-co-MaBP[3%]) in $CdCl_3$

3.2 Surface Attached Hydrogel Fabrication

The surface fabrication of thermoresponsive polymers is carried out with a photochemical technique, supporting wide array of functionalities.[66] By using surface-anchored benzophenone linkers, thin polymer layers with dry thicknesses of a few nanometers can be immobilized to various solid substrates in a simple way. Moreover, cross-link density and thickness can be independently controlled through this approach.[6] Thickness can be controlled by simply varying the concentration (w/v %) of the copolymer solution while cross-link density can be controlled during the synthesis by adjusting the ratio of the monomers or by blending the poly(NIPAAm-co-MaBP) copolymer with PNIPAAm homopolymer. Surface attached uniform poly(NIPAAm-co-MaBP) films are prepared by spin casting the copolymer dissolved in cyclohexanone on a 1% (3-aminopropyltrimethoxysilane) (APTES) treated substrate (LaSFN9 prism for ellipsometric measurements, quartz crystal resonator with gold electrodes for QCM-D experiments and glass circular cover slips for spinning disk experiments) followed by

ultraviolet (UV) irradiation of 365 nm for half hour to obtain cross-linked network. UV illumination activates a n,p* transition in the carbonyl group of benzophenone, which then covalently cross-links to a neighboring C-H group resulting in a stable C-C bond.

The same procedure is applied to circular glass cover slips for spinning disk and contact angle experiments. Prior to the thin film fabrication, circular glass cover slips were immersed in ethanol and placed in sonication bath for twenty minutes followed by plasma cleaning for five to fifteen minutes. After the APTES treatment, the cover slips were baked for 15 min at 120°C in order to evaporate the solvent and the polymer solution was subsequently spin-casted on the cover slips. The cross-linked networks were achieved by half-hour UV illumination (λ= 365 nm).

3.3 Synthesis of Poly(NIPAAm-co-3-APMA) and Poly(NIPAAm) Hydrogels

NIPAAm monomer (4 grams) was copolymerized with 3.5 mole percent (mol%) 3-APMA in 20 ml of DMF using 0.4 mol% AIBN as an initiator and 2 mol% MBAm as a cross-linker. The mixture was agitated by nitrogen for approximately 15 minutes in order to remove any residual oxygen. The reactants were then transferred to small test tubes in 1.25 ml aliquots and polymerized overnight in a constant temperature water bath at 70°C. The chemical synthesis is illustrated in figure 3.3. Poly(NIPAAm) hydrogel was synthesized in the same fashion except for the addition of 3-APMA.

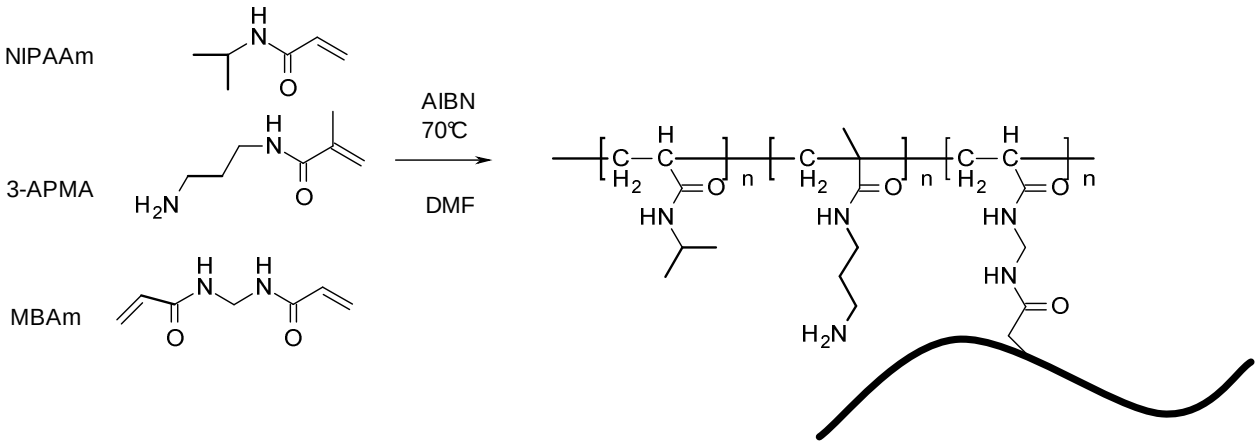

Figure 3.3 Chemical scheme of the poly(NIPAAm-co-3-APMA) synthesis.

The composition of the poly(NIPAAm-co-3-APMA) gel was confirmed by ^{1}H NMR spectroscopy. Adequate amount of gel pieces were washed repeatedly in Milli-Q water for a week and were then dried at 120℃ in order to remove the solvent residuals from the gel. They were then submerged in deuterated dimethylsulfoxide ($(CD_3)_2SO$) and the solution was sonicated for three days. For characterization, the ^{1}H NMR spectrum was recorded on an Agilent direct drive 500MHz (dd500) spectrometer using $(CD_3)_2SO$ as solvent and tetramethylsilane as internal standard. The amount of 3-APMA content was determined to be 3.5% via integration of the selected peaks at δ/ppm = 1 (s, $-CH_3$, NIPAAm) and 2.9 (m, $-CH_2$, 3-APMA).

3.4 Gly-Gly-His Conjugation to Poly(NIPAAm-co-3-APMA) Hydrogel

Amino acid conjugation to the copolymer gel was achieved by a modified Merrifield solid phase peptide synthesis (SPSS) method.[67] In this study, amino acids with a base-labile 9-Fluorenylmethoxycarbonyl (Fmoc) α-amino protecting group and an acid-labile trityl (Trt) side chain protecting group were covalently attached to the hydrogel through the amino moiety.[68] The mechanism is delineated in figure 3.4.

Prior to the first amino acid conjugation, the poly(NIPAAm-co-3-APMA) gels were cut into approximately 2 mm cubes to render facile diffusion of the reagents. The hydrogel cubes were then placed into Schlenk tubes and swelled in DMF overnight. They were subsequently transferred into a peptide reaction vessel and washed with DMF several times under nitrogen purge to remove any unreacted monomer. In a molar ratio of 2:2:1, a mixture of 2 ml of TBTU (120mg/ml in DMF), 2 ml of fmoc-Gly-OH (111.5mg/ml in DMF), and 130.6 µl of DIPEA was introduced to the reaction vessel and allowed to react for 2 hours under constant nitrogen. It is essential to note that the molar amount of amino acid and the conjugation reagents were at least three times or more of the molar amount of the 3-APMA used in the copolymerization process. The mixture was then drained and the gel cubes were washed with DMF and isopropanol for 6 to 8 hours through frequently alternating the solvents. Next, the fmoc protection group was removed by adding 20 ml of DMF with 20% piperidine into the peptide vessel under nitrogen purge for 20 min to 1 hour. The fmoc protection/deprotection procedures were repeated to conjugate the second amino acid, fmoc-Gly-OH, and the third amino acid, fmoc-His(Trt)-OH, to the gel. At each stage in the process, the Kaiser test was performed to ascertain the presence of free amines. The Kaiser test is a fast and sensitive color test that is capable of detecting as little as 5 µmole/g free terminal amino group.[69] The method indicates the reducing amount of free terminal amino groups through decreasing color intensities and enables one to detect incomplete couplings that are not detectable by amino acid analysis. Finally, the trityl side chain protecting group of histidine was cleaved by addition of 20 ml of deionized water with 5% TFA. The Gly-Gly-His conjugated gel was agitated with nitrogen for 5 minutes and then

immediately washed with Milli-Q water several times. The gel conjugate was then transferred to another container and stored in Milli-Q water with frequent water exchanges for 7 days to ensure complete removal of all reagents.

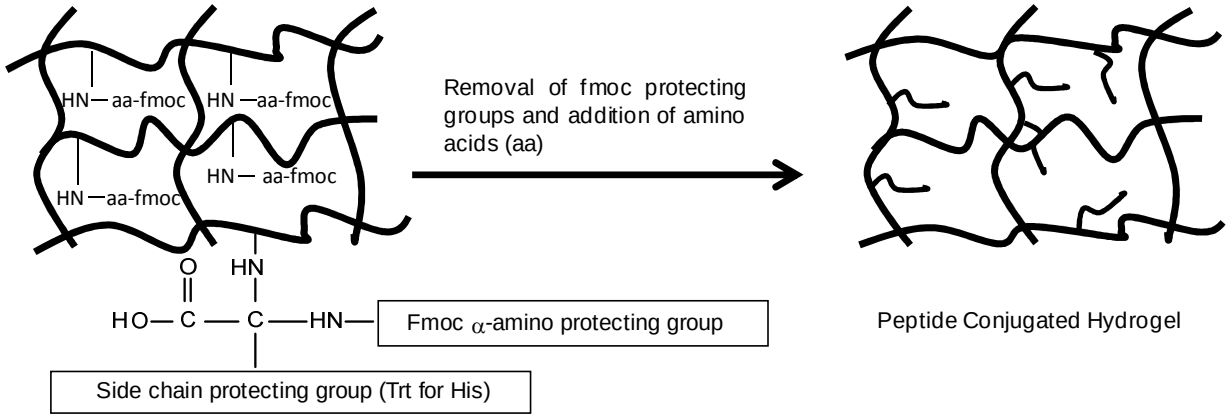

Figure 3.4 Schematic representation of the fmoc based solid phase synthesis of amino acids to poly(NIPAAm-co-3-APMA) gel.

3.5 Characterization Techniques

3.5.1 Variable Angle Ellipsometry with Polarizer-Rotating Compensator-Sample-Analyzer (PCSA) Configuration

One of the instruments used in this research is a home-built variable angle rotating compensator ellipsometer with a Polarizer-Compensator-Sample-Analyzer (PCSA) configuration as shown in figure 3.5. In this configuration, the incident polarization is modulated by a rotating compensator and the signal at the detector is Fourier analyzed. The ellipsometric parameters (Ψ and Δ) are determined by the amplitudes pertaining to second and fourth harmonics of the fundamental frequency compensator. Rotating compensator configuration can enable users to determine ellipsomeric Ψ and Δ values over the complete measurement range (Ψ=0-90° and Δ=0-

360°). Offsets and miscalibrations can be compensated by averaging over multizone measurements (the polarizer and the analyzer can be set at +/- 45° giving four measurements). Optical parameters of the sample can be calculated using an iteration method using empirical and theoretical Ψ and Δ values.

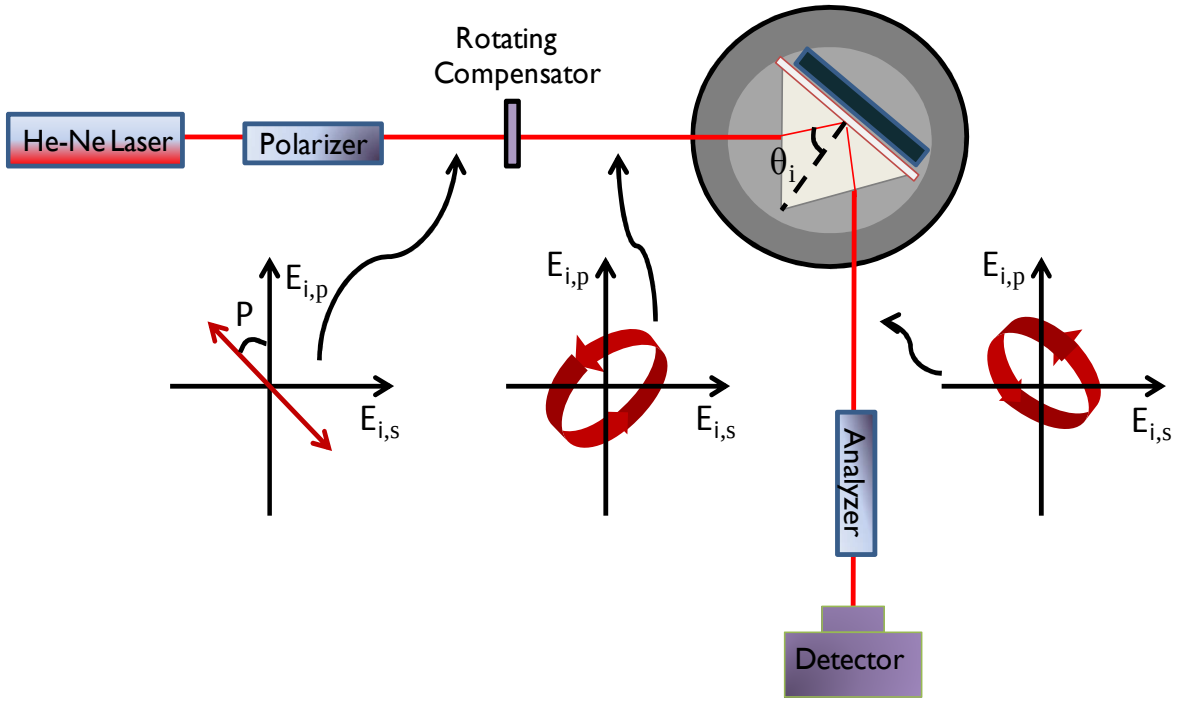

Figure 3.5 Schematic diagram of the home-built variable angle rotating compensator ellipsometer with PCSA configuration

3.5.1.1 Principles of Ellipsometry

Ellipsometry is a non-invasive, thereby highly accessible technique that is based on changes in polarized state of a monochromatic light due to interaction of the electric field component (E) of the electromagnetic wave with a surface. The method measures the change in the polarization ellipse of reflected light as a result of variations of refractive index in the interfacial zone. Figure 3.6 illustrates the elliptical state of polarization. Change in the polarization ellipse is characteristic of the surface structure

of the sample and thereby, can grant significant structural and chemical information. The method is widely used to characterize the state of responsive layers in both the collapsed and swollen states as well as adsorbed species to the interfacial layer.

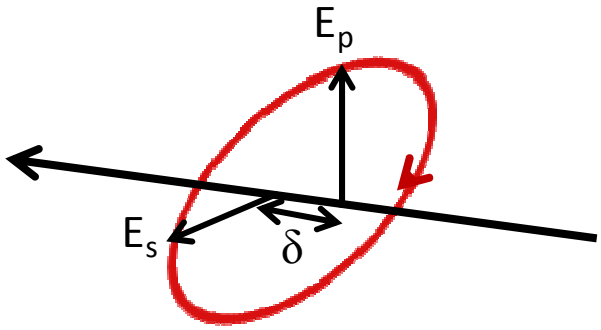

Figure 3.6 Diagram of the elliptical polarization

Electric field vector of an electromagnetic light possesses two orthogonal vector components that are parallel (E_p) and perpendicular (E_s) to the plane of incidence. Complex Fresnel coefficients of reflection can be determined from E_p and E_s for p- and s- polarized light as follows:

$$R_p = \frac{E_p^{reflected}}{E_p^{incident}} = |R_p|e^{i\delta_{rp}} \tag{3.1}$$

$$R_s = \frac{E_s^{reflected}}{E_s^{incident}} = |R_s|e^{i\delta_{rs}} \tag{3.2}$$

where δ_{rp} and δ_{rs} are the phase shift of the p- and s- polarized reflected light, respectively. Phase factors denote the phase difference before and after reflection of each component. The ratio between reflection coefficients is defined as the complex reflectance ratio (ρ) of the elliptically polarized light and is parameterized by two ellipsometric angles (Ψ, Δ):

$$\rho = \frac{R_p}{R_s} = \frac{|R_p|}{|R_s|} e^{i(\delta_{rp} - \delta_{rs})} = \tan \Psi e^{-i\Delta} \quad (3.3)$$

where Δ is the difference between the differential phase change of the parallel and the perpendicular component of the reflected light and Ψ is the amplitude ratio of the parallel and perpendicular reflection coefficients.

The thickness and refractive index are obtained by a layer model which uses an iteration procedure (least-squares minimization) that varies the unknown thickness and optical parameters to obtain the best fit of the theoretical ψ and Δ values calculated from Fresnel equations[70] to those from the experiment. The calculated Ψ and Δ values which match the experimental data best provide the optical constants and thickness parameters of the sample. The values of Δ can vary from 0 to 360° and those of Ψ vary from 0 to 90°.

3.5.1.2 Experimental Protocol for the Polymer Film Characterization

1) The substrate (LaSFN9 glass prism) was first cleaned with optical wipes and subsequently placed in plasma cleaner for 10 min.
2) Prism surface was amine functionalized with deposition of 1% solution of APTES (3-aminopropyltriethoxysilane) solution in acetone. The NH_2-terminated prism was baked at 120°C for 15 min in order to fully evaporate the solvent.
3) The polymer solution prepared from cyclohexanone was spin casted on the APTES treated substrate at 2000 rpm for 45 sec.
4) The substrate was exposed to UV light (λ=350 nm) for half an hour in order to have cross-linked networks

5) Before placing the substrate, a straight line alignment was performed by bringing sample holder and the detector to 90° position. The positions of the detector and the sample holder were delicately adjusted until the laser beam went through the center of the detector. Then, psi and delta values were measured for two different zones, zone 1 and zone 2. The readings for psi and delta values at each zone should be in agreement with each other with a maximum 5° discrepancy.
6) The substrate was vacuum sealed against the solution cell whose other side was sealed against the sample holder.
7) Then the sample holder position was brought to 45° and detector was rotated to be aligned with the sample. The readings of psi and delta at both zones were taken and verified to be in agreement between each zones.
8) Finally, the sample holder position was brought to 0° and the laser beam was checked to make sure that it hits the center of the substrate.
9) After verifying the alignment at 0°, the sample holder position was brought back to 45°and the alignment was performed as described at step 7.
10) The values of Ψ and Δ were measured for the dry film by scanning for the angle of incidence range from 20° to 50°.
11) After taking the dry film reading, the solvent (Deionized water, PBS buffer, protein solution, and metal ion salts in this dissertation) was injected to the solution cell and was allowed to remain in the cell for 15 minutes to 3 hrs for proper hydration of the polymer chains.
12) New values of Ψ and Δ were measured for the wet film by scanning for the angle of incidence range from 25° to 50°.

13) Finally, the optical parameters (thickness and refractive index) of the polymer film were calculated as described at section 3.2.2.

3.5.2 Quartz Crystal Microbalance with Dissipation (QCM-D)

The operation principle of QCM-D relies on the piezo electric effect which arises from the oscillation of the quartz resonator through application of an AC voltage. Alternating current between the electrodes of the AT-cut quartz crystal resonator generates a standing shear wave resulted in a mechanical deformation of the quartz crystal (figure 3.7). The oscillation frequency of the quartz resonator is perturbed by the mass accumulation or removal. The mass deposition induced disturbance in the resonance frequency (∆f) and the dissipation factor (D) are measured with resonance frequency as a function of time. Change in oscillation frequency is proportional to adsorbed mass (∆m), and dissipation is proportional to the structural changes of the adsorbed film such as stiffness. The relation of frequency change of the oscillating crystal to the mass adsorbed was established by Voinova and co-authors[71] for viscoelastic films and modified form was given by Patra and Toomey[72] as follows:

$$\Delta f = -\frac{h\rho\omega}{2\pi\rho_0 h_0}\left[1-\frac{\eta_s}{\eta}\left(\frac{(\tau_r\omega)^2}{1+(\tau_r\omega)^2}\right)\right]+\Delta f_s \tag{3.4}$$

$$\Delta D = -\frac{h\rho}{\rho_0 h_0}\left[\frac{\eta_s}{\eta}\left(\frac{(\tau_r\omega)}{1+(\tau_r\omega)^2}\right)\right]+\Delta D_s \tag{3.5}$$

where ρ_o and h_o are the density and thickness of the quartz resonator, respectively. The parameters of η and η_s represent the viscosity of the adsorbed layer and the solvent, respectively. The $\tau_r\omega$ is the ratio of the loss modulus to the storage modulus, also

known as tanδ. The Δf_s and ΔD_s are the changes in the resonant frequency and dissipation of the uncoated quartz oscillator in contact with the bulk solvent, respectively.

For rigid films ($\tau_r\omega \rightarrow 0$), frequency change is linear to the film thickness whereas the dissipation change is not affected by the film thickness, which indicates an oscillation without a loss. Hence, the equation 3.4 reduces to well-known Sauerbrey relation.[73-75]

$$\Delta f_{Sauerbrey} = -C_m \Delta m \tag{3.6}$$

where C_m is the mass sensitivity constant and it is equal to 56.6 Hz cm^2 μg^{-1} for a 5 MHz quartz crystal in air at room temperature.[73]

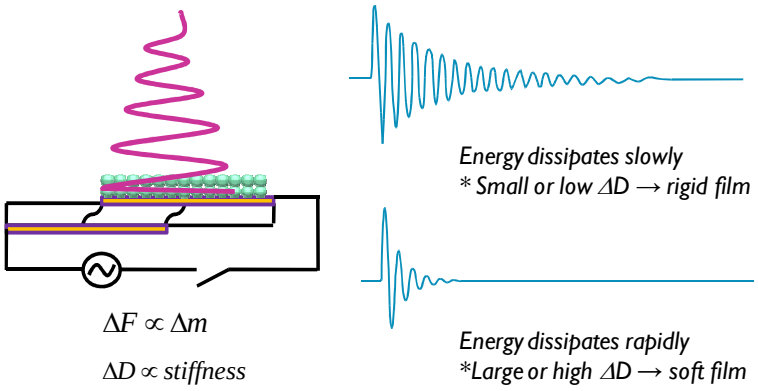

Figure 3.7 Principle of quartz crystal microbalance with dissipation

3.5.3 Spinning Disk

The principle of the technique relies on the measurement of the detachment stresses of the adhered substances from the adherent surface through hydrodynamic shear force generated by the fluid flow. The configuration of the spinning disk has been extensively studied[76, 77] and is shown in figure 3.8. Garcia and colleagues have

developed and authenticated a spinning disk device for osteobast-like cell adhesion on fibronectin adsorbed bioactive and nonreactive glasses.[78]

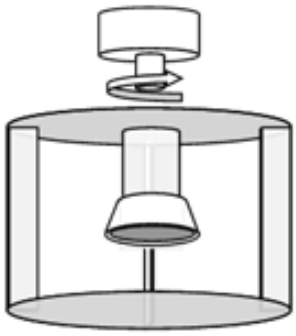

Figure 3.8 Spinning disk configuration

In the disk configuration, the sample substrate is sealed on a disk that is mounted on a rotating shaft and submerged in the cylinder filled with fluid. As the disk rotates, the fluid is drawn in axially from the surroundings and is forced to exit radially by the centrifugal force. For steady laminar flow, the resultant shear stress at the surface has a linear dependence on the radial distance from zero at the center as shown in figure 3.9 and it is given by equation 3.6

$$\tau = 0.800\, r \sqrt{(\rho\, \mu\, \omega^3)} \tag{3.6}$$

where *r* is the radial distance from the center of the disk (spinning axis), ρ is the fluid density, μ is the fluid viscosity, and ω is the rotational speed. Substances that remained adhered on the substrate surface after spinning are counted at specific radial positions with an automated stage and image analysis software and then normalized to the adsorbate count at the center of the surface where shear stress is negligible. Thereby, the experimental adherent fraction (f) of the adsorbate is obtained and the detachment profile (f versus τ) is fit to a sigmoid curve whose equation is as follows:

$$f = \frac{f_0}{1 + \exp\left[b\ (\tau - \tau_{50})\right]} \tag{3.7}$$

where f and τ are the experimental adherent fraction and shear stress at the disk and f_0, b, and τ_{50} are the fitted zero stress adherent fraction, decay slope and infection point, respectively. Inflection point, $\tau_{50,}$ stands for the shear stress to detach 50% of the molecules and is a measure of adhesion strength of the average population of adherent substances.

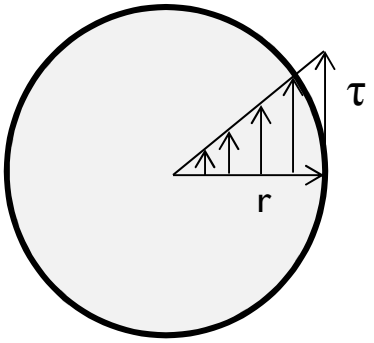

Figure 3.9 Resultant shear stresses at the surface by the hydrodynamic shear flow

CHAPTER 4 : IMMUNOGLOBULIN G (IGG) ADSORPTION ON GOLD AND SURFACE ATTACHED POLY(N-ISOPROPYLACRYLAMIDE) (PNIPAAM) FILMS

4.1 Introduction

Protein adsorption onto polymeric surfaces has been extensively studied over the past 20 years majorly due to its central role in cell adhesion which can determine the host response to a medical implant, formation of tissue or delivery of drugs to the target organ. It is, therefore, critical to gain control over the interactions of proteins with underlying surfaces. Number of efforts has been given to modulate the adsorption of proteins in desired way and switchable polymeric coatings have been one of the most promising methods to tune the adsorption behavior of proteins. These materials have both adsorbent and adsorption resistant properties that can be switched between an interactive protein adsorbing state and a non-interactive protein repelling state via an external stimulus such as temperature. A pioneering study by Hoffman in 1987 has attracted great interest for biomedical applications of thermally switchable hydrogels.[79] One of the most investigated stimuli responsive material is PNIPAAm with a hydrophilic to hydrophobic state transition temperature (LCST) of around 32°C. This is close to biological temperature of 37°C, thereby, it makes it very attractive for biomedical research and applications. Silva and co-workers characterized the non-specific adsorption of human immunoglobulin g (h-IgG) on to PNIPAAm based microgel and core-shell particles that can be used as hetero-bifunctional ligand careers for affinity

precipitation.[80] They observed significant influence of temperature on IgG adsorption to PNIPAAm microgel particles at pH 9 whereas temperature did not affect the IgG adsorption at pH 5. Their findings for adsorption onto charged core-shell particles did not reveal the influence of temperature on the IgG adsorption at both pH values. Studies with the conducting probe atomic force microscopy (CP-AFM) reported that adsorption of proteins to hydrophilic PNIPAAm surface is generally energetically unfavorable.[16, 33] On the other hand, some fouling below the LCST might occur if the residence time is sufficiently long enough for the initially loosely adsorbed proteins. Cheng Et al. reported a study of protein adsorption onto plasma polymerized PNIPAAm surfaces.[35] They observed low-fouling on the hydrated surfaces for three different proteins with the surface coverage less than 25 ng/cm^2 whereas surface coverage on collapsed PNIPAAm surfaces was greater than100 ng/cm^2. They also observed an irreversible adsorption of human fibrinogen and polyclonal anti-horse ferritin antibody on these coatings while they observed a partially reversible adsorption of bovine serum albumin (BSA). Huber Et al. reported a microfluidic device based on the ultra-thin (4nm) thermally switchable PNIPAAm coating that is capable of controlled uptake and release of proteins from solution.[10]

Although the use of switchable polymeric coatings has shown great potential to tune the adsorption behavior of proteins the adsorption mechanism is, however, still not fully understood. The intricacy of the adsorption mechanism is great because proteins can adopt different confirmations that directly affect protein functioning. Moreover, proteins cannot be treated as small solutes because of their large size, and the polymer surface is not flat such that it makes quantification very challenging. Entropic and

energetic approaches of adsorption can suggest the adsorption kinetics but cannot explain the increase in the absorbed amount due to the conformational change on the surfaces. In addition, the degree of conformational change is thought to be dependent on the strength, which is not yet known. Therefore, reliable measurement techniques that can produce rich and accurate information are necessary in order to elucidate the protein adsorption mechanism.

In this study, the adsorption of IgG onto gold and thermoresponsive cross-linked PNIPAAm coatings was investigated via a sensitive acoustic technique, quartz microbalance with dissipation (QCM-D) to establish the fundamental relationships between volume transition behavior in responsive thin films and adsorption phenomena.

4.2 Experimental Section

For QCM-D measurements, poly (NIPAAm-co-MaBP) was spin coated onto AT cut gold piezo electric crystal which was then induced to oscillate at its fundamental frequency (5Hz) and odd harmonics (n = 3, 5, 7, 9, 11, 13) via an alternating current applied between the electrodes. Solutions of IgG at 1-500 µg/ml were prepared from phosphate buffer silane (PBS) of pH 7.4. Each solution was allowed to flow through the bare and PNIPAAm coated sensor crystal at the rate of 0.1ml/min. The change in the resonance frequency (Δf) and the energy dissipation (ΔD) due to mass accumulation on the piezo electric sensor were recorded as a function of time at 15 and 40°C. The amount of adsorbed IgG (Γ) on gold sensor and collapsed PNIPAAm surfaces was obtained from an iteration method that searches for parameters (P_1, P_2, and P_3) and) that provide the best fit for equation 3.4. The equation 3.4 can be written as follows:

$$\frac{\Delta F}{n} = -P_1[1 - P_2\left(\frac{P_3^2 n^2}{1 + P_3^2 n^2}\right)] \quad (3.8)$$

where n is the harmonic value and P_1, P_2 and P_3 are given as

$$P_1 = \frac{\Gamma f_0}{\rho_0 h_0}, \quad P_2 = \frac{\eta_s}{\eta}, \quad P_3 = \tau_r \omega_0$$

4.2.1 QCM-D Characterization of IgG Adsorption on Gold Surface

Initially, the protein solution was adsorbed onto uncoated gold sensor surface in order to monitor the effect of temperature on the adsorption behavior of the protein. A solution of IgG at 0.5 mg/ml was flowed through the chamber that houses the gold sensor crystal. The change in frequency and dissipation is displayed in Figure 4.1. The frequency shift at both 15 °C and 40°C appeared to be the same (~ - 80 Hz) indicating that there is no influence of temperature on the amount of the proteins adsorbed to the gold surface. In the dissipation graph, we see an initial increase followed by stabilization to a plateau value of ~ 2.5×10^6 at both temperatures. This can be interpreted as the following: Adsorbed proteins initially, within a few minutes, form a softer layer on the gold surface. The continuing accumulation of protein molecules on the gold surface results in conformational changes that lead to a rigid film formation on the rigid gold surface. In order to be able to quantitatively explain this observation, we have obtained the adsorption kinetics of IgG at wide concentration range and analyzed for adsorbed amount and parameters of damping ($\tau_r \omega$ and η_s/η)

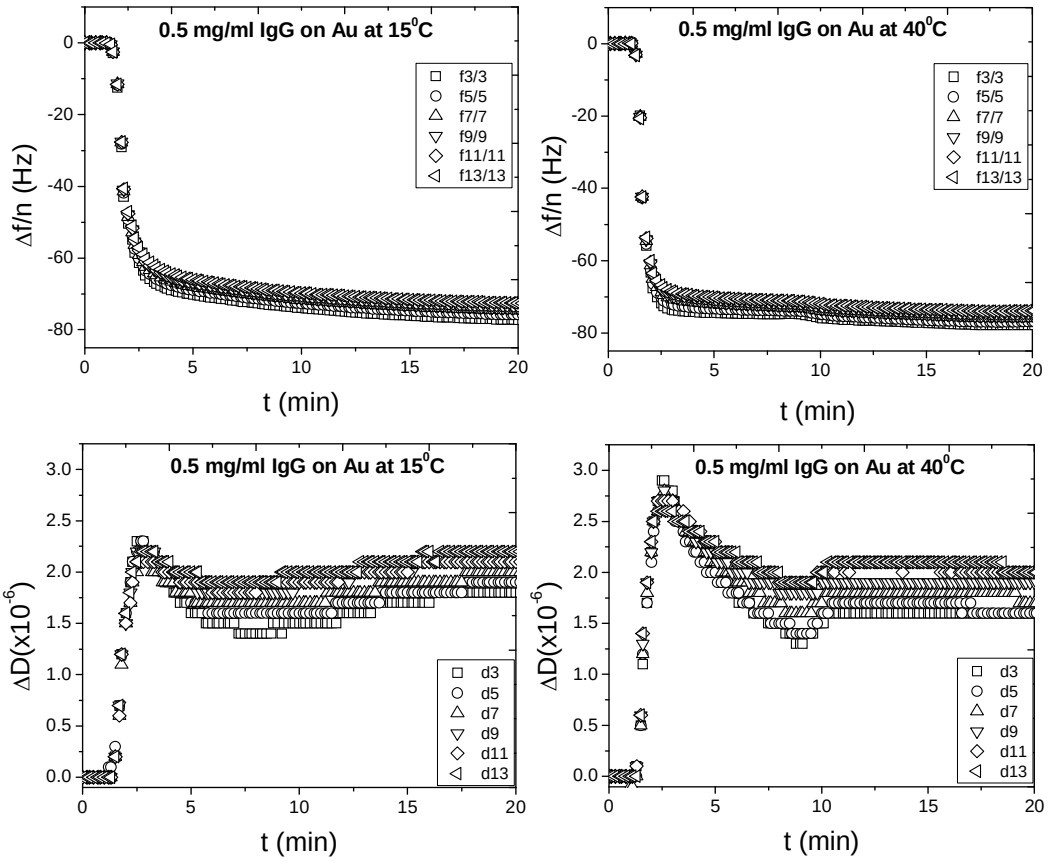

Figure 4.1 Frequency and dissipation change upon IgG adsorption on gold crystal surface at 15°C and 40°C.

The adsorption kinetics of IgG on gold surface and the adsorption isotherm were determined from frequency change measurements at 25°C and are shown in figure 4.2. The adsorption kinetic curve (figure 4.2a) shows that the adsorption rate is very fast in first 15 minutes, then; a well-defined plateau was reached within 30 min at higher IgG concentrations. It is also seen that higher surface coverage was obtained at higher IgG concentrations suggesting short residence time on the surface. Due to high concentration, protein molecules arrived at the surface might not have necessary time to relax and spread on the surface resulting in smaller average footprints. As a consequence more protein molecules will adsorb to the surface.

The adsorbed amount values for each IgG concentration were calculated from equation 3.4 for the rigid limit due to negligible variation in dissipation change. Although the adsorption isotherm (figure 4.3b) exhibits a Langmuir isotherm-like behavior the surface coverage value of 10.2 mg/m^2 at saturation is much higher than the theoretical surface coverage values for densely packed IgG monolayer which is 2mg/m^2 for flat-on orientation and 3.7 mg/m^2 for end-on orientation.[81] This suggests a multilayer formation on the surface since the IgG adsorption did not saturate at the monolayer level. A double layer formation upon IgG adsorption has been described by a few reports[82-84] and Zhou Et al. reported a supramonolayer formation with a surface coverage value of 6.09 mg/m^2 for the adsorption of IgG at a critical concentration of 0.46 mg/ml onto octadecanethiol (ODT) coated gold surface.[73]

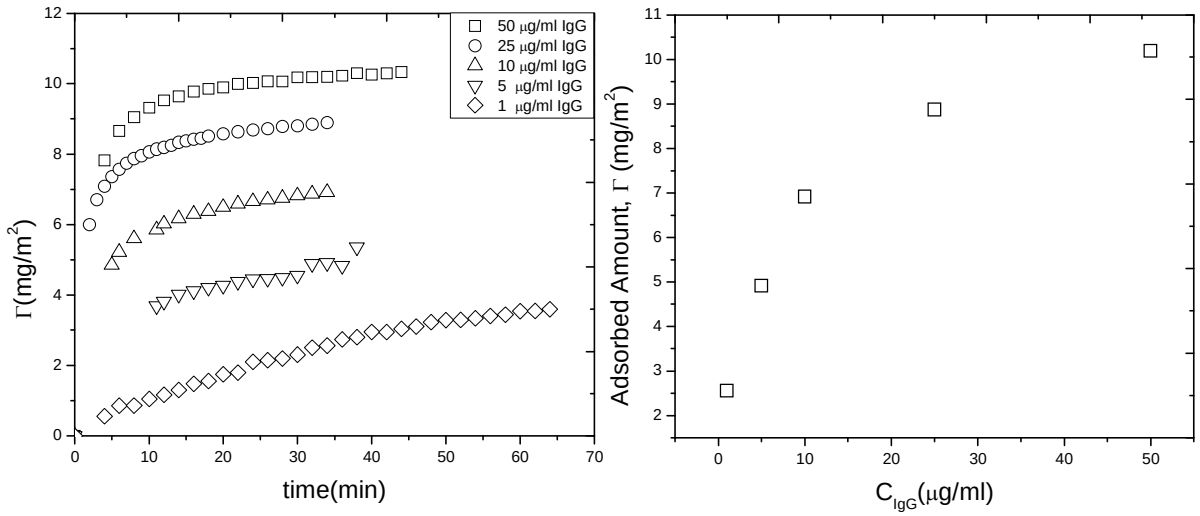

(a) (b)

Figure 4.2 a) Adsorption kinetics of IgG on gold sensor surface b) IgG adsorbed amount on gold surface with respect to concentration

Figures 4.3a and 4.3b provide information about the rigidity of the adsorbed layer. The ratio of the solvent viscosity to adsorbed protein layer viscosity shows no variation with respect to time for concentrations between 5-50 μg/ml indicating a very rigid film formation on the gold surface. For IgG bulk solution concentration of 1μg/ml, however, a softer film was initially observed. After 30 minutes of adsorption period, the ratio between solvent and protein viscosities overlaps with the rest of the data indicating a rigid behavior. Figure 4.3b shows the time dependent variations in the structure of the adsorbed protein layer, as well. The production of relaxation time and angular frequency ($\tau_r \omega$) is the ratio of loss modulus to storage modulus of the protein layer and also called tanδ. It is a measure of damping, in other words, energy dissipation in the protein film upon adsorption and it is equal to zero for a rigid material. Here, a similar behavior is also observed suggesting an instant rigid protein film formation on the gold surface between 5-50 μg/ml. For the concentration of 1μg/ml, a softer film was initially formed, then transformed to a rigid film after 30 min of adsorption time period.

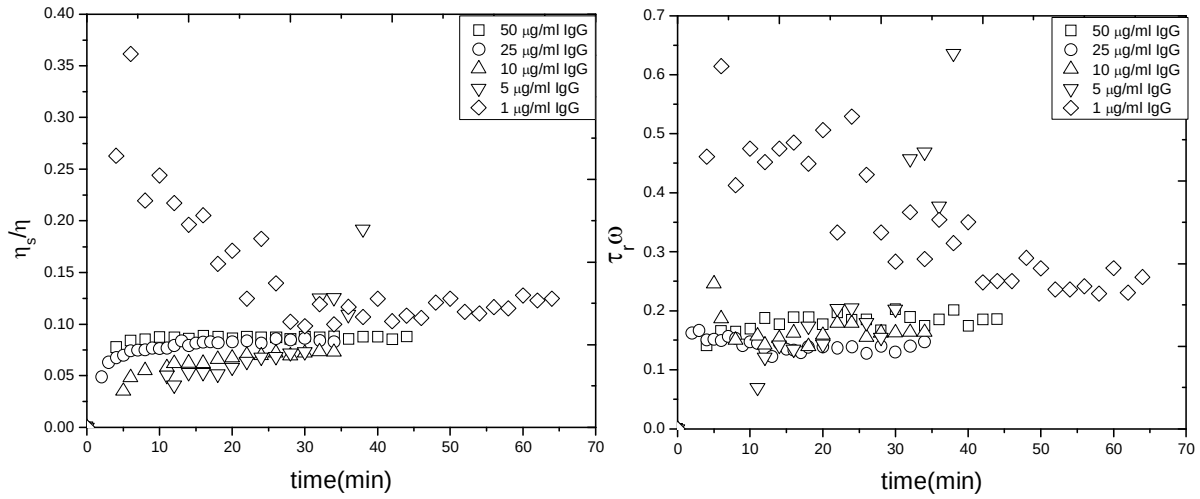

(a) (b)

Figure 4.3 a) The change in η_s/η with respect to time b) Change in $\tau_r \omega$ with respect to time

4.2.2 QCM-D Characterization of IgG Adsorption on Surface-Attached PNIPAAm Surfaces of Thicknesses

The variations in frequency and dissipation change are displayed in figure 4.4 for the adsorption of IgG of 0.5mg/ml to the PNIPAAm coated sensor at the hydrophilic (15°C) and the hydrophobic (40°C) states. It is shown that the frequency change is almost the same in both the hydrated and collapsed states suggesting approximately the same amount of adsorption on both hydrophilic and hydrophobic states. The dissipation is, however, larger in the case of adsorption to the hydrated layer indicating a large amount of water coupling with protein layer. This suggests a soft, viscoelastic protein layer formation on the swollen PNIPAAm surface. In the dissipation graph, large separation between the harmonic values was observed for the swollen PNIPAAm surface. This is also indicative of water coupling with the adsorbed material as an additional mass via direct hydration and/or entrapment within the adsorbed film. The higher frequency drop on the hydrophilic PNIPAAm surface could be a result of coupling of entrapped water to the oscillation of the adsorbed protein layer as an additional mass.

Figure 4.5 shows the adsorption kinetics of IgG with the bulk concentration of 0.5 mg/ml on PNIPAAm and gold surfaces at 40°C. The adsorption was observed to be faster and more on gold surface than collapsed PNIPAAm surface. This might be attributed to the following reason. Collapsed polymer surface might still possess some water entrapped within the matrix that can drive a competition for the available adsorption sites for IgG molecules resulting in slower adsorption kinetics. The adsorbed amount of IgG at saturation on collapsed PNIPAAm and gold surface was calculated to

be 6.1 mg/m^2 and 12.5 mg/m^2, respectively. In both surfaces the maximum adsorbed amount at saturation is higher than the highest possible surface coverage values for IgG monolayer which ranges 2mg/m^2 for flat-on orientation and 3.7 mg/m^2 for end-on orientation.[81] This suggests a multilayer formation on the surface since the IgG adsorption did not saturate at the monolayer level.

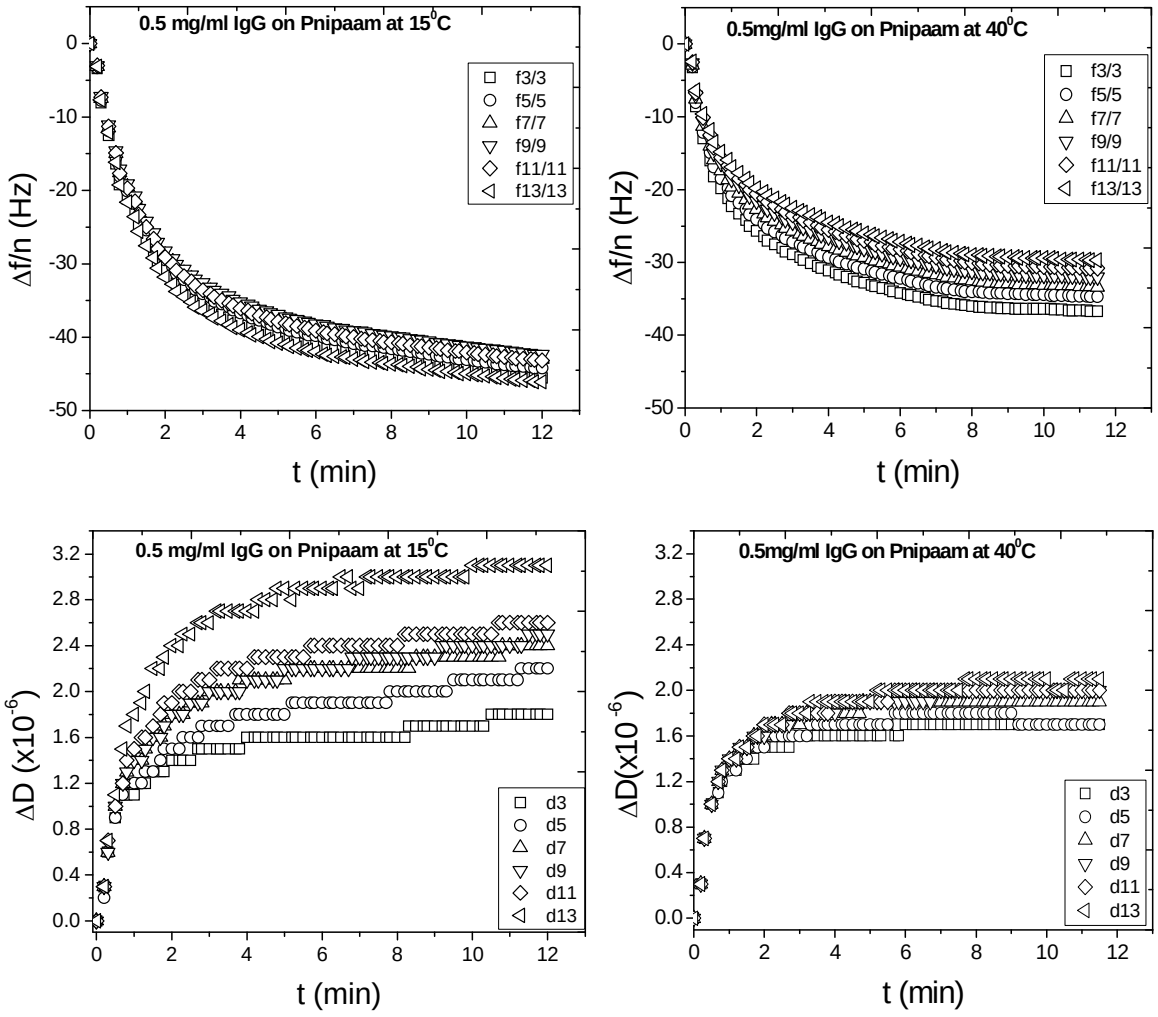

Figure 4.4 Frequency and dissipation change as a function of time upon IgG adsorption on PNIPAAm surfaces at 15 ^{o}C and 40 ^{o}C

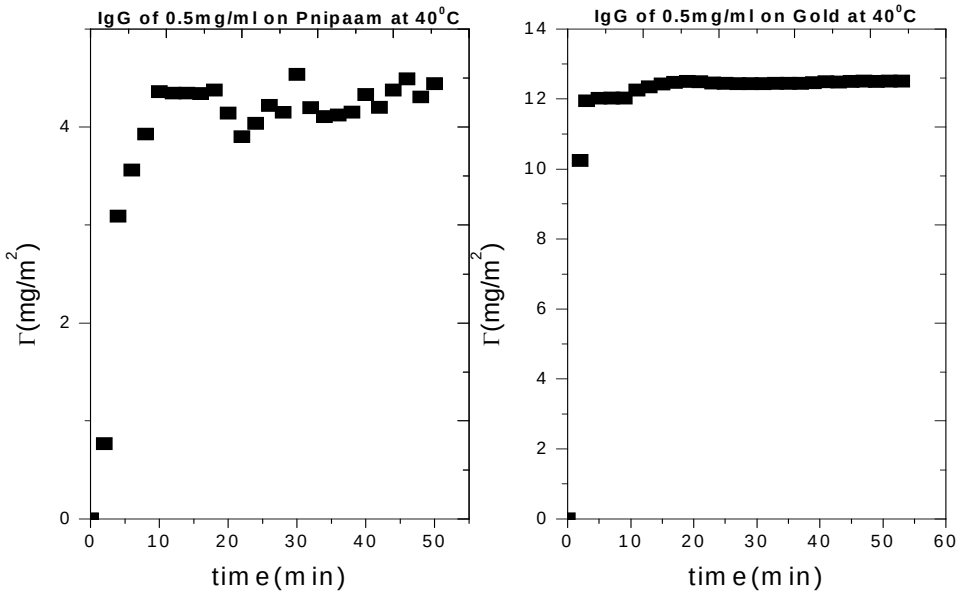

Figure 4.5 Adsorption kinetics of IgG on PNIPAAm and gold surfaces at 40°C.

Desorption behavior of IgG from PNIPAAm surface with 36 nm dry thicknesses is given in figure 4.6. In this study first PBS buffer was run through the PNIPAAm coated sensor at 40 °C and the frequency change was monitored upon temperature drop to 15 °C. Subsequently, IgG solution of 0.5 mg/ml was run through the PNIPAAm surface at 40 °C and the frequency change induced by mass removal was recorded as temperature was reduced from to 15 °C. The same amount of frequency change for both PBS buffer and IgG runs suggests that the frequency reduction is due to solvent effect and the adsorption of IgG is not reversible on the PNIPAAm surface. This indicates adsorption induced conformational changes in protein structure. Protein might have denatured to an elongated primary structure and completely relaxed or spread on the surface because of its high residence time.

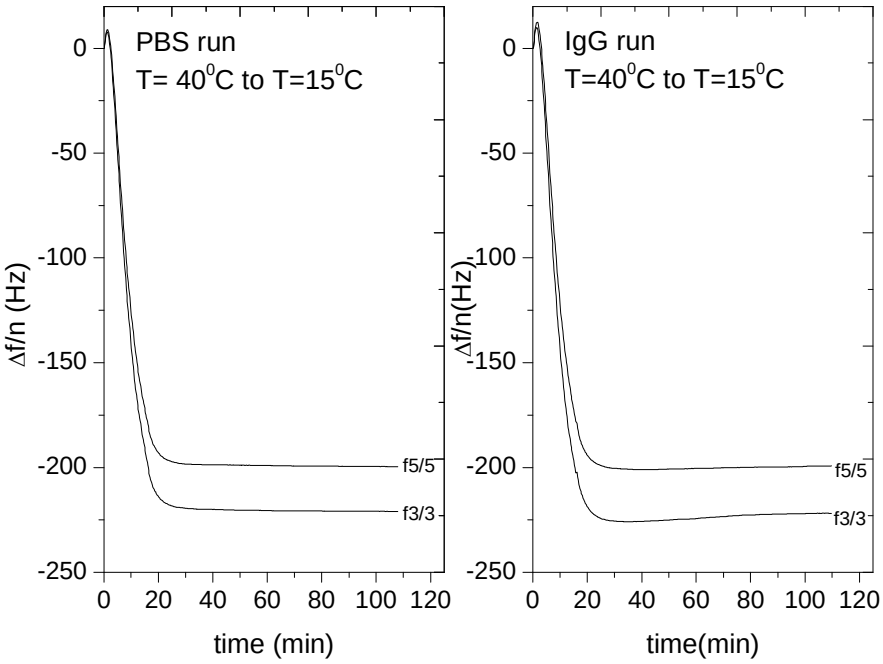

Figure 4.6 Desorption of IgG from PNIPAAm surface.

4.2.3 Fluorescence Study of Fluorescein Isothiocyanate (FITC) Conjugated IgG Adsorption on PNIPAAm

A fluorescence study of fluorescein isothiocyanate (FITC) conjugated IgG adsorption at 0.5 mg/ml was performed at 25°C and 37°C for 45 minutes adsorption time in order to visualize the adsorption at both hydrophilic and hydrophobic PNIPAAm surfaces with the dry thickness vaule of 10 nm (figure 4.7). From the average intensity values, it is determined that the adsorbed amount of IgG was about 50% greater on the hydrophobic surface than that on the hydrated surface. This finding conflicts with our observations from QCM-D which suggests the similar amount of adsorption at both surfaces.

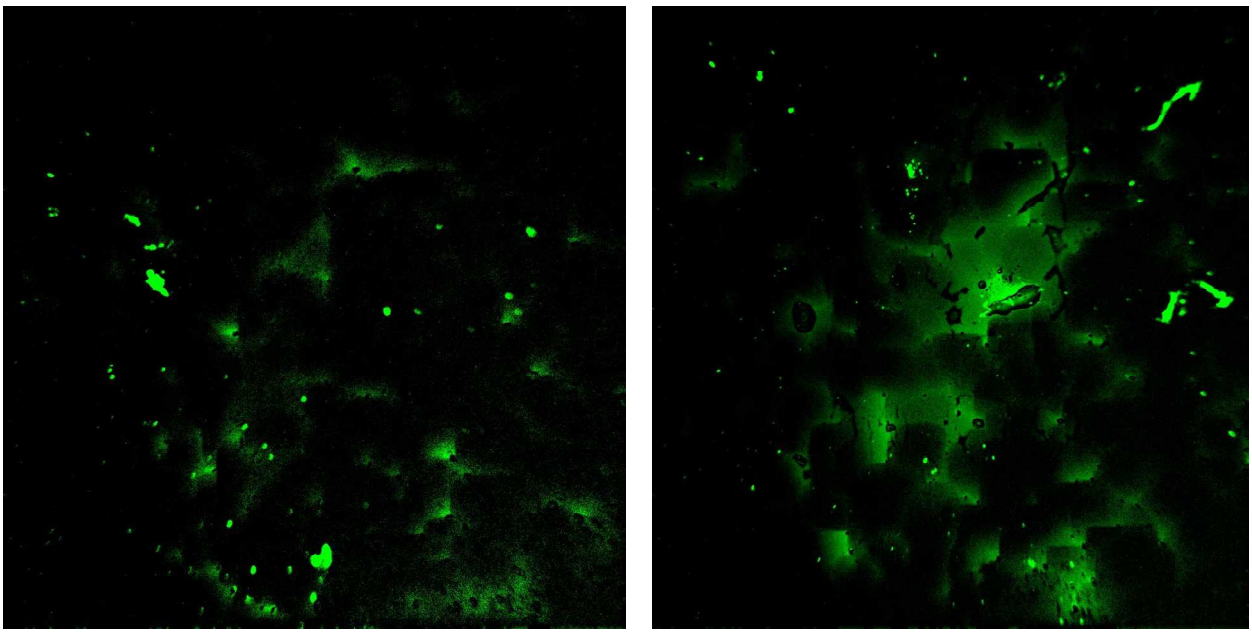

(a) 25 ^{o}C

Average Intensity 2.72

(b) 37°C

Average Intensity: 4.29

Figure 4.7 Adsorption of IgG-FITC to PNIPAAm (a) at 25 ℃ (b) at 37 ^{o}C

In order to obtain substantial information regarding the influence of volume transition of PNIPAAm on the IgG adsorption, it is an absolute necessity to conduct a different practice which can offer both an insight to the adsorption phenomena and a consistent quantification of the extent of adsorption on the surface of interest. The next chapter of this dissertation presents an empirical study on adhesion characteristics of PNIPAAm films using a mechanical tool, a spinning disk device, which is based on a hydrodynamic flow system that provides a wide linear range of hydrodynamic detachment forces on adherent substances to measure the adhesion strength on the adsorbent surface[85].

4.3 Conclusions

A study of temperature dependent immunoglobulin-g (IgG) adsorption onto gold and surface-attached PNIPAAm coatings was conducted by QCM-D and fluorescence techniques. The adsorbed protein amount per surface area on gold and collapsed PNIPAAm surfaces was characterized with QCM-D. Fluorescence probe was used to envision and determine the IgG adsorption on the PNIPAAm coatings with respect to volume phase transition of PNIPAAm. IgG adsorption on gold surface was independent of temperature and our data analysis revealed a rigid multilayer formation on the gold sensor surface. For adsorption on PNIPAAm, QCM-D showed that the frequency change was approximately the same in both hydrated and collapsed states; however, the dissipation was larger in the case of adsorption to the hydrated layer indicating formation of a soft viscoelastic protein. On the other hand, fluorescence study showed about 50% greater IgG amount adsorbed on the hydrophobic surface than that on the hydrated surface. Our calculations for IgG surface coverage using rigid film limit suggested a multilayer formation on the collapsed PNIPAAm surface as it was found on the gold surface. QCM-D studies also suggested a non-reversible adsorption behavior of IgG on PNIPAAm surfaces.

In order to be able to better understand and complement these results we employed a mechanical technique that could enable us quickly measure the adhesion of IgG on PNIPAAm surfaces. The next chapter presents our findings for temperature and film thickness dependent adhesion of polystyrene and IgG on PNIPAAm surfaces by using a hydrodynamic shear flow assay in spinning disk configuration.

CHAPTER 5 : PROBING ADHESION TO POLY(*N*-ISOPROPYLACRYLAMIDE) COATINGS USING A SPINNING DISK METHOD

5.1 Introduction

The majority of proteins change structure upon adsorption to a solid surface, which has important implications for the regulation of biological functions such as cellular response. It is widely recognized that “switchable” coatings, such as poly(*N*-isopropylacrylamide), or PNIPAAm, offer the ability to tune protein adsorption. Surface force apparatus (SFA)[86] and atomic force microscopy (AFM)[28, 30, 87] have been used to characterize surface forces and the morphology of proteins adsorbed on switchable surfaces. For instance, Kidoaki Et al. preliminarily investigated the variations in the intermolecular force between a PNIPAAm-grafted surface and model proteins, albumin and fibronectin, using AFM at below (25°C) and above (40°C) the critical temperature of PNIPAAm.[25] They reported a large repulsion force in the approach trace at 25°C regardless of the protein type whereas little repulsion force was monitored at 40°C. Moreover, their results showed no significant adhesion force in the retract trace for albumin at both temperatures. Cho Et al. conducted a similar study using AFM; however, they measured the changes in the intermolecular force between a PNIPAAm-grafted surface and bovine serum albumin (BSA) as a function of temperature (22-30°C). [33] Their result showed some contradiction with the results obtained by Kidoaki and co-workers. They observed no adhesion force in the retraction trace between 22°C

and 24°C. However, as the temperature was increased, the adhesion force increased and finally reached a plateau value of 1.1 nN at 30°C, which was considerably higher than the control values for bare and amine terminated substrates. Although both AFM and SFA techniques provide direct measurement of the surface forces with different time scale and sensitivity, they suffer from mechanical instability in different force measurements when the gradient of true force-distance curve exceeds the spring constant of the instrument.[88] In spite of the knowledge obtained on temperature dependent variations in the intermolecular forces between protein and switchable surfaces by these techniques, questions still remain regarding the relations between the specific architecture of the switchable surface and adhesion of biomolecules. In order to address this, we have implemented a spinning disk method to quickly measure adhesion to cross-linked PNIPAAm coatings.

The use of hydrodynamic detachment shear forces to determine the adhesion strength enables to perform a wide range of measurements in a short time period, which establish good statistics and confidence in the measured data. The spinning disk configuration for hydrodynamic shear system has the ability to produce large detachment forces that vary linearly with radial distance. The detachment forces produced are applicable to a large population of adsorbate in a single experiment.[78, 89, 90] There have been several studies that employed spinning disk method in order to quantify cell adhesion strengthening [78, 89, 91-93] and to characterize colloid adhesion on solid surfaces.[94, 95] We however, have not encountered any report on use of this method to study protein adsorption onto thermoresponsive surfaces in relation to volume phase transition behavior of the polymer. With the use of this robust and reliable technique,

we, for the first time, have been able to quantitatively ascertain the adhesion of the model protein, immunoglobulin g (IgG), on the thermoresponsive cross-linked coatings of PNIPAAm as a function of film thickness and cross-link density in correlation with volume phase transition behavior of the coatings. IgG is the main antibody isotype present in blood and extracellular fluid and it plays a primary role in secondary immune response. IgG facilitates phagocytosis by binding pathogens (opsonisation), thereby, allowing for their recognition by the phagocytic immune cells (macrophages). Therefore, understanding the IgG adsorption on solid interfaces has a major relevance in developing efficient biomaterial surfaces and detection systems such as immunological tests and biosensors. There have been number of reports that investigated the kinetics, equilibrium and binding strength of IgG adsorption on solid interfaces using different techniques.[73, 81, 96-109] For instance, LaGraaf and Cu-LaGraaf studied the attachment of IgG to oxygen plasma cleaned glass surfaces through microcontact printing (MCP) and physical adsorption during bath application.[109] By applying a Langmuir adsorption model, they determined the binding constants for the MCP stamped and bath applied IgG adsorption to be 1.7 (2)$\times 10^{7}$ M^{-1} and 7.8(7)$\times 10^{5}$ M^{-1}, respectively. This suggested that MCP brought IgG-inked PDMS stamp in direct contact with the plasma-cleaned, hydrophilic glass surface, where IgG has more affinity towards than hydrophobic PDMS stamp. In spite of the numerous empirical studies, the adsorption mechanism of IgG still remains not well understood because of the lack of experimental methods that give direct information on the adsorption kinetics under *in situ* conditions.

In this study, the quantitative measurements of IgG adhesion on PNIPAAm coatings were achieved by application of a wide range of detachment shear forces that

result from hydrodynamic drag and torque on the adherent IgG coated 10 μm sized polystyrene (PS) particles. The shear stress that detaches 50% of the adhered particles is defined as the measure of mean adhesion strength of the adhered particles. In order to determine the adhesion through hydrodynamic detachment shear forces, the model protein, IgG, was fluorescently labeled and covalently attached to carboxylated PS microsphere probes through carbodiimide chemistry as shown in figure 5.1.

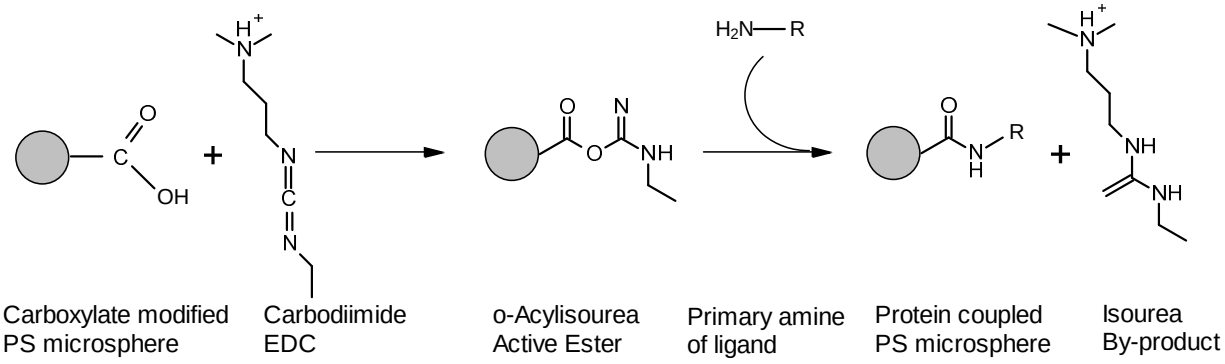

Figure 5.1 Schematic of the reactions for carbodiimide coupling of a protein to a PS microsphere

Latex particles such as PS microspheres are suitable for biomedical research as they readily adsorb proteins and ligands and facilitate procedures such as cell sorting and immunoprecipitation where they can act as a solid substrate for the antibody to couple with. They provide proper solid-phase supports in order to immobilize biomolecules, which especially has significance in reducing undesirable nonspecific protein adsorption. Particle size and size distribution determine surface availability for immobilization and the presence of surface functional groups is important to ensure the colloidal stability and to allow immobilization. Functionalized polymer particles that are covalently coupled with biomolecules can then be visualized through fluorescence. The interaction of protein molecules with polystyrene latex particles that have a well-defined

surface has been studied as a model system to understand interfacial behavior of proteins.[110]The main features of protein adsorption onto such particles exhibited that the adsorption process is rapid and irreversible and is governed by electrostatic and hydrophobic interactions[111], however hydrophobic interactions may influence conformational changes in the protein that can induce denaturation and influence accessibility and activity of the immobilized biomolecules. In order to control the conformations of the fixed biomolecules, one alternative solution could be to utilize interactions between a specific domain of the biomolecules and suitable active chemical groups on the colloid particle surface.

Adsorption of proteins onto PS latex particles has been extensively studied. Kawaguchi Et al studied adsorption of human serum albumin (HAS), γ-globulin, cycochrome, myoglobin and horseradish peroxide onto a series of PS latex particles of the same particle size but different surface structures.[112] They observed little affinity that the proteins had towards hydrophilic surfaces while the affinity increased with increasing hydrophobicity and surface charge. They found electrostatic interactions to be larger factor in determining the adsorption of polar and relatively small protein molecules. Duracher and colleagues examined bovine serum albumin adsorption onto positively charged core-shell latex particles with a PS core and a rich PNIPAAm shell layer as a function of pH, ionic strength and temperature.[113] They observed BSA adsorption onto such cationic and thermosensitive particles to be negligible below the LCST of PNIPAAm while BSA adsorption was much greater above LCST. Ionic strength and pH dependence of the adsorbed amount at the plateau of the adsorption isotherms revealed dominating role of electrostatic forces on the adsorption process. In another

study, influence of NaCl addition to negatively charged PS latex particles that were pre-coated with β-casein was investigated.[114] A reduction of 4-5nm in the β-casein layer thickness was attributed to less electrostatic repulsion due to suppression of ionization of the negatively charged groups that are located in the hydrophilic tail region of the protein and on the surface of the latex. In addition, an increase in NaCl concentration resulted in aggregation of the coated particles. Microspheres that are conjugated to drugs, fluorescence probes, radionuclides and photosensitizers have been used in enhancement of drug delivery and delivery of toxins. Polystyrene microsphere (1μm) - photosensitizer (chlorin e6) conjugates were reported as an efficient system for the delivery of photosensitizing drugs to carcinoma cells.[115] The adhesion of the drug particles to specific sites is important to the pharmaceutical industry, however, submicron or micron sized particle-surface interactions can be problematic in many industrial processes since the particulate contamination is becoming a major issue.

The particle adhesion and removal mechanism is comprehensively reviewed by Visser[116, 117] and several theories have been developed to explain the mechanics of particle contact on different surfaces. It is necessary to gain a better understanding of the mechanism in order to be able to properly interpret our experimental findings.

5.1.1 Mechanics of Particle Adhesion and Removal

Particles on a surface experience different forces. These forces are gravitational force, Van der Waals interactions and other attractive forces such as electrostatic and capillary. In 1882, Heinrich Hertz developed a theory to solve the contact mechanics of the two curved surfaces.[118] His theory assumed non adhesive contact of homogenous and frictionless surfaces that could be considered as elastic half-space. As a

modification for the Hertz contact theory, Johnson-Kendal-Roberts (JKR) incorporated the effect of adhesion inside the area of elastic contact between a sphere and a flat surface of an infinite half-plane.[119] According to JKR model, the adhesion force between a spherical of radius R and a flat surface of a half-plane and the contact radius when no external force is exerted are given by

$$F_A = \frac{3}{2}\pi\gamma R \tag{5.1}$$

$$a = \left(\frac{9\pi R^2\gamma}{E^*}\right)^{\frac{1}{3}} \tag{5.2}$$

where γ is the adhesion energy, E^* is the elastic modulus of the combined sphere-half plane system and it is given as

$$\frac{1}{E^*} = \left[\frac{1-\nu_1^2}{E_1} + \frac{1-\nu_2^2}{E_2}\right] \tag{5.3}$$

where ν is the Poisson ratio and subscript 1 and 2 corresponds to the sphere and substrate.

Visser proposed that the tangential force on a spherical particle in contact with a plane wall in a laminar flow is directly related to the shear stress acting on the wall.[117]

$$F_s \approx 32R^2\tau_{wall} \tag{5.4}$$

The free body diagram for the forces upon a particle under hydrodynamic shear flow is illustrated in figure 5.2.The possible actions for particle removal in hydrodynamic flow are categorized in three ways: Complete removal by lift, sliding over the surface and rolling over the surface. It is shown by performing centrifuge experiments that the

detachment mechanism for colloidal particles of 5 to 40 μm is rolling rather than sliding or lifting.[120] Therefore, the dominant mode for 10μm sized PS particle removal is rolling. In this case, the detachment occurs when the hydrodynamic shear moment is larger than adhesion resisting moment.

$$M_s \geq M_A = F_A.a \tag{5.5}$$

$$1.4(F_s R) \geq F_A.a \tag{5.6}$$

$$\tau_{wall} \geq \frac{a}{32R^3}\left(\frac{F_A}{1.4}\right) \tag{5.7}$$

For a laminar flow (Re ≤ 10) the shear stress on a particle is determined as

$$\tau_{wall} = 0.800\, r \sqrt{\rho\mu\omega^3} \tag{5.8}$$

where ω is the angular velocity; ρ and μ are the density and the viscosity of the fluid at the ambient temperature, respectively. By inserting term ($a.F_A$) from the JKR theory in to the equation 5.7, the wall shear stress between the articles and substrate can be obtained as follows:

$$\tau_{wall} \geq \frac{\left(\frac{9\pi R^2\gamma}{E^*}\right)^{\frac{1}{3}}\left(\frac{3}{2}\pi\gamma R\right)}{44.8R^3} \tag{5.9}$$

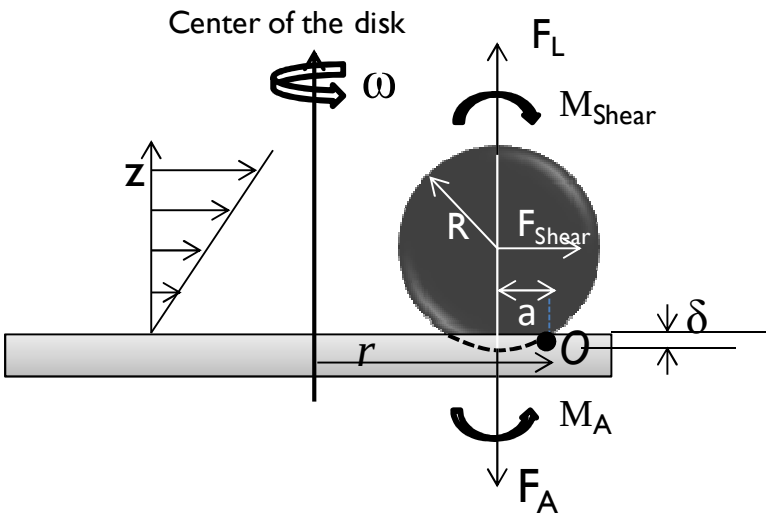

Figure 5.2 Free body diagram for a particle under a hydrodynamic shear flow.

5.2 Experimental Section

5.2.1 Materials

Immunoglobulin g (IgG) (M_w = 150 kDa), sodium chloride (NaCl), carbonate buffer, 2-(N-morpholino) ethanesulfonic acid (MES) buffer, borate buffer, ethanolamine, N-(3-dimethylaminopropyl)-N'-ethylcarbodiimide hydrochloride (EDAC), sodium phosphate monobasic, sodium phosphate dibasic, bovine serum albumin (BSA), sodium azide and glycerol were purchased from Sigma Aldrich. Fluorescein isothiocyanate (FITC) labeling kit was purchased from Invitrogen. Carboxyl functionalized and non-functionalized PS microspheres (2.5 % solids (w/v) aqueous suspension) were purchased from Polysciences. IgG solution was prepared in 0.01M phosphate buffer saline (PBS) at pH 7.4.

5.2.2 Experimental Procedure

Prior to the thin film fabrication, circular glass cover slips were immersed in ethanol and placed in sonication bath for twenty minutes followed by plasma cleaning for five to fifteen minutes. Cleaned glass cover slips were then deposited in 1% solution of 3-aminopropylmethoxysilane (APTES) in acetone for two minutes and were subsequently washed with acetone to remove impurities. The cover slips were dried by gentle air purge and baked for 15 min at 120°C in order to evaporate the solvent. After APTES treatment, the polymer solution was spin-casted on the substrates at 2000 rpm for 45 sec. The cross-linked networks were achieved by half-hour UV illumination at 365 nm. Polymer film thickness was simply adjusted by changing the weight/ volume (w/v %) percentage of the polymer solution. After polymer coating, substrates were submerged in 3 ml of NaCl solution at 0.014M and a solution of 10 μm sized PS microspheres was adsorbed on the substrates at 24°C for various deposition times. The microsphere distribution on PNIPAAm coated substrates before spinning is shown in figure 5.3.

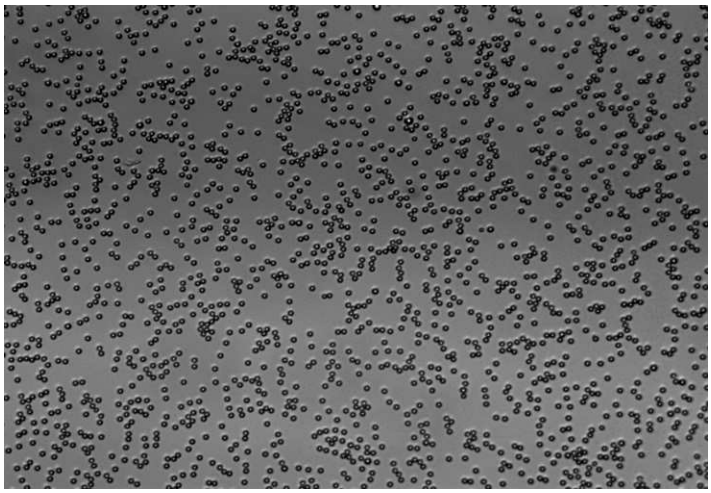

Figure 5.3 PS microspheres distribution on PNIPAAm surface before spinning

The average nearest neighbor distance of the 10 μm sized microspheres were determined using ImageJ and was calculated to be between 15 to 20 μm, indicating an adequate separation among microspheres. After confirming nearly homogenous microsphere coverage on the surface, samples were sealed on the shaft of the spinning disk device filled with 0.014M NaCl solution at 24°C or 42°C and were spun at maximum 5000 rpm for 5 min. The schematic of the procedure is given in figure 5.4. Although the spinning duration was not changed, the spinning speed was occasionally varied among the experiments in order to ascertain a nice sigmoid curve for the detachment profiles.

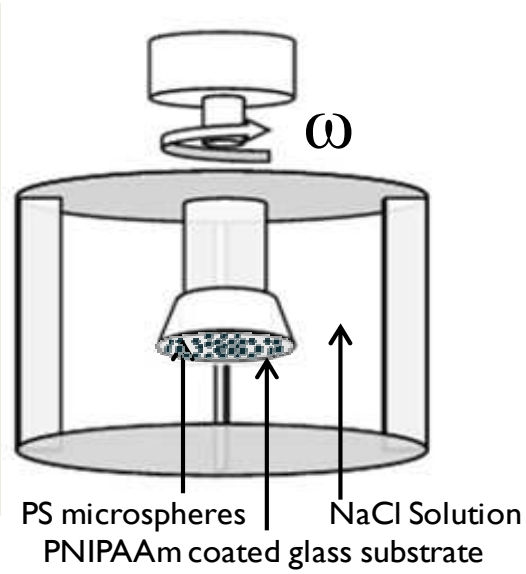

Figure 5.4 Schematic of the spinning procedure

It is important to mention that a significant challenge was encountered while removing the samples from the solution for the spinning procedure. The adhered PS micro particles started to aggregate immediately due to action of the lateral capillary forces between the particles as the surface began to dry.[121] The clustering of the microspheres on the PNIPAAm surface caused a major problem in the microsphere counting. In order to be able to overcome this difficulty, immediately after spinning, the

sample was wetted and placed in a plate containing spinning solution as the PS microsphere deposited side of the sample would be in contact with the solution. The excess solution was aspirated giving rise to an adequate seal between the microsphere adhered surface and the plate (figure 5.5). Thereby, the lateral mobility of PS beads on the surface was stabilized and reliable microsphere counting was achieved.

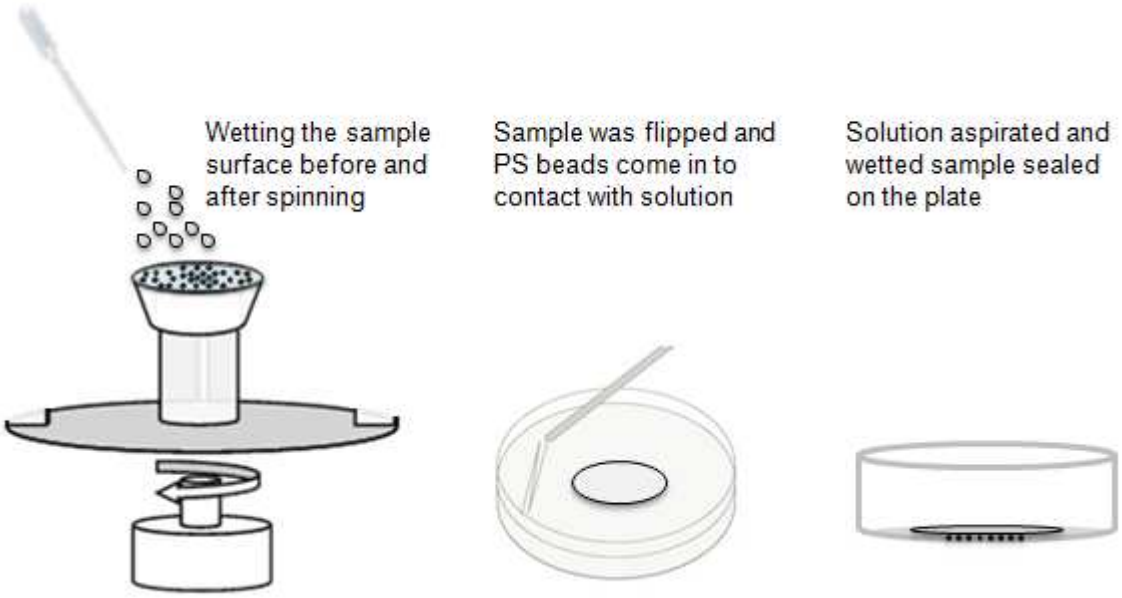

Figure 5.5 Procedure before microsphere counting

Following the spinning procedure, remaining adherent particles on the coatings were counted at specific radial positions with an automated stage and image analysis software installed in Nikon Fluorescence Microscopy. The microsphere counts were then normalized to the counts at the center of the surface where shear stress is negligible and the detachment profiles for each sample count were obtained. The change in viscosity of the spinning solution due to temperature adjustment was taken into account when calculating the detachment shear stresses.

The same experimental procedure was performed for IgG-FITC coated PS microsphere counting, as well. Prior to the IgG immobilization on PS probes, FITC was conjugated to IgG to visualize the IgG immobilization on the PS probes under the microscopy. FITC labeling was done through following the protein labeling protocol obtained from Invitrogen. The absorbance values of the IgG (at 280 nm) and the FITC dye (at 495 nm) in order to calculate the degree of labeling (DOB) were measured using Thermo Scientific NanoDrop 1000 Spectrophotometer. The estimated values of DOB for the labeling reactions performed in this study ranged between 4-8 FITC dye molecules per IgG molecule, which were in the optimal range. For IgG-FITC immobilization on PS probes, IgG-FITC was covalently attached to carboxylated PS probes through carbodiimide method using a protocol provided by Polysciences. The coupling efficiencies of the reactions performed in this study were 100%.

5.3 Results and Discussion

The adhesion characteristics of surface attached PNIPAAm coatings have been investigated as a function of coating thickness and structure in correlation with phase transition of the coatings. It is known that physical properties of a thin coating is greatly affected by its thickness[122]. For instance, it was reported that the polymer film thickness influenced the endothelial cell adhesion and proliferation.[123] Endothelial cells showed enhanced adherence on the poly(vinylacetic acid) film with 9% carboxyl concentration at 100nm thickness with respect to the films with 25, 50 and 200 nm thicknesses with the same 9% carboxyl concentration. Another study by the group of Okano also showed the significant influence of PNIPAAm grafted layer thickness on temperature induced hydrophilic/hydrophobic transition and cell adhesion/release behavior.[124]

In this study, the spinning disk experiments were performed at 24°C (hydrophilic state) and 42°C (hydrophobic state) for 10 μm sized bare polystyrene (PS) microspheres, carboxylated PS microspheres and IgG coated PS microspheres on poly(NIPAAm) photo-cross-linked coatings. Figure 5.6 exhibits a detachment profile for 10μm sized PS microspheres adsorbed on swollen (24°C) and collapsed (42°C) PNIPAAm surfaces at a dry thickness of 24nm. The adhesion strength is obtained from the shear stress value for the 50% detachment (τ_{50}) of the PS microspheres from PNIPAAm coatings. The thickness dependent adhesion behavior of hydrophobic bare PS microspheres is shown in figure 5.7. Here, PS microspheres were adsorbed on PNIPAAm surfaces with dry thicknesses ranging from 5 nm to approximately 144 nm (thicknesses are determined by ellipsometry) for overnight (~ 18 h) deposition time. Each data point represents the average of the adhesion strength values obtained from at least three samples (maximum five samples). The error bars correspond to the standard error among the samples counted for each data point. Measurements show a linear dependence between mean particle adhesion strength and PNIPAAm film thickness in the hydrophilic state. Adhesion ranged from 110 dynes/cm^2 to 184 dynes/cm^2 in the hydrated state and from 85 dynes/cm^2 to 154 dynes/cm^2 in the collapsed state indicating a strong dependence of coating thickness on microsphere adhesion. For thin film thicknesses (5nm-15nm) microsphere adhesion was greater in the hydrophilic state due to larger contact of the PS particles with the soft thin film. Interestingly, at a critical thickness (24nm) microsphere adhesion in the hydrophobic state began to outcompete adhesion in the hydrophilic state. Measurement of microsphere cm^2 adhesion on collapsed surfaces thicker than 24nm was not possible

as microsphere adhesion exceeded the measurement capacity of the experiment. This might result from the change in the morphology of the collapsed PNIPAAm films allowing for a larger contact area of the particles on the surface as the film thickness is raised. The higher adhesion force with increasing film thickness has been previously reported.[122, 125] For instance, Pourzand and co-workers investigated the film thickness dependence on adhesion force and its correlation to surface roughness in multilayered graphene using AFM.[125] Their findings showed that for relatively thicker layers (10-250nm), the adhesion force increased with increasing graphene layer thickness. This was correlated to the surface roughness of the layers, which increased as the layer thickness was increased from 10nm to 250 nm.

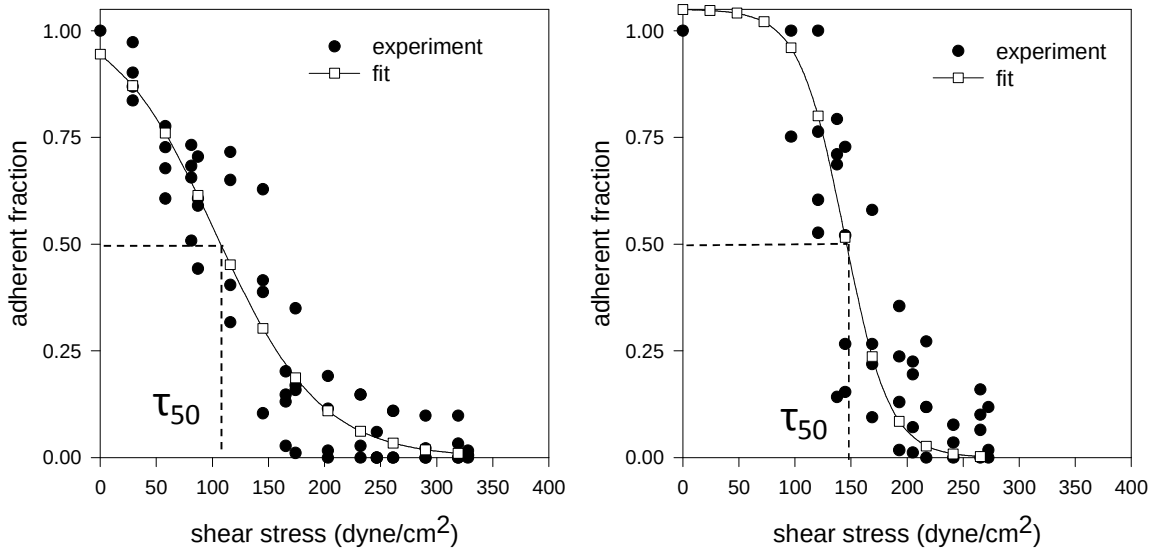

(a) τ_{50}=108 dyne/cm^2 at 24°C **(b)** τ_{50}=145 dyne/cm^2 at 42°C

Figure 5.6 Detachment profile of the 10μm sized bare PS particles from PNIPAAm with 24nm dry thickness (a) at 24℃ (b) at 42℃

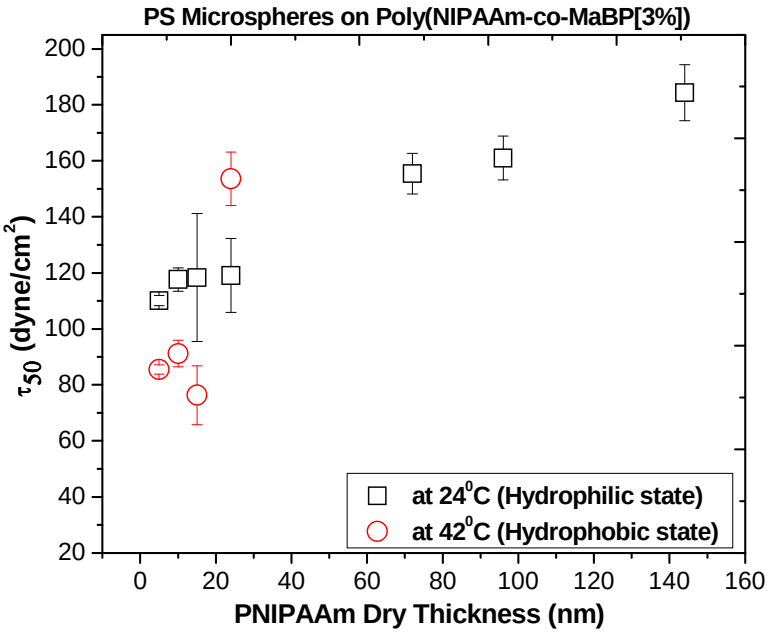

Figure 5.7 Thickness dependent adhesion of bare PS microsphere on PNIPAAM at hydrophilic (24 °C) and hydrophobic states (42 °C)

The effect of the PS microsphere concentration was also investigated and the results were presented in figure 5.8. The concentration of the nonfunctionalized PS microspheres deposited on PNIPAAm surface at both swollen and collapsed states was changed from 0.5 v/v % to 1.5 v/v%. The increase in the bare PS concentration in 0.014M NaCl solution did not significantly vary the adhesion strength of the microspheres on the PNIPAAm coatings with 24 nm dry thickness at both hydrophilic and hydrophobic states for overnight (~18 h) deposition time. Our findings indicate that the adhesion strengthening of the microspheres is independent of the initial deposition concentration on the PNIPAAm surfaces of same thicknesses.

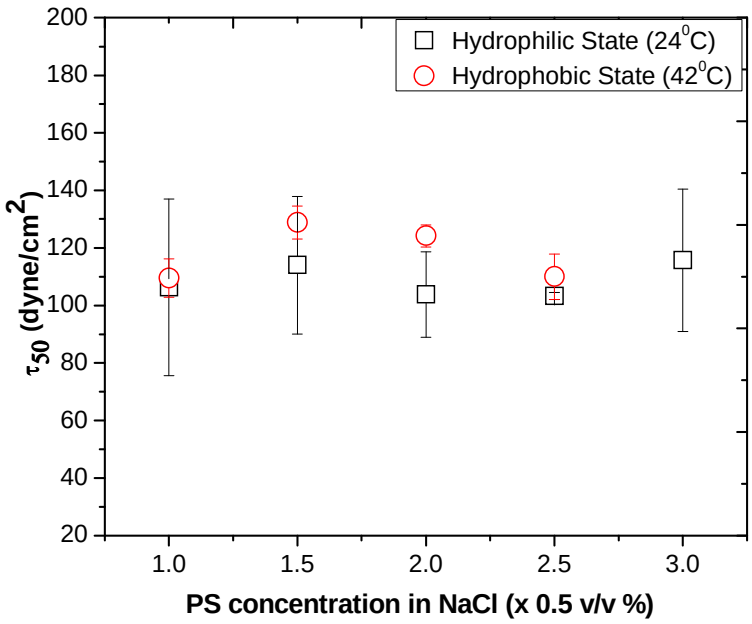

Figure 5.8 Mean detachment shear stresses for bare PS microspheres on PNIPAAm at 24 nm dry thickness as a function of PS microsphere concentration

The thickness dependent adhesion behavior of hydrophilic carboxyl functionalized PS microspheres is given in figure 5.9 for overnight (~18 h) adsorption. The adhesion of carboxylated microspheres did not seem to be significantly affected as the dry film thickness was increased from 10 nm to 124 nm. On the other hand, the adhesion trend was altered with respect to bare PS microsphere adhesion. The mean detachment shear stress values were observed to always be greater on the hydrophilic state compared to the hydrophobic state by a factor of 2. The higher adhesion of the hydrophilic PS microspheres on the hydrated PNIPAAm surfaces could be due to the hydrogen bond formation between carboxyl groups of the microspheres with water molecules within the PNIPAAm network. Additionally, high surface tension between the two hydrophilic surfaces could also contribute to the adhesion forces.

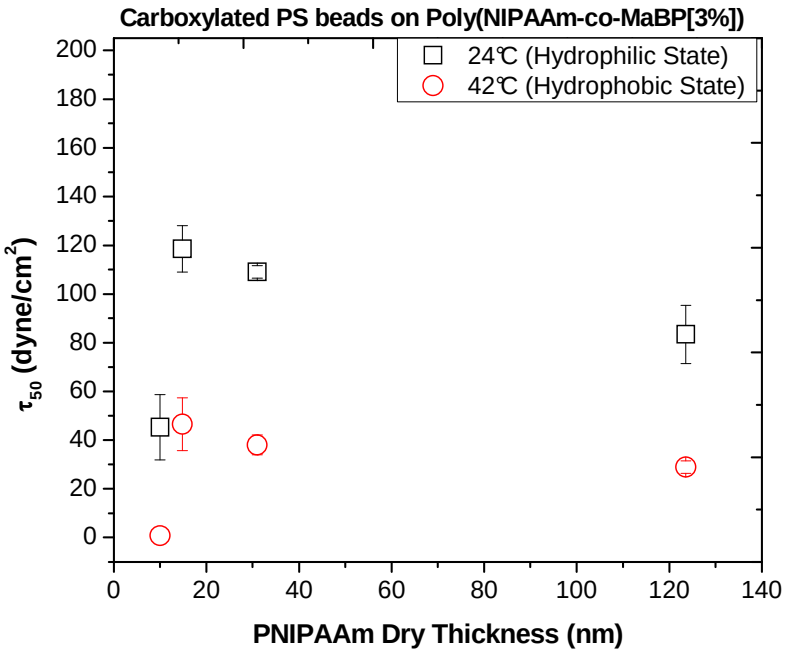

Figure 5.9 Thickness dependent mean detachment shear stresses of carboxylated PS microspheres on PNIPAAm at hydrophilic (24 °C) and hydrophobic states (42 °C) when samples were freshly coated.

The influence of film thickness on carboxylated PS adhesion was investigated by reusing the carboxylated PS adhered samples from previous experiments (figure 5.10). Pre-used samples were rigorously purged with deinonized water and placed in sonication bath to remove pre-adhered PS beads. The removal of the microspheres from the PNIPAAm surface was confirmed under microscopy. Interestingly, the adhesion trend is observed to increase linearly with thickness. The mean detachment shear stresses were greater on the hydrophilic state compared to the hydrophobic state by a factor of 2.5 between the dry thickness values of 10 nm and 36 nm. For the thicker film thickness (124 nm), the adhesion strength value was greater on the hydrophilic state by factor of 1.5.

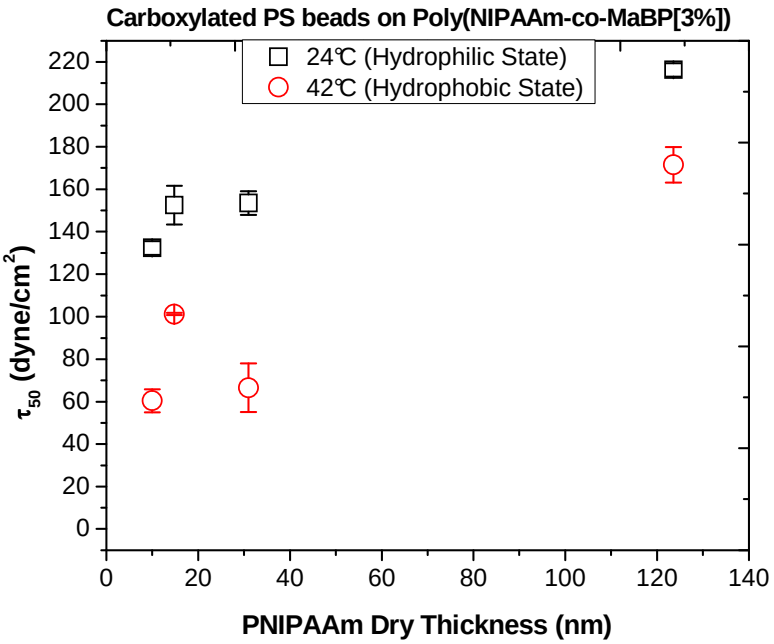

Figure 5.10 Thickness dependent adhesion of carboxylated PS microsphere on PNIPAAm at hydrophilic (24 °C) and hydrophobic states (42 °C) when coated samples were reused.

The influence of the microsphere deposition time on the adhesion behavior was also investigated the effect of the microsphere adsorption time on the adhesion strength. According to a study by Das Et al., the effect of the time of deposition was found to be insignificant for deposition times larger than approximately 30 min although it became very important for the deposition times less than approximately 5 min.[126] The results of our aging studies of carboxylated PS probes on 124 nm thick (dry thickness) PNIPAAm coatings with 3% crosslink density are shown in figure 5.11. It is observed that the adhesion at both hydrophilic and hydrophobic states increased linearly as the PS adsorption time was increased from 3hrs to 48 hrs. This indicates a strong influence of microsphere deposition time on the adhesion behavior of the microspheres on PNIPAAm regardless the state of the coatings. Strong time dependence of the microsphere adhesion on PNIPAAm surface is rather puzzling because the response

time of the surface attached PNIPAAm coatings is on the order of a few seconds. We would expect to reach saturation on adhesion within relatively shorter amount of time.

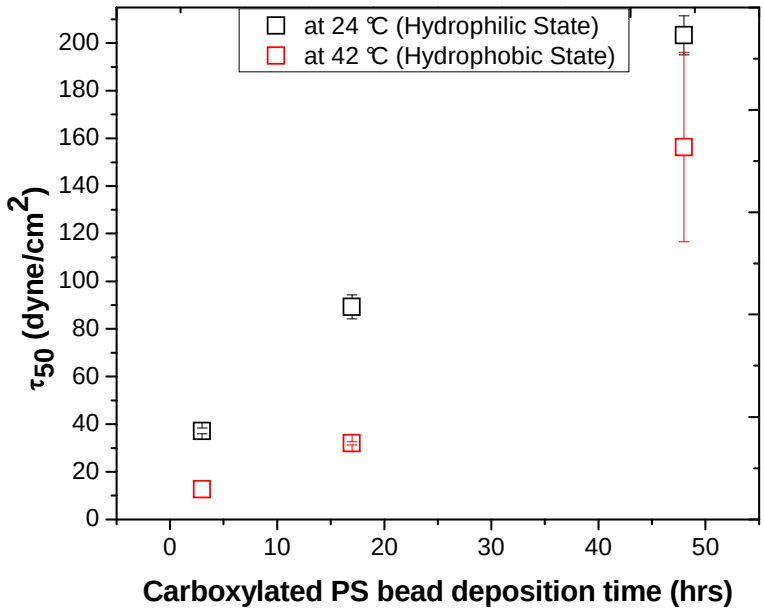

Figure 5.11 Detachment shear stresses of carboxylated PS microspheres as a function of deposition time

Figure 5.12 shows the detachment profile for IgG-FITC coated 10μm sized PS microsphere from the 1wt% PNIPAAm films (dry thickness of 32 nm) at both hydrophilic (24 °C) and hydrophobic states (42 °C). The fluorescence microscopy images were taken at the center of the samples and represent the IgG-FITC coated PS microsphere distributions on the swollen (left image) and collapsed (right image) PNIPAAm surfaces. On the other hand, the long adhesion time might increase the area of contact between the microspheres and the PNIPAAm surface, thereby increasing the adhesion of the microspheres on the PNIPAAm surface.

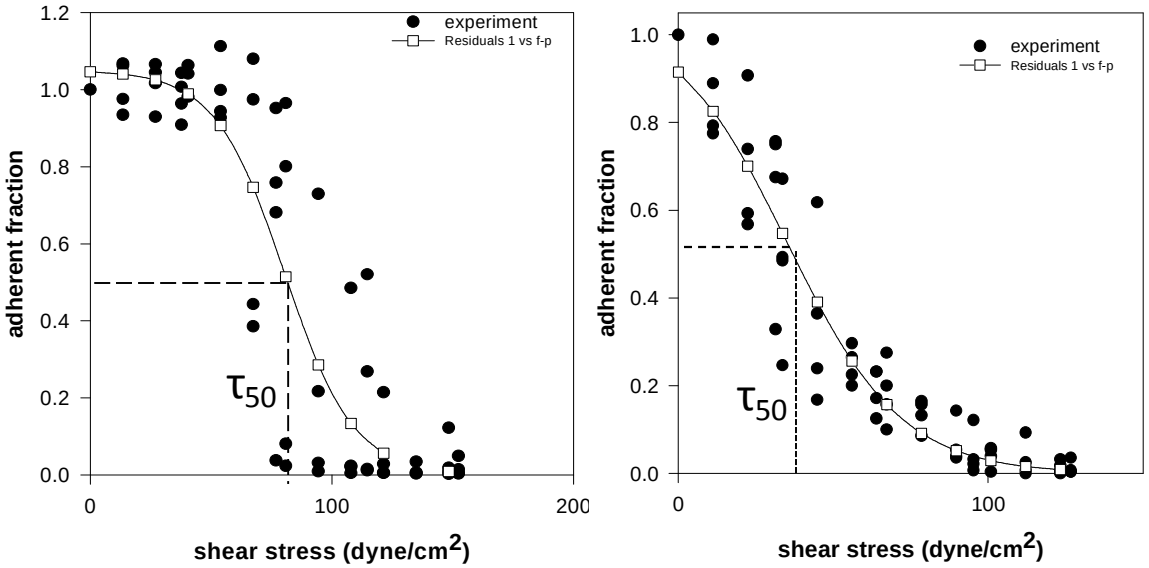

(a) τ_{50}=80.32 dyne/cm^2 at 24°C

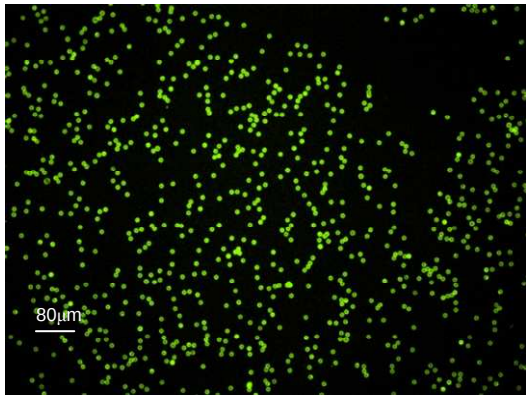

(b) τ_{50}=35.21 dyne/cm^2 at 42°C

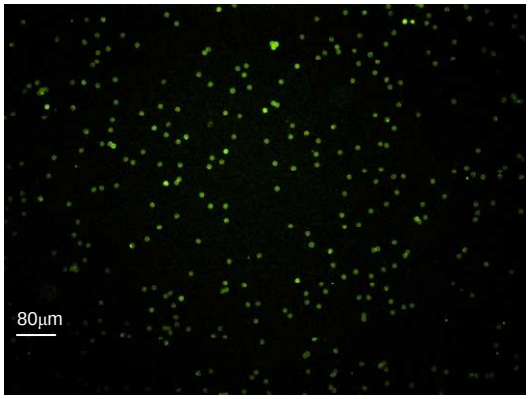

Figure 5.12 Detachment profile of the IgG-FITC coated 10μm sized PS particles from PNIPAAm with 32nm dry thickness (a) at 24°C (b) at 42°C

The thickness dependent adhesion behavior of IgG was investigated with respect to influence of cross-link density of PNIPAAm coatings in correlation with volume phase transition behavior. IgG-FITC coated 10 μm sized PS microspheres were adsorbed on PNIPAAm coatings containing 0.3% and 3% cross-link density at 24°C and 42°C for overnight (~16 h). The cross-link density was adjusted to 0.3% by simply blending the

(PNIPAAm-co-MaBP[3%]) copolymer with PNIPAAm homopolymer. The adhesion of the IgG on poly(NIPAAm-co-MaBP[3 mol%]) was given in figure 5.13. The IgG coated PS microsphere adhesion showed a similar trend as a function of film thickness for both hydrophilic and hydrophobic PNIPAAm surfaces. Here, the adhesion trend was altered when compared to carboxylated microsphere adhesion and the mean detachment shear stress values for the hydrophobic state were higher by approximately factor of 1.7 with respect to hydrophilic state. For a dry thickness of 10 nm the mean detachment shear stress values of hydrophilic and hydrophobic states were 36 dyne/cm^2 and 60 dyne/cm^2, respectively. These findings suggest a strong agreement with our QCM-D observations as the QCM-D results indicated a similar adsorbed amount of IgG on both hydrophilic and hydrophobic films. Between 10 nm and 31 nm the mean detachment shear stresses values for IgG adhesion on hydrated PNIPAAm coatings are observed to decrease by 3.5 fold on average with respect to carboxylated PS bead adhesion indicating lower adhesion of IgG on PNIPAAm coatings. Our findings also showed that the adhesion on both hydrated and collapsed coatings of PNIPAAm with 3% cross-link density did not change significantly with increasing coating thickness. On the other hand, as shown in figure 5.14, the IgG adhesion on PNIPAAm surfaces with 0.3% crosslink density scaled linearly with increasing thickness at both hydrophilic and hydrophobic states. Moreover, the reduction of the cross-link density by factor of 10 resulted in a strong dependence on thickness with approximately a 3-fold increase at the hydrophobic state as the thickness of the dry film was increased from 11 nm to 186nm.

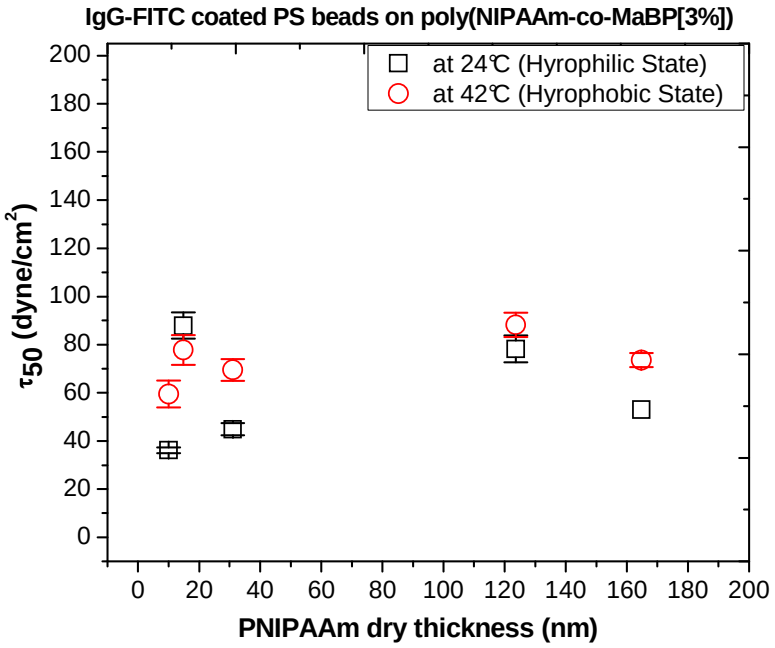

Figure 5.13 Thickness dependent adhesion of IgG coated PS microspheres on PNIPAAm with 3% MaBP at hydrophilic (24 °C) and hydrophobic states (42 °C)

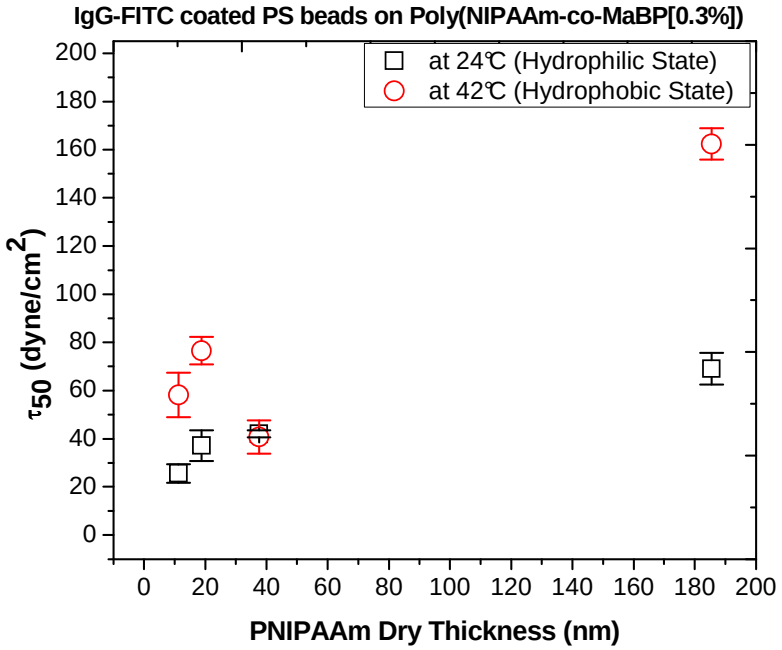

Figure 5.14 Thickness dependent adhesion of IgG coated PS microspheres on PNIPAAm with 0.3% MaBP at hydrophilic (24 °C) and hydrophobic states (42 °C)

The adhesion behavior of IgG on swollen and collapsed coatings of PNIPAAm is illustrated in figure 5.15 with respect to cross-link density. It is seen that the adhesion of IgG linearly increases at the collapsed state as the cross-link density is reduced. It is well known that change in cross-link density strongly affects the swelling/deswelling ability of the PNIPAAm coatings. Lowering cross-link density enables polymer networks swell in greater capacity. Figure 5.16 presents the ellipsometrically determined swelling ratio values of the PNIPAAm coatings with different cross-link densities. Swelling capacity of PNIPAAm coatings with 0.75% cross-link density is observed to be as twice as much with respect to swelling capacity of PNIPAAm coatings with 3% cross-link density. Again, change in swelling capacity of the coatings could affect the contact area and thereby adhesion of the IgG on the PNIPAAm surface.

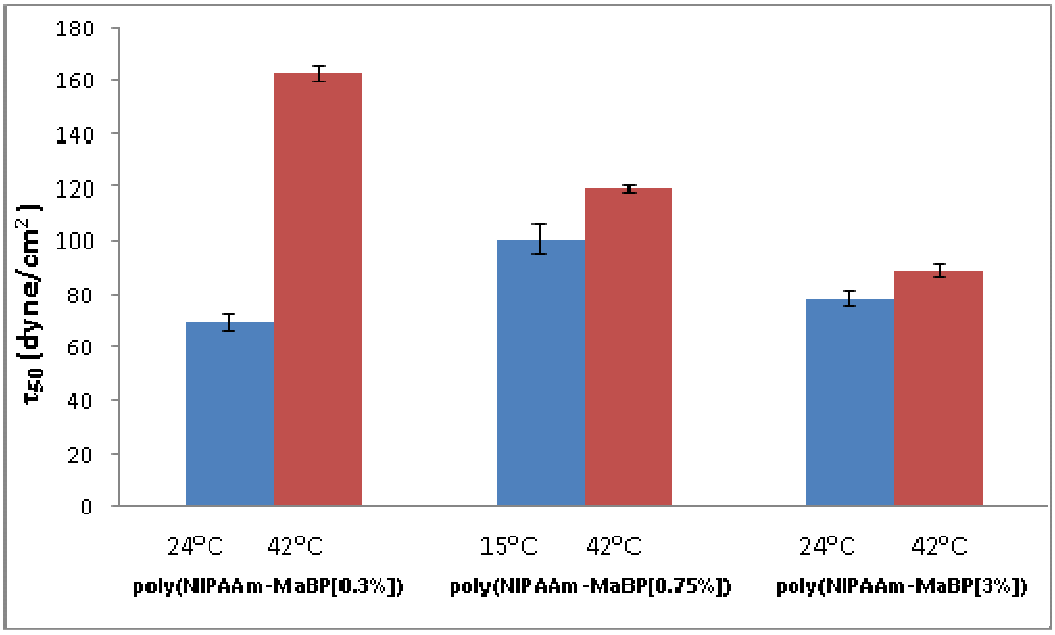

Figure 5.15 Temperature dependent adhesion of IgG coated PS microspheres on PNIPAAm films of various cross-link densities

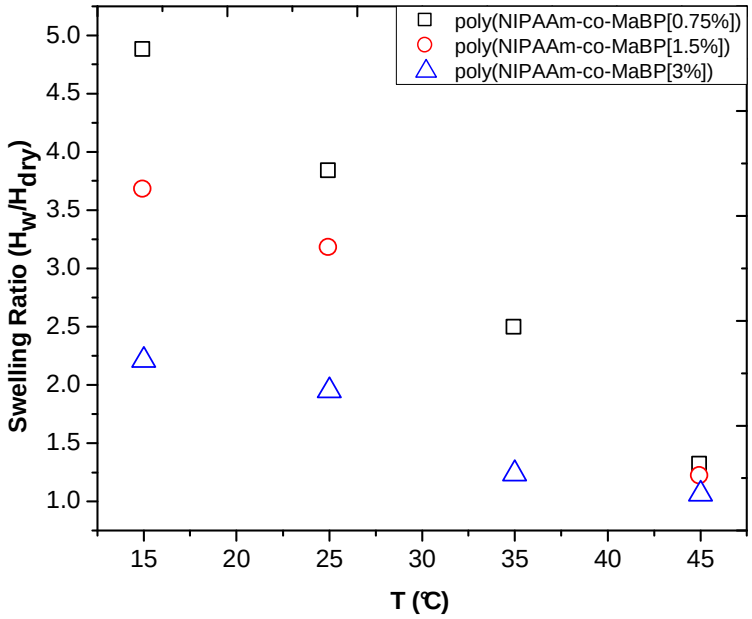

Figure 5.16 Change in the swelling ratios of PNIPAAm films of various cross-link densities as a function of temperature

To determine the difference in the wettability of PNIPAAm surfaces with different cross-link densities, we have performed dynamic sessile drop measurements at both hydrophilic and hydrophobic states. The results of advancing contact angles for PNIPAAm with 0.75% and 3% cross-link densities are given in table 5.1. It is seen that contact angle differs only by 10° and 6° between the PNIPAAm surfaces of 3% and 0.75% cross-link density at swollen and collapsed states, respectively. On the other hand, contact angle increases by 25° upon transition from swollen to collapsed state of PNIPAAm with 0.75% cross-link density. A more pronounced increase in contact angle is often observed with low polymer cross-linking density.[127]

Table 5.1 Contact angle values for PNIPAAm with 0.75% and 3% cross-link density

Dry Thickness (nm)	Contact Angle at 15°C	Contact Angle at 45°C
Poly(NIPAAm-MaBP[0.75%]) at 41.1nm	62.5° ± 5.8°	87.7° ± 1.3°
Poly(NIPAAm-MaBP[3%]) at 31.1nm	72.3° ± 1.6°	81.5° ± 2.2°

5.4 Conclusions

In this study, adhesion characteristics of surface attached PNIPAAm coatings have been investigated as a function of coating thickness, cross-link density, microsphere deposition time and microsphere concentration in correlation with phase transition of the coatings. The spinning disk experiments were performed at 24°C (hydrophilic state) and 42°C (hydrophobic state) and detachment shear stresses were generated on adherent substances through hydrodynamic flow. The strength of adhesion was determined from the mean detachment shear stress values.

The adhesion of hydrophobic bare PS microspheres scaled linearly with the thickness of the PNIPAAm coating in the hydrophilic state (24°C). The values of the detachment shear stresses were greater for the hydrophilic state than the hydrophobic state until the dry film thickness surpassed 24 nm. In the case of hydrophilic carboxylate PS microspheres, the trend was altered and the adhesion was observed to always be greater on the hydrophilic state compared to the hydrophobic state. The concentration of PS microsphere deposited on PNIPAAm surfaces did not significantly influenced the adhesion trend.

The adhesion IgG coated PS microspheres showed a similar trend as a function of film thickness for both hydrophilic and hydrophobic PNIPAAm surfaces with 3% crosslink density. The adhesion strength values for the hydrophobic state were higher by approximately factor of 1.4 with respect to hydrophilic state between dry thicknesses values of 165-185 nm. These results showed a strong agreement with QCM-D measurements. Moreover, by lowering the cross-link density by factor of 10 the adhesion strength value at the hydrophobic surface increased by approximately factor of 2.5 (from 69 dyne.cm^{-2} to 162 dyne.cm^{-2}) between dry thicknesses values of 165-185 nm. The IgG adhesion on PNIPAAm surfaces with 0.3% crosslink density scaled linearly with increasing thickness at both hydrophilic and hydrophobic states and exhibited a strong dependence on thickness with approximately a 3-fold increase at the hydrophobic state. This could be attributed to the possibility that the reduction in the crosslink density allows the polymer chains move more freely and reconstruct themselves locally resulting in larger contact with IgG coated microspheres.

The adhesion of IgG coated microspheres was observed to increase with decreasing crosslink density of the polymer network. This increase was not consistent with the swelling ratio and wettability data. The decrease in crosslink density results in decrease in the elastic modulus of the polymer network. The change in modulus could have a significant impact on the adhesion performance of the polymer layers. This finding reveals the modulus related adhesion behavior.

Finally, aging studies of carboxylated PS probes on PNIPAAm with 3% crosslink density showed that the adhesion strength at both hydrophilic and hydrophobic states increased linearly as the PS adsorption time was increased from 3hrs to 48 hrs. This

indicates a long relaxation process at the interface such that the adhesion does not reach equilibrium.

In conclusion, the adhesion of 10μm sized bare poly(styrene) (PS) microspheres, carboxylated PS microspheres and IgG coated PS microspheres on PNIPAAm photo-cross-linked coatings was successfully quantified using hydrodynamic shear flow assay in spinning disk configuration. Spinning disk method showed sensitivity towards coating thickness and structure as a significantly different trend was obtained for PS microsphere and IgG adhesion.

CHAPTER 6 : [1]POLY(N-ISOPROPYLACRYLAMIDE) NETWORKS CONJUGATED WITH GLY-GLY-HIS VIA A MERRIFIELD SOLID PHASE PEPTIDE SYNTHESIS TECHNIQUE FOR METAL ION RECOGNITION

6.1 Introduction

Responsive polymer-peptide hydrogel conjugates with embedded peptides offer the ability to modify or tune response characteristics. The swelling behavior of responsive polymers has been of considerable interest for many bio related applications such as drug/gene delivery[57, 58], tissue engineering[2, 19] and the biocatalysis.[128] Peptide-polymer conjugates covalently combine a peptide with a synthetic polymer and can be synthesized by one of two strategies.[129] The first is convergent synthesis, wherein the peptide and polymer precursors are synthesized individually and then coupled.[130-132] The second is divergent synthesis, wherein the conjugated unit is directly synthesized from a peptide macroinitor[133] or a synthetic polymer support.[134] Herein, we show that peptides can be grown directly in temperature responsive poly(NIPAAm) cross-linked gels via a solid phase synthesis technique in order to enhance recognition of heavy metal ions.

Stimuli responsive polymer mediated recognition of heavy metal ions from aqueous solution has gained special attention due to the potential for selectively binding metal ions in a controlled manner. Kuckling Et al., for example, investigated the effect of

[1] This chapter has been published in Macromolecular Chemistry and Physics, Volume 215, Issue 13, pages 1342-1349, July 2014. The permission is included in Appendix A.

various transition metal ions on the phase transition of the poly(NIPAAm) gels conjugated with cyclam in order to obtain a chemomechanical system that is switchable by transition-metal ion/ligand interactions. [135] Their results showed a significant decrease (~ 12°C) in the phase transition of the conjugated gel upon exposure to Cu^{2+} and Ni^{2+} ions, suggesting selective recognition through complexation between the ion and cyclam functional group. Although the incorporation of such chelating moieties into stimuli responsive polymers has allowed for the identification and collection of heavy metal ions [136-138], there still remain difficulties in the identification of a wide range of heavy metal ions.

Here, we use the Gly-Gly-His (GGH) tripeptide as a metal affinity ligand due to its well-known property of binding copper (II) cations.[139-141] Gly-Gly-His is known to mimic the native Cu(II) transport site of human albumin in blood,[139] and intravenous injection of a Gly-Gly-His derivatives have shown enhanced removal of Cu(II) via the kidney.[142] This implies the potential to use small peptide sequences in responsive gels to mimic biomolecular recognition of ions.

In this study, precursor responsive gels were first synthesized from N-isopropylacrylamide and the lysine-like monomer N-(3-aminopropyl)methacrylamide hydrochloride (3-APMA). The lysine-like monomer allows for direct conjugation of amino acids to the hydrogel through a modified Merrifield solid phase peptide synthesis (SPPS) technique. By covalently attaching the C-terminus of an amino to the hydrogel support, Gly-Gly-His can be readily synthesized directly in the gel. The major benefit of this method is that impurities are easily washed from the gel support after each reaction. Hence, a large number of individual steps for intermediates can be avoided. In addition,

solid support allows for automation of the peptide synthesis process, thereby, rapid synthesis of long, more complex peptides.

We tested the response of the NIPAAm-Gly-Gly-His conjugate to a wide range of metal ions including Cu^{2+}, Ni^{2+}, Zn^{2+}, and Na^{+} by using quartz crystal microbalance with dissipation (QCM-D). Specifically, the peptide-conjugated coatings of poly(N-isopropylacrylamide) showed distinctive “temperature dependent swelling fingerprints” that can be used for recognition of different metallic ions in aqueous solution. In the case of poly(NIPAAm) gels without Gly-Gly-His, the logarithm of the transition temperature was proportional to the ionic strength of ion, with NaCl having the largest salting out constant ($K_s' = 0.02\ M^{-1}$), followed by $CuCl_2$, $NiCl_2$, and $ZnCl_2$, each of which had a salting out constant of roughly $0.007\ M^{-1}$. In the case of the Gly-Gly-His conjugated poly(NIPAAm) gel, however, two distinct regimes were observed for the salting out constant of $CuCl_2$, $NiCl_2$, and $ZnCl_2$: a low ionic strength trend and a high ionic strength region. In the low ionic strength regime, the salting out constant was $0.08\ M^{-1}$, $0.07\ M^{-1}$, and $0.06\ M^{-1}$ for Cu, Ni, and Zn, respectively, which follows the known trend for binding of these ions with Gly-Gly-His. At high ionic strengths, the salting out constants were similar to the salting out constants associated with pure poly(NIPAAm), signifying that the gel was completely loaded and that salting out of the poly(NIPAAm) domain was dominant. In contrast, the NaCl showed only a single region with a salting out constant of $0.03\ M^{-1}$.

6.2 Experimental Section

6.2.1 Materials

N-isopropylacrylamide (NIPAAm), *N,N'*-Methylenebisacrylamide (MBAm), azobisisobutyronitrile (AIBN), anhydrous *N,N*-dimethylformamide (DMF), Isopropyl Alcohol (IPA), *N*,*N*-Diisopropylethylamine (DIPEA), piperidine, O-(Benzotriazol-1-yl)-N,N,N',N'-tetramethyluronium tetrafluoroborate (TBTU), trifluoroaceticacetic acid (TFA) and a Kaiser test kit were purchased from Sigma Aldrich. Fmoc-Glycine-OH and Fmoc-Histidine(Trt)-OH were purchased from LC Sciences. N-(3aminopropyl) methacrylamide hydrochloride (3-APMA) was purchased from Polysciences and all reagents were used as received. Cu(II)Cl, Zn(II)Cl, Ni(II)Cl and NaCl were also purchased from Sigma and their solutions were prepared in water that was purified with a Milli-Q system (Millipore).

6.2.2 QCM-D Measurements

QCM-D measurements were performed with a Q-Sense E (Sweden). A small sample of the hydrogel was placed on a gold-coated crystal and compressed under a glass slide so that a thickness on order 50 μm was obtained. The crystal was then spun at 500 rpm for 15 sec in order to obtain proper adhesion and coverage of gel to the crystal surface. Both the frequency and dissipation of the hydrogel coated crystal were measured in contact with water and the cation solutions as a function of temperature (1 ℃/minute ramp). The data from the third harmonic (15 MHz) is presented for all of the measurements of this study. Moreover, a correction was made by subtracting the bare crystal frequency/dissipation values in water (or the cation solutions) as a function of temperature from those of the hydrogels in water and the cation solutions. The

response temperature (T_c) was calculated by taking the value of the third data point after a change in the slope of the frequency or dissipation trend.

6.3 Results and Discussions

In this study, the temperature-dependent swelling behavior of poly(NIPAAm)-GGH conjugate gels was characterized in the presence of NaCl, $CuCl_2$, $NiCl_2$, and $ZnCl_2$ solutions. The conjugate gels were prepared from precursor poly(NIPAAm) gels copolymerized with an amine-substituted monomer, 3-APMA. The peptide sequence was then subsequently synthesized directly in the gel using a Merrifield solid phase peptide synthesis technique, with each amino acid coupling reaction verified by the Kaiser test. Briefly, the Kaiser test was performed after each amino acid conjugation to ensure no free amines and therefore complete coupling. Occasionally, the conjugation reaction was repeated until the Kaiser test resulted in no color change (negative test). Detailed procedure of the hydrogel synthesis and the peptide conjugation is given in chapter III.

To characterize the swelling behavior of the conjugate gels, a quartz crystal microbalance with dissipation (QCM-D) was used. As the dry gel coatings are on the order of several μm, the QCM-D data can be interpreted with respect to the “thick” viscoelastic layer limit.[71] Assuming that the shear modulus, μ, is much larger than the shear viscosity, η, the response of the shift in the resonant frequency, *f* and the dissipation factor, *D*, are:

$$\Delta f \cong -\frac{\eta f}{\rho_o h_o}\sqrt{\frac{\rho}{\mu}} \tag{6.1}$$

$$\Delta D \cong +\frac{1}{\pi f(\rho_o h_o)}\sqrt{\rho\mu} \tag{6.2}$$

where ρ is the density of the layer, and ρ_o and h_o refer to the density and thickness of the quartz crystal, respectively. The density of poly(NIPAAm) is 1.1 mg/ml and the density of water is 1.0 mg/ml. Hence, as the layer collapses the density increases, causing changes in both the frequency and dissipation.

Figure 6.1 shows the both the frequency and dissipation of the poly(NIPAAm), poly(NIPAAm-co-3-APMA) and poly(NIPAAm-co-3-APMA)-GGH gels in pure water and 0.2 M $CuCl_2$ as a function of temperature. For the poly(NIPAAm) gels, the frequency and dissipation show abrupt changes at approximately 33 ℃ (pure water) and 30 ℃ (0.2 M $CuCl_2$), which is taken to be the transition temperature, T_c, between the swollen and collapsed states. Unlike the pure poly(NIPAAm) gel, however, no abrupt transition is observed in either the frequency or dissipation for the poly(NIPAAm-co-3-APMA) gel. A small increase in *f* and a small decrease in *D is* observed, however, for the poly(NIPAAm-co-3-APMA) gel, which may be attributed to a reduction in the shear modulus with increasing temperature. Finally, the conjugated GGH gel shows an abrupt transition near 37 ℃ in pure water. Addition of 0. 2 M $CuCl_2$ to the conjugated GGH gel induces a broad transition at 22 ℃.

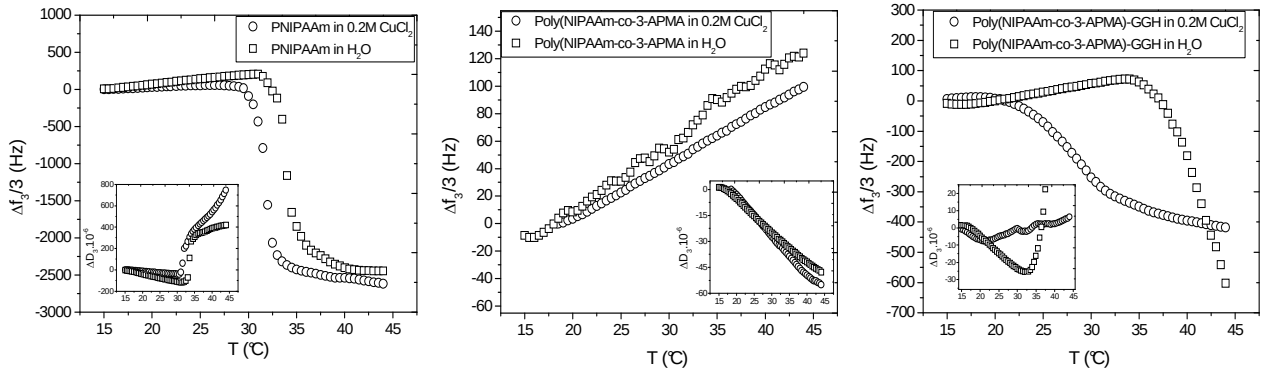

(a) (b) (c)

Figure 6.1 Frequency and dissipation shift as a function of temperature for (a) pure PNIPAAm gels, (b) poly(NIPAAm-co-3-APMA) gels, (c) poly(NIPAAm-co-3-APMA)-GGH gels in $CuCl_2$ and deionized water

Similar measurements were made for a range of salt concentrations (0-0.2 M) including $CuCl_2$, $NiCl_2$, $ZnCl_2$ and NaCl. The resultant transition temperatures, T_c, are shown in Figure 6.2, with the exception of the poly(NIPAAm-co-3-APMA) gels, which did not display a transition temperature over the range of salt concentrations studied. The results for pure poly(NIPAAm) in Figure 6.2a indicate that the effect of each salt is small. In each case, the maximum decrease in the transition temperature was approximately 3 ℃ at 0.2 M salt concentration. This so-called “salting-out” effect is the result of two possible mechanisms.[143, 144] First, ions interfere with the hydrogen bonding between the amide group and surrounding water molecules. Second, ions destabilize the structure of water that surrounds the isopropyl group and backbone of poly(NIPAAm), which increases surface tension. Such an effect has been well-documented in poly(NIPAAm) systems [145, 146] The resultant transition temperatures for the tripeptide conjugated gel are shown in Figure 6.2b. Whereas the dependence of the transition temperature for pure poly(NIPAAm) was linear and quite small with respect to

each ion over the range of 0 – 0.2 M, the poly(NIPAAm)-GGH conjugate is non-linear and quite significant (up to a 15 °C difference), particularly for $CuCl_2$. Between 0.05 and 0.2 M, a trend emerges, in which $CuCl_2$ has the largest effect on the transition temperature followed by $NiCl_2$ and $ZnCl_2$, respectively.

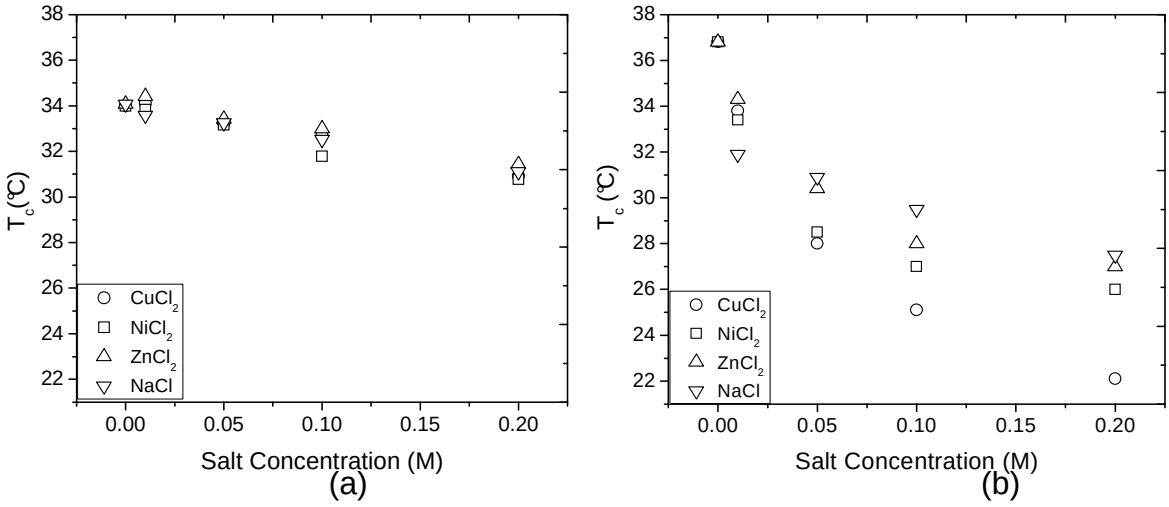

Figure 6.2 Transition temperature (T_c) with respect to salt concentration for (a) PNIPAAm gels, (b) poly(NIPAAm-co-3-APMA)-GGH gels.

The complete QCM-D temperature-scans (from 15 to 40°C) of the poly(NIPAAm-co-3APMA)-GGH conjugate gels are shown in figure 6.3 for each divalent ion. All measurements were referenced to a frequency shift of zero at 15°C for comparison purposes. Interestingly, the overall change in frequency at the transition temperature is largest for $ZnCl_2$ (~ - 1400 Hz), followed $NiCl_2$ (~ - 700 Hz) and then $CuCl_2$ (- 400 Hz). This trend may be understood by the initial shrinkage or contraction of the GGH conjugate gels upon introduction of the each salt solution at 15°C.

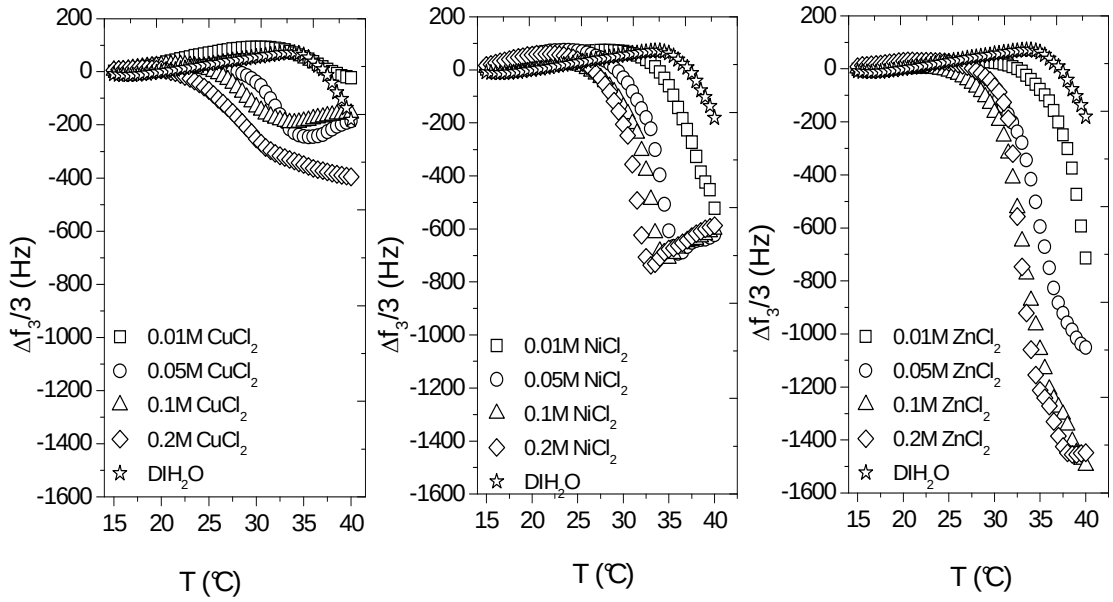

Figure 6.3 Frequency shift as a function of temperature for poly(NIPAAm-co-3-APMA)-GGH gels in heavy metal ion solutions between 0 – 0.2 M.

In order to interpret the results in a more quantifiable manner, we examined the transition temperature of both the poly(NIPAAm) and poly(NIPAAm-co-3APMA)-GGH gels in each salt solution as a function of the ionic strength. Cohn[147] provided a relationship that describes the salting-out of proteins in both strong electrolytes and non-electrolytes:

$$\log S = \beta - K_s' \, I \tag{6.3}$$

where *S* is the solubility, *I* is the ionic strength, β is the intercept (or the logarithm of the solubility at zero ionic strength), and K_s' is the salting out constant. We hypothesize that the transition temperature of the responsive poly(NIPAAm) gels scales with solubility, and thus we can express Equation 3 in terms of the transition temperature T_c

$$\log(T_c) = \log(T_0) - K_s' \, I \tag{6.4}$$

Here, T_o is the transition temperature at zero ionic strength. Figure 6.4 shows the best fits of log (T_c (K)) to equation 6.4 for pure poly(NIPAAm) gel with respect to ionic strength of the NaCl, $CuCl_2$, $NiCl_2$, and $ZnCl_2$ solutions. The salting out constants $K'_s{}'$ are presented in Table 6.1. NaCl has a significantly greater salting out coefficient (0.02 M^{-1}) than $ZnCl_2$, $CuCl_2$ or $NiCl_2$, which each have a salting out constant similar to one another (0.007 M^{-1}). In general, the salting out efficiency of monovalent cations is larger than divalent cations, as ranked in the Hofmeister series, i.e. $NH_4^+ > K^+ > Na^+ > Li^+ > Mg^{2+} > Ca^{2+} > Zn^{2+}$.[148]

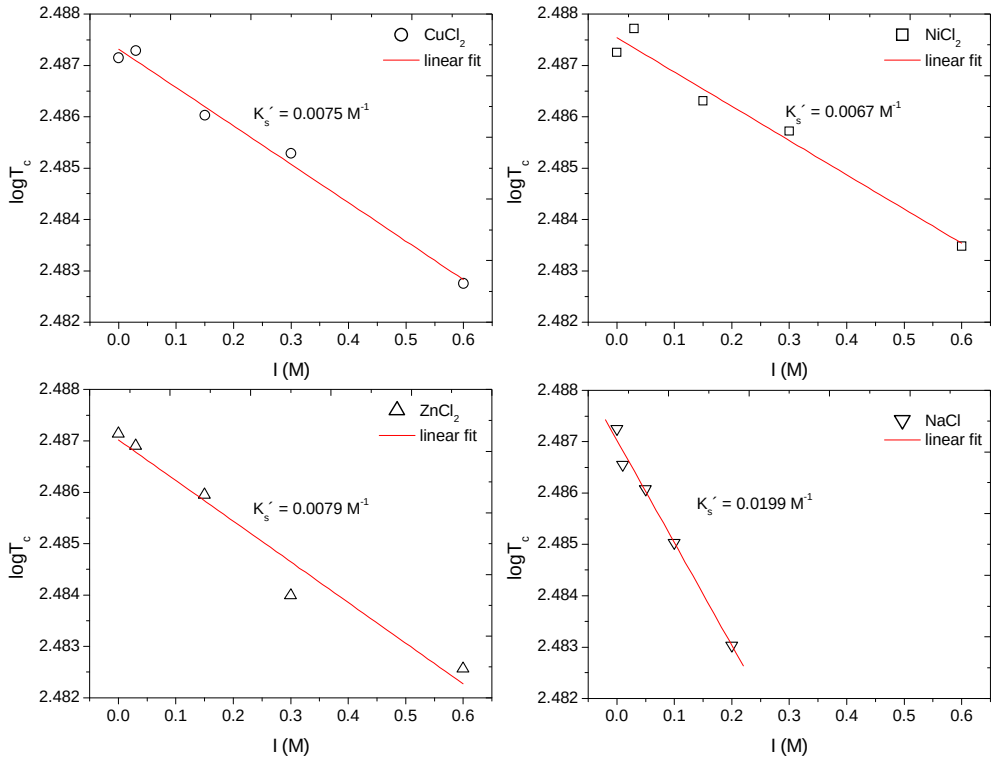

Figure 6.4 Logarithm of the transition temperature (T_c) as a function of ionic strength (I) for pure PNIPAAm with the introduction of the heavy metal ion solutions.

Table 6.1 Fitted values from T_c data of pure PNIPAAm gel.

Ion	Log(T_o)	K_s' (M^{-1})
Cu^{2+}	2.4873 ± 0.00014	0.0075 ± 0.00045
Ni^{2+}	2.4875 ± 0.00020	0.0067 ± 0.00066
Zn^{2+}	2.4870 ± 0.00027	0.0079 ± 0.00088
Na^{+}	2.4870 ± 0.00013	0.0199 ± 0.00126

Figure 6.5 shows the best fits of log (T_c (K)) to equation 6.4 for the poly(NIPAAm-co-3APMA)-GGH gels. In contrast to the pure poly(NIPAAm) gels, a two-regime dependence is observed for the divalent ions.

In the low ionic strength regime, the salting out constant was 0.08 M^{-1}, 0.07 M^{-1}, and 0.06 M^{-1} for Cu^{2+}, Ni^{2+}, and Zn^{2+}, respectively, as reported in Table 2. These salting out constants represent an increase, by a factor of ~11 for Cu^{2+} and Ni^{2+}, and by a factor of ~7 for Zn^{2+} over pure poly(NIPAAm). In the second regime, at ionic strengths greater than 0.15 M, the salting out constants are dramatically decreased for all three ions and are within a factor of two of the salting out constants associated with pure poly(NIPAAm). NaCl has only a single region with a salting out constant of 0.03 M^{-1}.

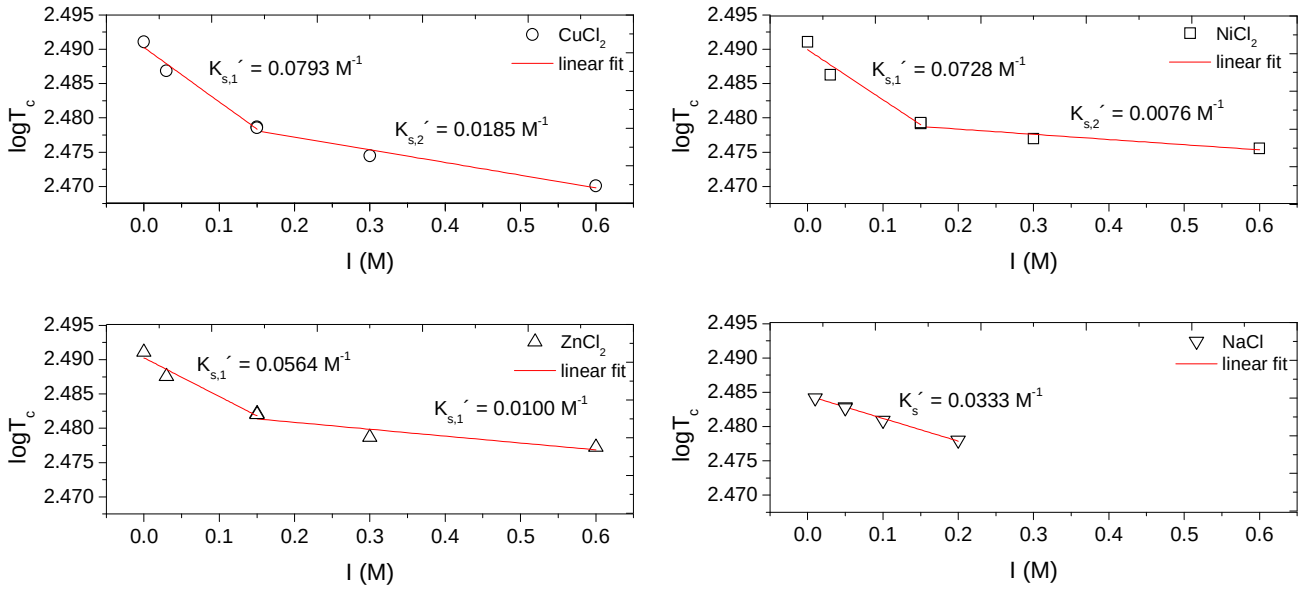

Figure 6.5 Logarithm of the transition temperature (T_c) as a function of ionic strength (I) for pure poly(NIPAAm-co-3-APMA)-GGH gel with the introduction of the heavy metal ion solutions.

Table 6.2 Fitted values from T_c data of poly(NIPAAm-co-3-APMA)-GGH gel

Ion	Poly(NIPAAm-co-3APMA)-GGH		Pure PNIPAAm	$K_{s,1}´ / K_s´$	$K_{s,2}´/ K_s´$
	First region	Second region	$K_s´$ (M^{-1})		
	$K_{s,1}´$ (M^{-1})	$K_{s,2}´$ (M^{-1})			
Cu^{2+}	0.0793 ± 0.0119	0.0185 ± 0.0033	0.0075 ± 0.0005	10.5733	2.4667
Ni^{2+}	0.0728 ± 0.0167	0.0076 ± 0.0024	0.0067 ± 0.0006	10.8657	1.1343
Zn^{2+}	0.0564 ± 0.0117	0.0100 ± 0.0045	0.0079 ± 0.0009	7.1392	1.2659
Na^+	0.0333 ± 0.0018		0.0199 ± 0.0013	1.6734	

At low ionic strengths the large augmentation of the salting out constant between the GGH modified gel and pure poly(NIPAAm) gel indicates that the precipitation of poly(NIPAAm-co-3APMA)-GGH is due to metal-peptide complexation. The tripeptide GGH is known to form a chelate ring with Cu^{2+} through the nitrogen of the imidazole ring

in histidine, the two deprotonated amide nitrogens in glycine and the terminal α-amine. The configuration of Cu^{2+} complexation is shown in figure 6.6. In addition to Cu(II), the binding of transition metals such as Ni^{2+}, and Zn^{2+} to imidazole units in proteins is presented in detail in the literature.[149] The order of association constants for metals binding to imidazole is reported to be $Cu^{2+} > Ni^{2+} > Zn^{2+}$.

As the ionic strength is increased above 0.15 M, the metal-ion binding sites of the GGH peptide saturate and screening of the NIPAAm subunits dominate, as indicated in the similarity of the salting out constants between the poly(NIPAAm-co-3APMA)-GGH gel and pure poly(NIPAAM).

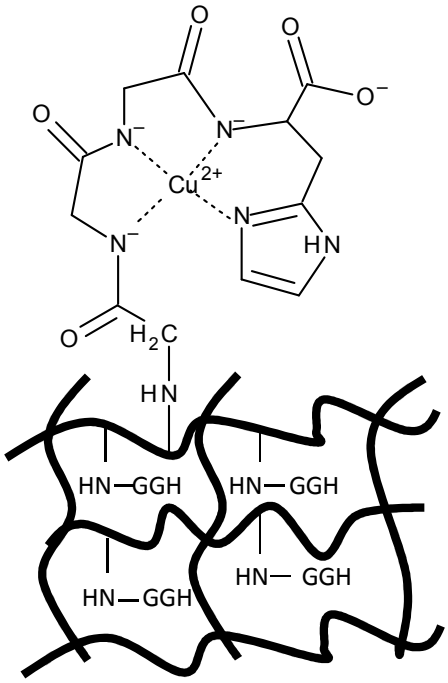

Figure 6.6 A schematic of the Cu^{2+} complexation with the poly(NIPAAm-co-3-APMA)-GGH gel.

6.4 Conclusion

In this study, GGH peptides were successfully grown into an amine-functionalized poly(NIPAAm) gel using a Merrifield solid phase peptide synthesis technique. The peptide/gel conjugate showed a significantly different temperature response than either poly(NIPAAm) or the poly(NIPAAm-co-3-APMA) precursor. In the case of poly(NIPAAm) gels without GGH, the logarithm of the transition temperature was proportional to the ionic strength of ion, with NaCl having the largest salting out constant, followed by $CuCl_2$, $NiCl_2$, and $ZnCl_2$, each having a smaller but similar salting out constant. In the case of the GGH conjugated poly(NIPAAm) gel, however, the trend was reversed, with NaCl having the smallest salting out constant, at least at low ionic strengths. This reversal is believed to be due to complex formation between GGH and the divalent ions. Overall, these results show the ability to easily and quickly grow peptides in responsive gel frameworks in order to modify response behavior. The “built-in-logic” strategy offers an innovative approach to the synthesis of polymer/peptide conjugates that can be used as selective detection systems.

CHAPTER 7 : CONCLUSION AND FUTURE WORK

In this dissertation, adsorption of model protein immunoglobulin g (IgG) on gold and surface attached cross-linked PNIPAAm thin films was studied using quartz crystal microbalance with dissipation (QCM-D). This study was further complemented by a mechanical technique, spinning disk configuration, in order to quickly measure the adhesion of IgG on these thin coatings through detachment shear stresses as the polymer surface was altered between hydrophilic and hydrophobic. Through spinning disk, adhesion of polystyrene (PS) microspheres and model protein immunoglobulin g (IgG) to surface attached cross-linked PNIPAAm thin films have been quantified as a function of film thickness, polymer cross-link density, microsphere deposition time and microsphere concentration.

Our adsorption study results from QCM-D suggested a rigid protein multilayer formation on both gold and collapsed PNIPAAm coating. On hydrated PNIPAAm surfaces, however, the higher dissipation value suggested a soft viscoelastic protein layer formation. The amount of adsorbed protein on both swollen and collapsed PNIPAAm surfaces observed to be similar, indicated by the same amount of frequency drop. The results from spinning disk measurements revealed strong dependence of the bare PS adhesion on polymer film thickness at the collapsed state. In the case of carboxyl functionalized charged PS microspheres, the adhesion trend was altered and is observed to be higher at the swollen state. An interesting study would be to further

investigate this behavior through FTIR to test whether hydrogen bond is being formed between carboxyl groups of the microspheres with water molecules within the PNIPAAm network. Additionally, it was an interesting finding to obtain higher adhesion values when samples were reused. The causes of this behavior could be investigated and its significance in control over adhesion could be evaluated. Another very important study would be to determine the effect of other architectures of PNIPAAm coatings such as brushes and grafted monolayers on the adhesive characteristics. As discussed in previous chapters of this dissertation, different architectural structures have been reported to influence the volume phase transition behavior of PNIPAAm, which could significantly impact the adhesive characteristics. In addition, it would be rather complementary to directly measure the adhesion force between PNIPAAm surfaces of different architectures and PS surface as well as IgG coated surfaces via surface force apparatus (SFA).

In this dissertation, the metal affinity peptide, Gly-Gly-His, conjugated poly(NIPAAm-co-3-APMA) cross-linked bulk networks were also synthesized and the temperature induced swelling behavior was characterized using QCM-D while in contact with metal ion solutions . Our findings showed that GGH conjugated PNIPAAm gel showed the highest recognition towards Cu^{2+} followed by Ni^{2+} and Zn^{2+}. Several experiments were conducted to characterize the influence of the heavy metal ions on the phase transition behavior of the surface attached cross-linked coatings of poly(NIPAAm-co-3-APMA) with dry thickness of 31 nm. Our preliminary results obtained from ellipsometry are shown in figure 6.1.

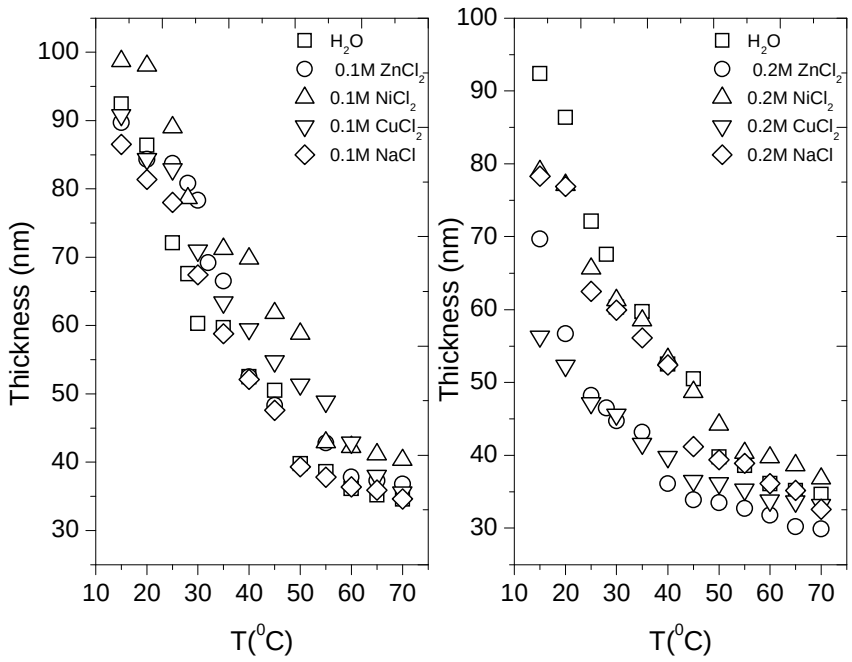

Figure 7.1 Change in surface attached poly(NIPAAm-co-3-APMA) coating thickness as a function of temperature for each metal salt solutions.

As can be seen, ellipsometry enabled us to characterize the temperature dependent phase transition behavior of surface attached coatings of poly(NIPAAm-co-3-APMA) under the influence of metal salts whereas the phase transition of bulk poly(NIPAAm-co-3-APMA) could not be captured via QCM-D. This can suggest that lateral confinement of the poly(NIPAAm-co-3-APMA) networks introduce significant structural changes that could considerably affect the phase transition behavior of the polymer. In addition, different experimentation techniques with different sensitivities could also result in different observations of these two polymer systems. A gradual volume transition was observed at both 0.01M and 0.02M concentrations, which this behavior did not differ with respect to type of metal salt at 0.01M. At 0.02M our results indicated that the influence of $CuCl_2$ on the phase transition was the highest followed by

$ZnCl_2$. These results need to be confirmed and measurements need to be conducted for more metal salt concentrations. Moreover, the influence of other parameters such as pH could be investigated, as well.

Overall conclusions of this dissertation can be laid out as follows:

- Hydrodynamic shear flow assay in spinning disk configuration was for the first time applied to characterization of the adhesive characteristics of surface attached cross-linked PNIPAAm networks.
- The adhesion of IgG on surface attached cross-linked PNIPAAm networks was successfully quantified through hydrodynamics detachment shear stresses.
- The results on adhesion of surface attached thin cross-linked PNIPAAm networks showed an agreement with our QCM-D findings. These results indicated that protein adsorption takes place at both hydrophilic and hydrophobic states and the strength of adhesion does not differ significantly on both surfaces.
- Spinning disk method is very sensitive to structural changes caused by surface confinement and polymer cross-link density.
- The synthesis of a metal affinity peptide was, for the first time, done within the PNIPAAm bulk gel via solid phase peptide synthesis introducing a relatively simple and quick way to produce polymer peptide conjugates.
- It is shown that Gly-Gly-His conjugated PNIPAAm hydrogels allow for selective recognition towards heavy metal ions, specifically for Cu^{2+}.

Experimental findings of this dissertation provide an aid to develop the current understanding of the adhesive performance of the responsive polymers. The

contributions of this research lead to possible new explorations into respective research fields in the design of responsive polymer based novel materials.

REFERENCES

1. Edahiro, J.; Sumaru, K.; Tada, Y.; Ohi, K.; Takagi, T.; Kameda, M.; Shinbo, T.; Kanamori, T.; Yoshimi, Y., In situ control of cell adhesion using photoresponsive culture surface. *Biomacromolecules* 2005, 6, (2), 970-974.

2. Yamada N., O. T., Sakai H., Karikusa F., Sawasaki Y., Sakurai Y. , Thermoresponsive Polymeric Surfaces - Control of Attachment and Detachment of Cultured Cells. *Makromol. Chem., Rapid Commun* 1990, 11, 571-576.

3. Cole, M. A., Jasieniak, M., Voelcker, N.H., Thissen, H., Griesser, H.J., Control Over Protein Adsorption with Thermosensitive Stimuli-Responsive Coatings. *European Cells and Materials* 2007, 14, (3), 50.

4. Dejardin, P., *Proteins at Solid-Liquid Interfaces*. Springer: Berlin Heidelberg, 2006.

5. Tanaka, T., Fillmore, D. J., Kinetics of Swelling of Gels. *Journal of Chemical Physics* 1979, 70, 1214-1218.

6. Toomey, R.; Freidank, D.; Ruehe, J., Swelling Behavior of Thin, Surface-Attached Polymer Networks. *Macromolecules* 2004, 37, (3), 882-887.

7. Harmon, M. E., Jakob, T. A. M., Knoll, W.; Frank, C. W., A surface plasmon resonance study of volume phase transitions in N-isopropylacrylamide gel films. *Macromolecules* 2002, 35, (15), 5999-6004.

8. Harmon, M. E.; Kuckling, D.; Frank, C. W., Photo-Cross-Linkable PNIPAAm Copolymers. 2. Effects of Constraint on Temperature and pH-Responsive Hydrogel Layers. *Macromolecules* 2003, 36, (1), 162-172.

9. Harmon, M. E.; Kuckling, D.; Pareek, P.; Frank, C. W., Photo-cross-linkable PNIPAAm copolymers. 4. Effects of copolymerization and cross-linking on the volume-phase transition in constrained hydrogel layers. *Langmuir* 2003, 19, (26), 10947-10956.

10. Dale L. Huber, R. P. M., Michael A. Samara, Byung-Il Kim, Bruce C. Bunker, Programmed Adsorption and Release of Proteins in a Microfluidic Device. *Science* 2003, 301, 352-354.

11. Schild, H. G., Poly(N-isopropylacrylamide)-Experiment, Theory, and Application. *Progress in Polymer Science* 1992, 17, 163-249.

12. Hoffman, A. S., Environmentally Sensitive Polymers and Hydrogels - Smart Biomaterials *MRS Bulletin* 1991, 16, 42-46.

13. Tanaka, T., Phase Transitions in Gels and a Single Polymer. *Polymer* 1979, 20, 1404-1412.

14. Heskins, M., Guillet, G.E., James E. , Solution Properties of poly (N-isopropylacrylamide). *Journal of Macromolecular Science, Chemistry* 1968, 2, 1441-1455.

15. Yamazaki, A., Winnik, F. M., Cornelius, R. M., Brash, J. L., Modification of liposomes with N-substituted polyacrylamides: identification of proteins adsorbed from plasma. *Biochimica Et Biophysica Acta-Biomembranes* 1999, 1421, (1), 103-115.

16. Cho, E. C., Kim, Y. D., Cho, K., Thermally responsive poly (N-isopropylacrylamide) monolayer on gold: synthesis, surface characterization, and protein interaction/adsorption studies. *Polymer* 2004, 45, (10), 3195-3204.

17. Cheng, X., Canavan, H. E., Graham, D. J., Castner, D. G., Ratner, B. D., Temperature dependent activity and structure of adsorbed proteins on plasma polymerized N-isopropyl acrylamide. *Biointerphases* 2006, 1, (1), 61-72.

18. Yu, Q., Zhang, Y., Chen, H., Wu, Z., Huang, H., Cheng, C., , Protein adsorption on poly(N-isopropylacrylamide)-modified silicon surfaces: Effects of grafted layer thickness and protein size. *Colloids and Surfaces B-Biointerfaces* 2010, 76, (2), 468-474.

19. Takezawa, T., Mori, Y., Yoshizato, K. , Cell Culture on a Thermoresponsive Polymer Surface. *Nature Biotechnology* 1990, 8, 854-856.

20. Harimoto, M., Yamato, M., Hirose, M., Isoi, Y., Kikuchi A., Okano, T. , Novel Approach for Achieving Double-Layered Cell Sheets Co-Culture: Overlaying Endothelial Cell Sheets onto Monolayer Hepatocytes Utilizing Temperature-Responsive Culture Dishes. *Journal of Biomedical Materials Research* 2002, 62, (3), 464-470.

21. Hoffman, A. S., Environmentally sensitive polymers and hydrogels. "Smart" biomaterials. *MRS Bull.* 1991, 16, (9), 42-6.

22. Lahann, J.; Langer, R., Smart materials with dynamically controllable surfaces. *MRS Bull.* 2005, 30, (3), 185-188.

23. Yakushiji, T.; Sakai, K.; Kikuchi, A.; Aoyagi, T.; Sakurai, Y.; Okano, T., Effects of cross-linked structure on temperature-responsive hydrophobic interaction of poly(N-isopropylacrylamide) hydrogel-modified surfaces with steroids. *Anal. Chem.* 1999, 71, (6), 1125-1130.

24. de las Heras Alarcon, C.; Farhan, T.; Osborne, V. L.; Huck, W. T. S.; Alexander, C., Bioadhesion at micro-patterned stimuli-responsive polymer brushes. *J. Mater. Chem.* 2005, 15, (21), 2089-2094.

25. Kidoaki, S.; Ohya, S.; Nakayama, Y.; Matsuda, T., Thermoresponsive Structural Change of a Poly(N-isopropylacrylamide) Graft Layer Measured with an Atomic Force Microscope. *Langmuir* 2001, 17, (8), 2402-2407.

26. Ishida, N.; Kobayashi, M., Interaction forces measured between poly(N-isopropylacrylamide) grafted surface and hydrophobic particle. *J. Colloid Interface Sci.* 2006, 297, (2), 513-519.

27. Wiedemair, J.; Serpe, M. J.; Kim, J.; Masson, J.-F.; Lyon, L. A.; Mizaikoff, B.; Kranz, C., In-Situ AFM Studies of the Phase-Transition Behavior of Single Thermoresponsive Hydrogel Particles. *Langmuir* 2007, 23, (1), 130-137.

28. Junk, M. J. N.; Berger, R.; Jonas, U., Atomic Force Spectroscopy of Thermoresponsive Photo-Cross-Linked Hydrogel Films. *Langmuir* 26, (10), 7262-7269.

29. Kushida, A.; Yamato, M.; Konno, C.; Kikuchi, A.; Sakurai, Y.; Okano, T., Decrease in culture temperature releases monolayer endothelial cell sheets together with deposited fibronectin matrix from temperature-responsive culture surfaces. *J. Biomed. Mater. Res.* 1999, 45, (4), 355-362.

30. Huber, D. L.; Manginell, R. P.; Samara, M. A.; Kim, B.-I.; Bunker, B. C., Programmed adsorption and release of proteins in a microfluidic device. *Science (Washington, DC, U. S.)* 2003, 301, (5631), 352-354.

31. Kurkuri, M. D.; Nussio, M. R.; Deslandes, A.; Voelcker, N. H., Thermosensitive Copolymer Coatings with Enhanced Wettability Switching. *Langmuir* 2008, 24, (8), 4238-4244.

32. Cunliffe, D.; de Alarcon, C.; Peters, V.; Smith, J. R.; Alexander, C., Thermoresponsive surface-grafted poly(N-isopropylacrylamide) copolymers: Effect of phase transitions on protein and bacterial attachment. *Langmuir* 2003, 19, (7), 2888-2899.

33. Cho, E. C.; Kim, Y. D.; Cho, K., Temperature-dependent intermolecular force measurement of poly(N-isopropylacrylamide) grafted surface with protein. *J. Colloid Interface Sci.* 2005, 286, (2), 479-486.

34. Cheng, X.; Wang, Y.; Hanein, Y.; Bohringer, K. F.; Ratner, B. D., Novel cell patterning using microheater-controlled thermoresponsive plasma films. *J Biomed Mater Res A* 2004, 70, (2), 159-68.

35. Cheng, X.; Canavan, H. E.; Graham, D. J.; Castner, D. G.; Ratner, B. D., Temperature-dependent activity and structure of adsorbed proteins on plasma polymerized N-isopropyl acrylamide. *Biointerphases* 2006, 1, (1), 61-72.

36. Malmsten, M., *Biopolymers at Interfaces*. Marcel Dekker, Inc.: New York, 1998; Vol. 75.

37. Andrade, J. D., *Surface and Interfacial Aspects of Biomedical Polymers*. Plenum Press: New York, 1985; Vol. 2.

38. Horbert, T. S., Brash, J., *Proteins at Interfaces, Amer. Chem. Soc. Sym. Series 343* 1987.

39. Andrade, J. D., Hlady, V., Wei, A.P., Ho, C.H., Lea, A.S., Jeon, S.I., Lin, Y.S., Stroup, E., in Piskin E. ed. , *Biologically Modified Biomaterial Surfaces*. Elsevier: 1991.

40. Andrade, J. D., Hlady, V. , *Journal of Biomaterials Science, Polymer Edition* 1991, 2, 161-171.

41. Norde, W., in E. Piskin, ed., *Biologically Modified Biomaterial Surfaces*. Elsevier: 1991.

42. Ramsden, J. J., Puzzles and paradoxes in protein adsorption. *Chemical Society Reviews* 1995, 24, (1), 73-78.

43. Andrade, J. D., Hlady, V. , Protein Adsorption and Materials Biocompatibility: A Tutorial Review and Suggested Hypotheses. *Adv. Polym. Sci.* 1986, 79, 1-63.

44. Nakanishi, K.; Sakiyama, T.; Imamura, K., On the adsorption of proteins on solid surfaces, a common but very complicated phenomenon. *J. Biosci. Bioeng.* 2001, 91, (3), 233-244.

45. Park P. K., J. B. E., Williams S. K., Carter T. L., Rose D. G., Martinez-Hernandez A., Carabasi R. A. III, Thrombus-free, human endothelial surface in the midregion of a Dacron vascular graft in the splanchnic venous circuit-Observations after nine months of implantation. *J. Vasc. Surg.* 1990, 11, 468-475.

46. Langer, R.; Vacanti, J. P., Tissue Engineering. *Science* 1993, 260, (5110), 920-926.

47. Horwitz, F. A., Integrins and Health. *Scientific American* May 1997, 68-75.

48. Michael, K. E.; Vernekar, V. N.; Keselowsky, B. G.; Meredith, J. C.; Latour, R. A.; Garcia, A. J., Adsorption-induced conformational changes in fibronectin due to interactions with well-defined surface chemistries. *Langmuir* 2003, 19, (19), 8033-8040.

49. Clark, W. R.; Macias, W. L.; Molitoris, B. A.; Wang, N. H. L., Plasma protein adsorption to highly permeable hemodialysis membranes. *Kidney Int.* 1995, 48, (2), 481-8.

50. Nerem, R. M., Vacanti, J. P., Lanza, R. P., Langer, R. S. ed. , *Principles of Tissue Engineering (2nd ed.)*. Academic Press: Boston, 2000.

51. Williams, D. F., *The Williams Dictionary of Biomaterials*. Liverpool University Press: Liverpool, 1999.

52. Hench, L. L.; Thompson, I., Twenty-first century challenges for biomaterials. *J. R. Soc. Interface* 7, (Suppl. 4), S379-S391.

53. Lud, S. Q.; Nikolaides, M. G.; Haase, I.; Fischer, M.; Bausch, A. R., Field effect of screened charges: electrical detection of peptides and proteins by a thin-film resistor. *ChemPhysChem* 2006, 7, (2), 379-384.

54. Chen, Z. Y., Qian, S. Z., Abrams, W. R., Malamud, D., Bau, H. H., Thermosiphon-based PCR reactor: Experiment and modeling. *Analytical Chemistry* 2004, 76, (13), 3707-3715.

55. Lagally, E. T., Scherer, J. R., Blazej, R. G., Toriello, N. M., Diep, B. A. , Ramchandani, M., Sensabaugh, G. F., Riley, L. W., Mathies, R. A., Integrated portable genetic analysis microsystem for pathogen/infectious disease detection. *Analytical Chemistry* 2004, 76, (11), 3162-3170.

56. Zangmeister, R. A., Tarlov, M. J., DNA displacement assay integrated into microfluidic channels. *Analytical Chemistry* 2004, 76, (13), 3655-3659.

57. Bae, Y. H.; Okano, T.; Kim, S. W., "On-off" thermocontrol of solute transport. II. Solute release from thermosensitive hydrogels. *Pharm. Res.* 1991, 8, (5), 624-8.

58. Bae, Y. H.; Okano, T.; Kim, S. W., "On-off" thermocontrol of solute transport. I. Temperature dependence of swelling of N-isopropylacrylamide networks modified with hydrophobic components in water. *Pharm. Res.* 1991, 8, (4), 531-7.

59. Baszkin, A., Norde W. , *Physical Chemistry of Biological Interfaces* Marcel Dekker: New York, 2000.

60. Sina Burket, E. B., Marco Kuntzsch, Martin Müller, Klaus-Jochen Eichhorn, Cornelia Bellmann, Petra Uhlmann, and Manfred Stamn Protein Resistance of PNIPAAm Brushes: Application to Switchable Protein Adsorption *Langmuir* 2010, 26, (3), 1786-1795.

61. Adamson, A., W., *Physical Chemistry of Surfaces*. 4th ed.; Wiley: New York, 1983.

62. Kipling, J. J., *Adsorption from Solutions of Nonelecrolytes*. Academic Press: New York, 1965.

63. Vidyasagar, A.; Majewski, J.; Toomey, R., Temperature Induced Volume-Phase Transitions in Surface-Tethered Poly(N-isopropylacrylamide) Networks. *Macromolecules (Washington, DC, U. S.)* 2008, 41, (3), 919-924.

64. Carlini, C.; Ciardelli, F.; Donati, D.; Gurzoni, F., Polymers containing side-chain benzophenone chromophores: a new class of highly efficient polymerization photoinitiators. *Polymer* 1983, 24, (5), 599-606.

65. Carlini, C.; Gurzoni, F., Optically active polymers containing sidechain benzophenone chromophores. *Polymer* 1983, 24, (1), 101-6.

66. Prucker, O.; Naumann, C. A.; Ruehe, J.; Knoll, W.; Frank, C. W., Photochemical Attachment of Polymer Films to Solid Surfaces via Monolayers of Benzophenone Derivatives. *J. Am. Chem. Soc.* 1999, 121, (38), 8766-8770.

67. Merrifield, R. B., Solid phase peptide synthesis. I. The synthesis of a tetrapeptide. *J. Am. Chem. Soc.* 1963, 85, (14), 2149-54.

68. Carpino, L. A.; Han, G. Y., 9-Fluorenylmethoxycarbonyl amino-protecting group. *J. Org. Chem.* 1972, 37, (22), 3404-9.

69. Kaiser, E.; Colescott, R. L.; Bossinger, C. D.; Cook, P. I., Color test for detection of free terminal amino groups in the solid-phase synthesis of peptides. *Anal. Biochem.* 1970, 34, (2), 595-8.

70. Azzam, R. M. A., Bashara, N.M., *Ellipsometry and Polarized Light*. Elsevier Science 1987.

71. Voinova, M. V., Rodahl, M., Jonson, M., Kasemo, B., Viscoelastic acoustic response of layered polymer films at fluid-solid interfaces: Continuum mechanics approach. *Physica Scripta* 1999, 59, (5), 391-396.

72. Patra, L.; Toomey, R., Viscoelastic Response of Photo-Cross-Linked Poly(N-isopropylacrylamide) Coatings by QCM-D. *Langmuir* 26, (7), 5202-5207.

73. Zhou, C., Friedt, J-M., Angelova, A., Choi, K-H., Laureyn, W., Frederix, F., Francis, L.A., Campitelli, A., Engelborghs, Y., Borghs, G. , Human Immunoglobulin Adsorption Investigated by Means of Quartz Crystal Microbalance Dissipation, Atomic Force Microscopy, Surface Acoustic Wave, and Surface Plasmon Resonance Techniques. *Langmuir* 2004, 20, 5870-5878.

74. Hook, F., Voros, J., Rodahl, M., Kurrat, R., Boni, P., Ramsden, J. J., Textor, M., Spencer, N. D., Tengvall, P., Gold, J., Kasemo, B. , A Comperative Study of Protein Adsorption on Titanium Oxide Surfaces Using In-Situ Ellipsometry, Optical Waveguide Lightmode Spectroscopy, and Quartz Crystal Microbalance/Dissipation *Coloids and Surfaces, B.* 2002, 24, (2), 155-170.

75. Hook, F., Voros, J., Rodahl, M., Brzezinski, P., Kasemo, B., Energy Dissipation Kinetics for Protein and Antibody-Antigen Adsorption under Shear Oscillation on a Quartz Crystal Microbalance *Langmuir* 1998, 14, (4), 729-734.

76. Sparrow, E. M., Gregg, J. L., , Mass transfer, flow, and heat transfer about a rotating disk *J Heat Transfer, Trans ASME* 1960, 294-302.

77. Levich, V. G., *Physicochemical Hydrodynamics*. Prentice Hall: Englewood Cliffs, NJ, 1962.

78. Garcia, A. J., Ducheyne, P., Boettiger, D., Quantification of Cell Adhesion Using Spinning Disk Device and Application to a Surface-Reactive Materials. *Biomaterials* 1997, 18, (16), 1091-1098.

79. Hoffman, A. S., Applications of thermally reversible polymers and hydrogels in therapeutics and diagnostics. *J. Controlled Release* 1987, 6, 297-305.

80. Silva, C. S. O.; Baptista, R. P.; Santos, A. M.; Martinho, J. M. G.; Cabral, J. M. S.; Taipa, M. A., Adsorption of human IgG on to poly(N-isopropylacrylamide)-based polymer particles. *Biotechnol. Lett.* 2006, 28, (24), 2019-2025.

81. Bujis, J., Lichtenbelt, J.W.T., Norde, W., Lyklema, J.,, Adsorption of monoclonal IgGs and their F(ab')2 fragments onto polymeric surfaces. *Colloids and Surfaces B-Biointerfaces* 1995, 5, 11-23.

82. Petrash, S., Cregger, T., Zhu, B., Pokidysheva, E., Foster, M. D.,Brittain, W. J., Sevastianov, V., Majkrzak, C. F., , *Langmuir* 2001, 178, 7645-7651.

83. Grabbe, E. S., *Langmuir* 1993, 9, 1574-1581.

84. Song, D., Forciniti, D. J., *Colloid Interface Sci.* 2000, 221, 25-37.

85. Garcia, A. J.; Gallant, N. D., Stick and grip. Measurement systems and quantitative analyses of integrin-mediated cell adhesion strength. *Cell Biochem. Biophys.* 2003, 39, (1), 61-73.

86. Schmitt, F. J.; Park, C.; Simon, J.; Ringsdorf, H.; Israelachvili, J., Direct Surface Force and Contact Angle Measurements of an Adsorbed Polymer with a Lower Critical Solution Temperature. *Langmuir* 1998, 14, (10), 2838-2845.

87. Burkert, S.; Bittrich, E.; Kuntzsch, M.; Muller, M.; Eichhorn, K.-J.; Bellmann, C.; Uhlmann, P.; Stamm, M., Protein Resistance of PNIPAAm Brushes: Application to Switchable Protein Adsorption. *Langmuir* 26, (3), 1786-1795.

88. Li, T.-D. Atomic Force Microscopy Study of Nano-Confined Liquids. Georgia Institute of Technology, Atlanta, 2008.

89. Horbett, T. A., Waldburger, J.J., Ratner, B.D., Hoffman, A.S., Cell Adhesion to a Series of Hydrophilic-Hydrophobic Copolymers Studied with a Spinning Disk Apparatus. *J. Biomed. Mater. Res.* 1998, 22, (5), 383-404.

90. Weiss, L., The Measurement of Cell Adhesion. *Exp. Cell Res.Suppl.* 1961, 8, 141-153.

91. Mohandas, N., Hockmuth, R.M., Spaeth, E.F., Adhesion of red cells to foreign surfaces in the presence of flow. *J. Biomed. Mater. Res.* 1974, 8, 119-136.

92. Pratt, K. J., Jarrel, B.E., Williams, S.K., Carabasi, R.A., Rupnick, M.A., Hubbard, F.A., Kinetics of Endothelial Cell-Surface Attachment Forces. *J. Vasc. Surg.* 1997, 7, 591-599.

93. Gallant, N. D., Michael, K.E., Garcia, A.J., Cell Adhesion Strengthening: Contributions of adhesive area, integrin binding and focal adhesion assembly. *Mol. Biol Cell* 2005, 16, 4329-4340.

94. Sharma, M. M.; Chamoun, H.; Sarma, D. S. H. S. R.; Schechter, R. S., Factors controling the hydrodynamic detachment of particles from surfaces. *J. Colloid Interface Sci.* 1992, 149, (1), 121-34.

95. Visser, J., Adhesion Of Colloidal Polystyrene Particles To Cellophane As A Function Of Ph And Ionic-Strength. *Journal of Colloid and Interface Science* 1976, 55, (3), 664-677.

96. Buijs, J.; van, d. B. P. A. W.; Lichtenbelt, J. W. T.; Norde, W.; Lyklema, J., Adsorption dynamics of IgG and its F(ab')2 and Fc fragments studied by reflectometry. *J. Colloid Interface Sci.* 1996, 178, (2), 594-605.

97. Buijs, J.; Norde, W.; Lichtenbelt, J. W. T., Changes in the Secondary Structure of Adsorbed IgG and F(ab')2 Studied by FTIR Spectroscopy. *Langmuir* 1996, 12, (6), 1605-13.

98. Buijs, J.; White, D. D.; Norde, W., The effect of adsorption on the antigen binding by IgG and its F(ab')2 fragments. *Colloids Surf., B* 1997, 8, (4/5), 239-249.

99. Lau, K. H. A.; Bang, J.; Hawker, C. J.; Kim, D. H.; Knoll, W., Modulation of Protein-Surface Interactions on Nanopatterned Polymer Films. *Biomacromolecules* 2009, 10, (5), 1061-1066.

100. Gyss, C.; Bourdillon, C., Enzymic electrocatalysis as a strategy for electrochemical detection in heterogeneous immunoassays. *Anal. Chem.* 1987, 59, (19), 2350-5.

101. Ortega-Vinuesa, J. L.; Tengvall, P.; Lundstrom, I., Molecular packing of HSA, IgG, and fibrinogen adsorbed on silicon by AFM imaging. *Thin Solid Films* 1998, 324, (1,2), 257-273.

102. Molina-Bolivar, J. A.; Galisteo-Gonzalez, F.; Hidalgo-Alvarez, R., Particle enhanced immunoassays stabilized by hydration forces: a comparative study between IgG and F(ab')2 immunoreactivity. *J. Immunol. Methods* 1998, 211, (1-2), 87-95.

103. Gaucher, G.; Asahina, K.; Wang, J.; Leroux, J.-C., Effect of Poly(N-vinyl-pyrrolidone)-block-poly(D,L-lactide) as Coating Agent on the Opsonization, Phagocytosis, and Pharmacokinetics of Biodegradable Nanoparticles. *Biomacromolecules* 2009, 10, (2), 408-416.

104. Awsiuk, K.; Bernasik, A.; Kitsara, M.; Budkowski, A.; Petrou, P.; Kakabakos, S.; Prauzner-Bechcicki, S.; Rysz, J.; Raptis, I., Spectroscopic and microscopic characterization of biosensor surfaces with protein/amino-organosilane/silicon structure. *Colloids Surf., B* 2012, 90, 159-168.

105. Awsiuk, K.; Budkowski, A.; Petrou, P.; Bernasik, A.; Marzec, M. M.; Kakabakos, S.; Rysz, J.; Raptis, I., Model immunoassay on silicon surfaces: Vertical and lateral nanostructure vs. protein coverage. *Colloids Surf., B* 2013, 103, 253-260.

106. Malmsten, M.; Lassen, B.; Holmberg, K.; Thomas, V.; Quash, G., Effects of hydrophilization and immobilization on the interfacial behavior of immunoglobulins. *J. Colloid Interface Sci.* 1996, 177, (1), 70-8.

107. Lassen, B.; Malmsten, M., Competitive protein adsorption studied with TIRF and ellipsometry. *J. Colloid Interface Sci.* 1996, 179, (2), 470-477.

108. Lassen, B.; Malmsten, M., Structure of protein layers during competitive adsorption. *J. Colloid Interface Sci.* 1996, 180, (2), 339-349.

109. LaGraff, J. R.; Chu-LaGraff, Q., Scanning Force Microscopy and Fluorescence Microscopy of Microcontact Printed Antibodies and Antibody Fragments. *Langmuir* 2006, 22, (10), 4685-4693.

110. Elgersma, A. V.; Zsom, R. L. J.; Norde, W.; Lyklema, J., The adsorption of bovine serum albumin on positively and negatively charged polystyrene lattices. *J. Colloid Interface Sci.* 1990, 138, (1), 145-56.

111. Norde, W.; Lyklema, J., Thermodynamics of protein adsorption. Theory with special reference to the adsorption of human plasma albumin and bovine pancreas ribonuclease at polystyrene surfaces. *J. Colloid Interface Sci.* 1979, 71, (2), 350-66.

112. Kawaguchi, H.; Amagasa, H.; Hagiya, T.; Kimura, N.; Ohtsuka, Y., Interaction between proteins and latex particles having different surface structures. *Colloids Surf.* 1985, 13, (4), 295-311.

113. Duracher, D.; Veyret, R.; Elaissari, A.; Pichot, C., Adsorption of bovine serum albumin protein onto amino-containing thermosensitive core-shell latexes. *Polym. Int.* 2004, 53, (5), 618-626.

114. Brooksbank, D. V., Davidson, C. M. , Horne, D. S., Leaver, J. , Influence of electrostatic interactions on b-casein layers adsorbed on polystyrene latices. *J Chem Soc Faraday Trans* 1993, 89, 3419-3425.

115. Bachor, R.; Shea, C. R.; Gillies, R.; Hasan, T., Photosensitized destruction of human bladder carcinoma cells treated with chlorin e6-conjugated microspheres. *Proc. Natl. Acad. Sci. U. S. A.* 1991, 88, (4), 1580-4.

116. Visser, J., Particle adhesion and removal: a review. *Part. Sci. Technol.* 1995, 13, (3-4), 169-96.

117. Visser, J. In *Colloid and other forces in particle adhesion and particle removal (a review)*, 1978; Soc. Chem. Ind.: 1978; pp 121-41.

118. Hertz, H., *J. Reine Angew Mathematik* 1881, 95, 156-171.

119. Johnson, K. L.; Kendall, K.; Roberts, A. D., Surface Energy and the Contact of Elastic Solids. *Proceedings of the Royal Society of London. Series A, Mathematical and Physical Sciences.* 1971, 324, 301-313.

120. Sharma, M. M.; Chamoun, H.; Sarma, D. S. H. S. R.; Schechter, R. S., Factors controlling the hydrodynamic detachment of particles from surfaces. *J. Colloid Interface Sci.* 1992, 149, (1), 121-34.

121. Thill, A.; Spalla, O., Capillary against Adhesion Forces during Drying of Particle Submonolayers on a Solid Substrate. *Langmuir* 2002, 18, (12), 4783-4789.

122. Kamat, S. V.; Puri, V.; Puri, R. K., The effect of film thickness on the structural properties of vacuum evaporated poly(3-methylthiophene) thin films. *ISRN Polym. Sci.* 2012, 570363, 8 pp.

123. Bhattacharyya, D.; Xu, H.; Deshmukh, R. R.; Timmons, R. B.; Nguyen, K. T., Surface chemistry and polymer film thickness effects on endothelial cell adhesion and proliferation. *J. Biomed. Mater. Res., Part A* 2010, 94A, (2), 640-648.

124. Akiyama, Y.; Kikuchi, A.; Yamato, M.; Okano, T., Ultrathin Poly(N-isopropylacrylamide) Grafted Layer on Polystyrene Surfaces for Cell Adhesion/Detachment Control. *Langmuir* 2004, 20, (13), 5506-5511.

125. Pourzand, H.; Pai, P.; Tabib-Azar, M. In *Thickness Dependent Adhesion Force and Its Correlation to Surface Roughness in Multilayered Graphene* IEEE Sensors Conference, Baltimore 2013; IEEE Baltimore 2013; pp 1-4.

126. Das, S. K.; Sharma, M. M.; Schechter, R. S., Adhesion and hydrodynamic removal of colloidal particles from surfaces. *Part. Sci. Technol.* 1995, 13, (3-4), 227-47.

127. Cole, M. A.; Voelcker, N. H.; Thissen, H.; Griesser, H. J., Stimuli-responsive interfaces and systems for the control of protein-surface and cell-surface interactions. *Biomaterials* 2009, 30, (9), 1827-1850.

128. Park, T. G.; Hoffman, A. S., Effect of temperature cycling on the activity and productivity of immobilized Î²-galactosidase in a thermally reversible hydrogel bead reactor. *Appl. Biochem. Biotechnol.* 1988, 19, (1), 1-9.

129. Dehn, S.; Chapman, R.; Jolliffe, K. A.; Perrier, S., Synthetic Strategies for the Design of Peptide/Polymer Conjugates. *Polym. Rev. (Philadelphia, PA, U. S.)* 51, (2), 214-234.

130. Stoica, F.; Alexander, C.; Tirelli, N.; Miller, A. F.; Saiani, A., Selective synthesis of double temperature-sensitive polymer-peptide conjugates. *Chem. Commun. (Cambridge, U. K.)* 2008, (37), 4433-4435.

131. Maslovskis, A.; Tirelli, N.; Saiani, A.; Miller, A. F., Peptide-PNIPAAm conjugate based hydrogels: synthesis and characterisation. *Soft Matter* 7, (13), 6025-6033.

132. Molawi, K.; Studer, A., Reversible switching of substrate activity of poly-N-isopropylacrylamide peptide conjugates. *Chem. Commun. (Cambridge, U. K.)* 2007, (48), 5173-5175.

133. Trzebicka, B.; Robak, B.; Trzcinska, R.; Szweda, D.; Suder, P.; Silberring, J.; Dworak, A., Thermosensitive PNIPAM-peptide conjugate - Synthesis and aggregation. *Eur. Polym. J.* 49, (2), 499-509.

134. Roesler, A.; Klok, H.-A.; Hamley, I. W.; Castelletto, V.; Mykhaylyk, O. O., Nanoscale Structure of Poly(Ethylene Glycol) Hybrid Block Copolymers containing Amphiphilic Î²-Strand Peptide Sequences. *Biomacromolecules* 2003, 4, (4), 859-863.

135. Kuckling, D.; Pareek, P., Synthesis of transition-metal-ion-selective poly(N-isopropylacrylamide) hydrogels by the incorporation of an aza crown ether. *J. Polym. Sci., Part A: Polym. Chem.* 2003, 41, (11), 1594-1602.

136. Galaev, I. Y.; Kumar, A.; Mattiasson, B., Metal-copolymer complexes of N-isopropylacrylamide for affinity precipitation of proteins. *J. Macromol. Sci., Pure Appl. Chem.* 1999, A36, (7 & 8), 1093-1105.

137. Saitoh, T.; Satoh, F.; Hiraide, M., Concentration of heavy metal ions in water using thermoresponsive chelating polymer. *Talanta* 2003, 61, (6), 811-817.

138. Iyer, G.; Yoon, Y.-S.; Coleman, M. R.; Nadarajah, A., Development of environmentally responsive hydrogels with metal affinity behavior. *J. Appl. Polym. Sci.* 2007, 105, (3), 1210-1220.

139. Lau, S.-J.; Kruck, T. P. A.; Sarkar, B., Peptide molecule mimicking the copper(II) transport site of human serum albumin. Comparative study between the synthetic site and albumin. *J. Biol. Chem.* 1974, 249, (18), 5878-84.

140. Camerman, N.; Camerman, A.; Sarkar, B., Molecular design to mimic the copper(II) transport site of human albumin. The crystal and molecular structure of copper(II)-glycylglycyl-L-histidine-N-methyl amide monoaquo complex. *Can. J. Chem.* 1976, 54, (8), 1309-16.

141. Shullenberger, D. F.; Eason, P. D.; Long, E. C., Design and synthesis of a versatile DNA-cleaving metallopeptide structural domain. *J. Am. Chem. Soc.* 1993, 115, (23), 11038-9.

142. Shearer, W. T.; Bradshaw, R. A.; Gurd, F. R. N.; Peters, T., Jr., Amino acid sequence and copper(II)-binding properties of peptide (1-24) of bovine serum albumin. *J. Biol. Chem.* 1967, 242, (23), 5451-9.

143. Zhang, Y.; Furyk, S.; Bergbreiter, D. E.; Cremer, P. S., Specific Ion Effects on the Water Solubility of Macromolecules: PNIPAM and the Hofmeister Series. *J. Am. Chem. Soc.* 2005, 127, (41), 14505-14510.

144. Patra, L.; Vidyasagar, A.; Toomey, R., The effect of the Hofmeister series on the deswelling isotherms of poly(N-isopropylacrylamide) and poly(N,N-diethylacrylamide). *Soft Matter* 7, (13), 6061-6067.

145. Jhon, Y. K.; Bhat, R. R.; Jeong, C.; Rojas, O. J.; Szleifer, I.; Genzer, J., Salt-induced depression of lower critical solution temperature in a surface-grafted neutral thermoresponsive polymer. *Macromol. Rapid Commun.* 2006, 27, (9), 697-701.

146. Ishida, N.; Biggs, S., Salt-induced structural behavior for poly(N-isopropylacrylamide) grafted onto solid surface observed directly by AFM and QCM-D. *Macromolecules (Washington, DC, U. S.)* 2007, 40, (25), 9045-9052.

147. Cohn, E. J., The physical chemistry of the proteins. *Physiol. Rev.* 1925, 5, 349-437.

148. Flores, S. C.; Kherb, J.; Cremer, P. S., Direct and Reverse Hofmeister Effects on Interfacial Water Structure. *J. Phys. Chem. C* 116, (27), 14408-14413.

149. Glusker, J. P., Structural aspects of metal liganding to functional groups in proteins. *Adv. Protein Chem.* 1991, 42, 1-76.

APPENDIX A: COPYRIGHT PERMISSIONS

A.1 Permission to Use Published Contents in Chapter 6

Rightslink Printable License https://s100.copyright.com/App/PrintableLicenseFrame.jsp?publi

JOHN WILEY AND SONS LICENSE TERMS AND CONDITIONS

Sep 25, 2014

This is a License Agreement between Gulnur Sanden ("You") and John Wiley and Sons ("John Wiley and Sons") provided by Copyright Clearance Center ("CCC"). The license consists of your order details, the terms and conditions provided by John Wiley and Sons, and the payment terms and conditions.

All payments must be made in full to CCC. For payment instructions, please see information listed at the bottom of this form.

License Number	3476240289848
License date	Sep 25, 2014
Licensed content publisher	John Wiley and Sons
Licensed content publication	Macromolecular Chemistry and Physics
Licensed content title	Poly(N-isopropylacrylamide) Networks Conjugated with Gly-Gly-His via a Merrifield Solid-Phase Peptide Synthesis Technique for Metal-Ion Recognition
Licensed copyright line	© 2014 WILEY-VCH Verlag GmbH & Co. KGaA, Weinheim
Licensed content author	Gulnur Efe-Sanden,Ryan Toomey
Licensed content date	May 26, 2014
Start page	1342
End page	1349
Type of use	Dissertation/Thesis
Requestor type	Author of this Wiley article
Format	Print and electronic
Portion	Full article
Will you be translating?	No
Title of your thesis / dissertation	Quantification of Protein Adhesion Strength to Surface Attached Poly (N-isopropylacrylamide) (PNIPAAm) Networks by Hydrodynamic Detachment Shear Stresses
Expected completion date	Dec 2014
Expected size (number of pages)	120
Total	0.00 USD
Terms and Conditions	

TERMS AND CONDITIONS

This copyrighted material is owned by or exclusively licensed to John Wiley & Sons, Inc. or one of its group companies (each a"Wiley Company") or handled on behalf of a society with which a Wiley Company has exclusive publishing rights in relation to a particular work (collectively "WILEY"). By clicking accept in connection with completing this